Eco-Efficient Fleet Allocation using Climate-Optimized Aircraft and Alternative Fuels

Claire Garretsen

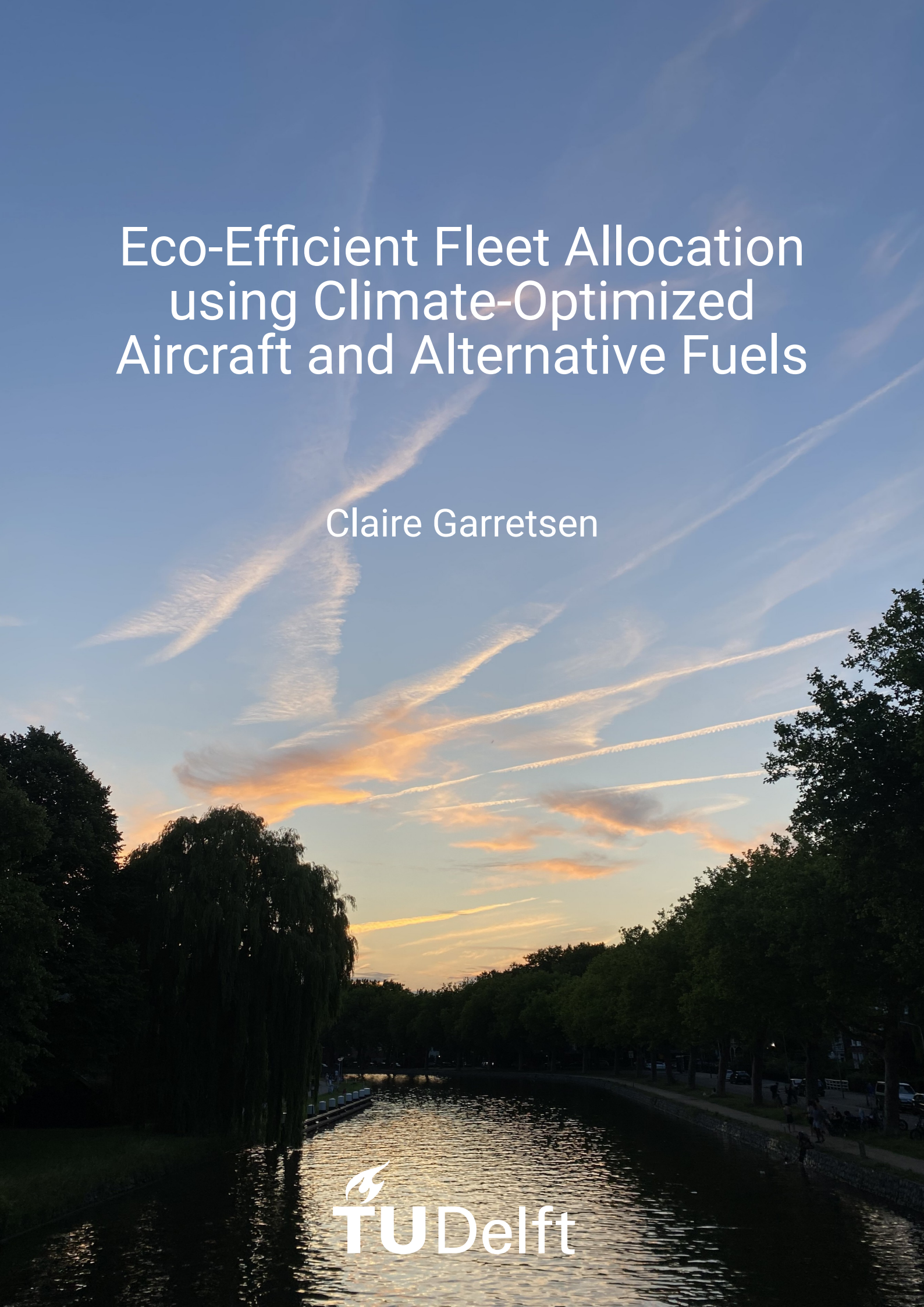

TU Delft

Eco-Efficient Fleet Allocation using Climate-Optimized Aircraft and Alternative Fuels

by

Claire Garretsen

to obtain the degree of Master of Science
at the Delft University of Technology,
to be defended publicly on the 22nd of September, 2025.

Student number:	5099927	
Project duration:	January 6, 2025 – September 22, 2025	
Thesis committee:	Dr. Ir. P Proesmans,	TU Delft, Supervisor
	Dr. Ir. F Yin,	TU Delft, Chair
	Dr. Ir. E van Kampen,	TU Delft, Examiner

TU Delft

Acknowledgements

This thesis marks the end of my master's in Aerospace Engineering at TU Delft. These past years have been educational, inspiring, and memorable. I am thankful to the university for giving me the opportunity to learn and grow, both academically and personally, throughout my studies.

During these past nine months, I had the pleasure of working with my supervisor, Pieter-Jan Proesmans. He has supported me throughout the process, from even before the start of the thesis with support on finding a thesis topic that excites me, to the final stages of this thesis. He has provided me with critical ideas and practical advice, and his openness and reliability have been invaluable. I also want to acknowledge my gratefulness to Feijia Yin. With her constructive feedback during the process, she helped me narrow down my scope and strengthen my arguments. Her suggestions steered me towards greater clarity and focus.

Lastly, I want to thank my family and friends. I am surrounded by love, kindness, and humor, and their encouragement and reassurance have made all the difference.

Claire Garretsen
Delft, September 2025

Contents

List of Figures

II Literature Study

III Supporting work

List of Tables

Nomenclature

Abbreviations and Acronyms

χ	Climate Impact Tax [USD/K]
aCCF	Algorithmic Climate Change Function
AFP	Airframe Purchase price [USD]
ATR_H	Average Temperature Response for a Time Horizon of H years [K],[K/kg(fuel)]
CCF	Climate Change Function
COC	Cash Operating Costs [USD]
CORSIA	Carbon Offsetting and Reduction Scheme for International Aviation
ECHAM	European Centre HAMburg general circulation model
ECMWF	European Centre for Medium-Range Weather Forecasts
EI	Emission Index [kg(x)/kg(fuel)]
EMAC	ECHAM/MESSy Atmospheric Chemistry model
EPP	Engine Purchase Price [USD]
GHG	Green house gas
ICAO	International Civil Aviation Organization
ISSR	Ice-Supersaturated Region
LR	Long-Range
MESSy	Modular Earth Submodel System
MILP	Mixed Integer Linear Programming
MTOM	Maximum Take-Off Mass [kg]
OEM	Operating Empty Mass [kg]
PCFAs	Persistent Contrail Formation Areas
REG	Regional
SAC	Schmidth-Appleman Criterion
SAF	Sustainable Aviation Fuel
SMR	Small-Medium Range
XDSM	Extended Design Structure Matrix

Chemical Formulas

CH_4	Methane
CO_2	Carbon Dioxide

CO	Carbon Monoxide
H_2O	Water
H_2	Hydrogen
NO_x	Nitrogen Oxides
SO_x	Sulfur Oxides
LH_2	Liquid Hydrogen

Introduction

The aviation industry accounts for around 5% of the net global anthropogenic radiative forcing [55]. As the industry is expected to continue to grow, the need for the industry to reduce its climate impact becomes imperative. Researchers have studied different fuel types, aircraft designs, and operational measures to reduce the climate impact (e.g. [62, 71, 72, 76, 94]), but this thesis is the first to research the effect of the combination of sustainable fuels and aircraft types in a fleet, when used to lower the overall climate impact using a fleet allocation model.

The aircraft from Proesmans [76] form the basis of this research. He designed different aircraft for cost and climate-optimal objectives, which include aircraft designed for conventional kerosene, a 50%-blend of sustainable aviation fuel and kerosene, and liquid hydrogen. The effects of these aircraft on the overall climate impact when used by a homogeneous fleet (single fuel type and single design) have been evaluated in his research, but the effects of a mixed fleet using different aircraft types and fuel types have not been studied.

The research methodology consists of three main steps:

1. the climate impact calculations, conducted using the CLIMaCCF library [21].
2. the flight and aircraft acquisition cost calculations, based on direct operating costs and the weekly acquisition costs per aircraft.
3. the eco-efficient fleet allocation, solved using dynamic programming, to maximize the overall profit for different levels of climate impact tax.

The research provides insights for airlines, aircraft manufacturers, and policymakers, and supports the navigation toward a more sustainable aviation industry. Results reveal the profitability of different aircraft designs and fuel types, the changes in the overall profit and climate impact, and the effect of the eco-efficient fleet allocation using climate impact taxes on the network.

This thesis consists of three parts. Part I contains the work of this thesis in the form of a scientific paper. Part II provides the research proposal, which was written during earlier stages of the thesis process, and Part III elaborates on the first two parts by providing additional insights into the conducted work.

I

Scientific Paper

Eco-Efficient Fleet Allocation using Climate-Optimized Aircraft and Alternative Fuels

Claire Garretsen*

Delft University of Technology, Delft, The Netherlands

Abstract

The aviation industry needs to reduce its climate impact. There are various research areas currently being investigated to accomplish this, such as the use of alternative fuels, the design of climate-optimized aircraft and/or aircraft designed for those fuels, and the use of operational mitigation strategies. This research focuses on the overlap of these three, examining the effect of alternative fuels and aircraft on a future airline through the use of climate impact taxes in a fleet allocation model. Kerosene and liquid hydrogen climate and cost-optimized aircraft are used in the fleet allocation for regional, small-medium, and long-range aircraft. Sustainable aviation fuel (SAF) allocation is incorporated through the possibility of adding a 50% SAF blend to the kerosene aircraft. This research calculates the climate impact of flights, including CO_2 as well as non-CO_2 climate effects, with the CLIMaCCF library using ERA5 reanalysis data from ECMWF. These calculations are provided as inputs to the fleet allocation model, which uses dynamic programming and examines the changes in the airline's profit and overall climate impact for different levels of climate impact tax. The results find a Pareto front between the climate impact reduction and the overall profit, resulting in a climate impact reduction potential of 10-15% at the expense of around 1% profit loss, and around 50-60% at 20-30% profit loss. Increasing climate impact tax levels move the fleet composition through a transition from kerosene, to 50% SAF blend, to liquid hydrogen. The transition differs per aircraft category (regional, small-medium range, and long-range), and shows that the climate-optimized aircraft are scarcely used due to their increased flight time and flight costs, for all levels of climate impact tax.

1 Introduction

In 2005, Lee et al. [51] found that the aviation sector contributed 4.9% (range 2-14%, with 90% likelihood range) to the net global anthropogenic radiative forcing. Later, in 2018, the net effective radiative forcing due to aviation was estimated to be around $+100.9\ (mW)m^{-2}$ (range 55-145, with 95% likelihood range), with more than half of the radiative forcing contributions due to non-CO_2 effects [50]. With a global growth forecast of 3.8% passenger increase per year from 2023 to 2043 [37], the climate impact of aviation is expected to grow in the next decades. This means that there is a strong need for the aviation sector to reduce its climate impact and become more sustainable.

Aircraft emissions influence anthropogenic climate change due to CO_2 and non-CO_2 effects. The climate impact of CO_2 emissions from kerosene aircraft is proportional to the amount of fuel that is burned. Increased atmospheric CO_2 concentrations contribute to global warming and have other negative effects on Earth's climate, such as rising sea levels, ocean acidification, decreased water supplies, severe droughts, and increased health risks for humanity and nature (e.g. [52, 81]).

Climate effects from non-CO_2 emissions are more complicated, as they significantly depend on the altitude, latitude, time of emission, and atmospheric conditions (e.g. [23, 75]). These non-CO_2 effects include, but are not limited to, contrail formation, nitrogen oxides (NO_x) emissions, and water vapor (H_2O) emissions.

To mitigate the complex climate impacts from aviation, considerable research is being conducted. The three main research directions, as also highlighted by Noorafza et al. [62], are: 1) sustainable fuels (e.g. [38, 61]), 2) sustainable aircraft designs (e.g. [16, 66]), and 3) operational improvements (e.g. [56, 62, 87]). These directions are interdependent. For example, some sustainable fuels need aircraft designed for these fuels, and operational measures need to be made to accommodate those sustainable aircraft and fuels. These three directions have been researched in the past; however, there is limited knowledge on the combination of them and how they impact the network and the fleet, as well as overall climate impact and profit.

This research provides insights into the effect of combining these different climate impact mitigation measures in a fleet. It considers two types of sustainable fuels in addition to kerosene: drop-in sustainable aviation fuel (SAF) and liquid hydrogen (LH_2), and two types of aircraft designs: climate and cost-optimized aircraft designs.

*MSc Student, Sustainable Air Transport, Faculty of Aerospace Engineering, Delft University of Technology

Through an eco-efficient fleet allocation model, the changes in the fleet, overall climate impact, and profit are examined. In the context of this research, eco-efficient refers to optimizing the combined objective of profit maximization and climate impact minimization. Since SAF is currently blended with conventional kerosene [4], this research uses only climate and cost-optimized aircraft designs for kerosene and LH_2. Aircraft specifically designed for SAF are excluded, and instead it is assumed that SAF can be allocated to kerosene aircraft up to a blending ratio of 50%. The focus of this research is summarized as follows:

> **The objective is to examine changes in the fleet, the allocation of SAF, and the overall profit and climate impact by allocating different types of aircraft employing different fuels to an airline.**

To guide this research, the following research questions are developed:
Research question: To what extent can a future airline reduce its climate impact while considering changes in operating costs by allocating climate-optimized aircraft and alternative fuels in its fleet?
Sub-question 1: To what extent do the fuel and aircraft type affect the fleet composition, the satisfied demand, the flight frequencies, and the flight routes when reducing the overall climate impact?
Sub-question 2: What is the trade-off between climate impact and profit for the allocation of different aircraft types, sizes, fuels, and combinations thereof in a network?

A fleet allocation model is developed, which includes the climate impact, the overall profit, and the trade-off thereof. Such a trade-off is often referred to as an eco-efficient solution (e.g. [29, 60, 66]). With this, changes in the fleet, network, satisfied demand, overall climate impact, and profit can be researched to provide insights into the impact of the use of novel aircraft and fuels at the fleet level. This research does not consider demand variations, nor does it consider flight trajectory optimization or other mitigation measures such as changes in flight altitude or intermediate stop operations.

This paper continues with a review of the literature in section 2, where the three research directions are discussed in more detail, followed by section 3, which describes the methodology used in this research. In section 4, the results are explained and discussed, followed by section 5, which describes the sensitivity analyses and the uncertainties. In section 6 and section 7, a broader discussion and the overall conclusions are presented. Lastly, in section 8, the recommendations for future research are provided.

2 Literature Review

This chapter provides an overview of the literature on sustainable air transport. As explained previously, the three main research directions include sustainable fuels (section 2.1), sustainable aircraft designs (section 2.2), and operational climate impact mitigation (section 2.3).

2.1 Fuel Types

The developments towards more sustainable aviation include different fuel types or energy sources, such as SAF, hydrogen, electricity, or a hybrid thereof. This research focuses on kerosene, SAF, and hydrogen-powered aircraft because each of these emits particles during flight, unlike electric aircraft, where the climate impact heavily depends on whether the electricity is produced from renewable sources. The emissions of the different fuel types are described in this section, as well as the differences in contrail properties. Moreover, the assumption is made that the aircraft powertrain uses turbofan engines, as it is the most widely used propulsion technology for commercial aircraft [68].

2.1.1 Kerosene

Kerosene combustion leads to the production of CO_2 and H_2O, and various other byproducts: unburned hydrocarbons, NO_x, carbon monoxide (CO), soot, aerosols, and sulfur oxides (SO_x) [24]. CO_2 and H_2O emissions are proportional to the amount of fuel burned, but the other molecules depend on factors such as fuel properties, flight altitude, and thrust settings. For example, flight altitude and thrust settings influence the amount of emissions, as well as the climate impact of those emissions [85], which in turn varies per emission. Consequently, a lower flight altitude increases the amount of NO_x emissions, but decreases the radiative forcing [48]. This results in an altitude trade-off, where the climate-optimal altitude might not be the same as the cost-optimal or fuel-optimal altitude [42]. As cost-optimality and fuel-optimality are closely related, airlines could prefer those altitudes to save costs over climate-optimal altitudes. Next to the fuel costs, the flight speed has been found to influence an airline's competitive advantage, which could indirectly affect the airline's profit [3] and an airline's decision to sacrifice some fuel costs for shorter flight times.

Contrail formation depends on the exhaust temperature and ambient conditions such as temperature and relative humidity [77]. Schmidt [76] and Appleman [6] were the first to formulate the criteria for contrail formation, called the Schmidt-Appleman Criterion [25, 77]. This states that contrails are formed when water condensates onto the exhaust and ambient air particles and freezes, forming ice particles [25]. When the ice particles remain in the atmospheric air for at least 10 minutes, contrails become persistent [37]. Persistent contrails generally have a warming effect on the Earth (e.g. [50, 91]); however, Lee et al. [50] showed that confidence levels are low and calculations come with large uncertainties. The contrail properties differ for alternative fuels, such as the number of ice particles, and the ice water contents [87].

2.1.2 Hydrogen

Although the use of hydrogen combustion in aircraft eliminates the climate effects of CO_2, SO_x, and black carbon [37], other effects from contrails, H_2O emissions, and NO_x emissions remain. The magnitudes of the effects differ from kerosene aircraft due to changes in fuel composition. As an example, hydrogen combustion leads to increased levels of H_2O emissions. Moreover, contrail characteristics change because hydrogen engines generally do not emit soot particles. At lower altitudes, the climate impact of hydrogen combustion is generally smaller because precipitation decreases the lifetime of H_2O [85]. At altitudes below 8-10 kilometers, the effects of H_2O emissions are insignificant, as clouds and precipitation are common.

The two most common ways to use hydrogen for aircraft propulsion are through turbo-machinery or hydrogen fuel cells. Liquid hydrogen (LH_2) combustion is preferred for medium to long-range aircraft as it reduces storage and weight constraints (e.g. [1, 20, 88]). Therefore, hydrogen combustion, and specifically liquid hydrogen (LH_2) combustion, is considered in this research.

The impact of hydrogen aircraft depends significantly on the formation of the contrails. The impact of those contrails come with lots of uncertainties. Kaufmann, Dischl, and Voigt [43] perform a statistical evaluation of the probability of contrail formation based on the ambient atmospheric conditions for kerosene and hydrogen-powered aircraft. They argue that the probability of contrail formation for hydrogen and kerosene propulsion is similar, as ambient temperatures are usually low enough for water droplets to freeze, and that the persistence is typically dependent only on the ice-supersaturated regions (ISSRs). They assume hot gaseous emission, similar to kerosene exhaust, whereas Adler and Martins [1] provide further insights into the impact of cooler exhaust on the climate. Ström and Gierens [83] present the first numerical simulation of contrails from hydrogen (cryogenic LH_2) combustion. They compare the contrails from hydrogen combustion to kerosene, and find that the contrails from hydrogen combustion are optically thinner (2D evaluation) and show lower ice crystal number density; however, they measure similar amounts of ice mass and sedimentation rates, even though the average ice crystal size is 4 to 6 times larger for hydrogen. This study does not consider the effect of background ambient particles, which have been found to influence the contrail formation and characteristics [10]. Bier et al. [10] model ambient aerosol particles back into the plume, and find that the ice crystal number is reduced by 80-90% and that the optical visibility is significantly reduced. By comparing the two, they find that for kerosene, the number of ice particles depends on the amount of emitted soot particles at low enough temperatures, whereas the number of ice particles for hydrogen combustion continues to increase when temperature decreases, because of the high amount of emitted water vapor and the entrainment of aerosol particles back into the plume. Moreover, they argue contrail formation starts at temperatures around 10 Kelvin higher than for kerosene, and that the probability of persistent contrail formation is higher for hydrogen aircraft. This research is in line with other findings (e.g. [43, 77]). Megill and Grewe [58] argue that hydrogen aircraft could significantly increase persistent contrail formation (71.4%), but stress the importance of recognizing the difference between persistent contrail formation and the resulting contrail cirrus coverage and climate impact. There is a consensus that an increase in contrail formation does not mean that the resulting radiative forcing increases similarly [58, 70, 77].

2.1.3 Sustainable Aviation Fuel

Drop-in Sustainable Aviation Fuel (SAF) is an alternative fuel for the aviation industry. SAF is a certified jet fuel and is derived from renewable sources, such as used cooking oils, fats, plant oils, waste, etc [63]. Another method is to use renewable energy to produce hydrogen from water, and to convert it to a synthetic fuel using captured CO_2 [1]. SAF is blended with kerosene, generally up to a 50% blending ratio (called drop-in SAF, but often referred to as SAF), to reduce the climate impact and net-CO_2 emissions. It requires minimal changes to the aircraft and infrastructure [14]; however, the availability is heavily constrained because the production levels are low and expensive. The production capacity is currently being improved to meet the RefuelEU aviation regulations [71], which force EU airports to use fuel containing at least 2% SAF in 2025, 6% SAF in 2030, and 70% SAF in 2050.

The International Civil Aviation Organization (ICAO) adopted the Carbon Offsetting and Reduction Scheme

[1] `https://www.bp.com/en/global/air-bp/news-and-views/views/what-is-esaf.html`, accessed August 25th, 2025

for International Aviation (CORSIA)[2]. It plans to regulate the CO_2 emissions from the aviation sector for all member states. The ICAO defines renewable fuel as SAF (or CORSIA SAF) when it meets specific criteria [38]. Currently, the SAF blending ratios are approved by the European Union Aviation Safety Agency and the Federal Aviation Administration for up to 50%, but developments towards the use of 100% SAF are being made [2, 12]. SAF reduces the net CO_2 emission; however, other effects remain, such as NO_x, black carbons, H_2O, contrails, and aerosols. SAF is thus only to a certain extent more sustainable than conventional aviation fuel.

The use of drop-in SAF has been found to increase persistent contrail occurrence compared to kerosene fuel; however, it increases the mean ice particle size, which in turn shortens the contrail lifetime as it increases the sedimentation rate. The slight increase in the probability of contrail occurrence due to a higher amount of water vapor emission is counteracted by the larger decrease in contrail lifetime due to lower amounts of non-volatile particle matter and larger ice particle size [87].

Teoh et al. [86] argue that around 12% of all flights over the North Atlantic are responsible for around 80% of the net radiative forcing due to contrail formation. Because SAF could thus be used to lower the climate impact of contrails, Teoh et al. [87] argue that SAF should not be distributed equally among flights, but instead be allocated at higher blending ratios to flights responsible for the most warming contrails. They elaborate on this by pointing out that careful allocation of the scarce amounts of SAF is necessary to mitigate the impact of those specific flights. They argue the climate impacts from contrails can be decreased by a factor of 9-15 when allocating higher blending ratios to certain flights, compared to uniformly distributing the available SAF among aircraft.

Next to reducing the climate impact, careful SAF allocation could potentially also alleviate pressure from the supply chain. Eurocontrol [21] shows that only 39 of the 1657 EU airports were responsible for 80% of the volumetric kerosene uptake in 2019. Providing the same total amount of SAF to only these airports would lead to equal amounts of CO_2 reductions and fewer logistical complications for the SAF supply chain. This research aims to explore whether the allocation of SAF to particular flights can minimize the overall climate impact, which includes examining possibilities to lower the pressure on the supply chain, when, for example, certain airports are consistently using or not using SAF.

2.2 Sustainable Aircraft Designs

Besides using alternative fuels and redesigning aircraft and engines to accommodate those fuels, aircraft are specifically designed for a lower climate impact. Dallara and Kroo [16] design multiple narrow-body aircraft using a linear climate model with altitude variation. They combine three objectives: minimal operating costs, emissions, and average temperature response (ATR). Similarly, Proesmans and Vos [67] examine how aircraft design variables change when minimizing aircraft for cash operating cost (COC), fuel usage, and climate impact (ATR). Their research includes the aircraft designs for kerosene, drop-in SAF, and LH_2 fuels, and they compare these optimized aircraft for regional (REG), small-medium (SMR), and long-range (LR) categories. Dallara and Kroo [16] and Proesmans and Vos [67] both demonstrate that the trade-off between climate impact and operating cost generates a Pareto front. For the SMR kerosene aircraft, the trade-off is presented in Figure 1. The main differences between climate and cost-optimized aircraft design variables are lower cruise altitudes, lower flight speeds, higher wing aspect ratios, lower engine overall pressure ratios, and higher engine bypass ratios in climate-optimized aircraft [16, 67].

[2] `https://www.icao.int/environmental-protection/CORSIA`, accessed March 4th, 2025

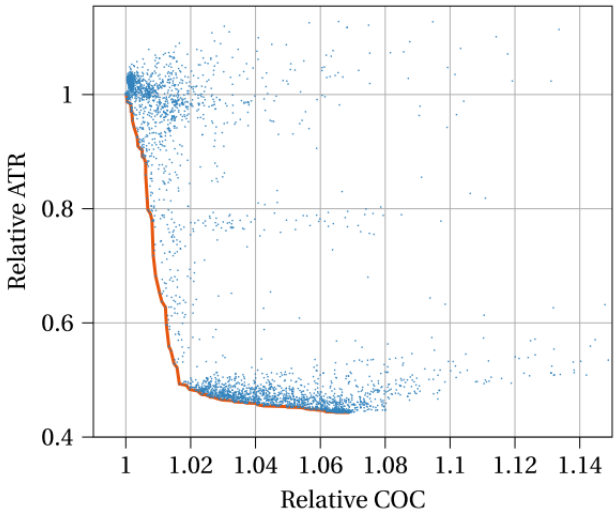

Figure 1: Eco-efficient distribution presenting the trade-off between operating costs and climate impact for the kerosene SMR aircraft design optimization, from Reference [66].

2.3 Operational Climate Impact Mitigation Measures

Proesmans and Vos [67] performed a fleet allocation on a simplified hub-and-spoke network to demonstrate the changes in the number of aircraft in the fleet, using the aircraft optimized for minimal cash operating costs (COC), minimal average temperature response over 100 years (ATR_{100}), and minimal multi-objective (MO) corresponding to the eco-efficient solution (the kinks in the Pareto distribution, as shown in Figure 1). In all optimizations, they assume all aircraft in the fleet use the same fuel type, either kerosene, SAF, or LH_2. Results show that more ATR-optimized (climate-optimized) aircraft are needed compared to a fleet that uses COC-optimized (cost-optimized) aircraft, due to a higher block time and a lower productivity of ATR-optimized aircraft. Their research focuses on the allocation of aircraft types to obtain the maximum profit, but it does not consider a mixed fleet (ATR and COC-optimized aircraft, and/or different fuels combined in one fleet), nor does it look at fleet allocation incorporating the climate impact into the objective function.

Noorafza et al. [62] developed a multi-objective framework for network planning and design, incorporating the objective of minimizing the climate impact (ATR). This objective is relatively new, as airlines primarily focus on maximizing profit, which only extends to the incorporation of fuel costs into the objective function (e.g. [40, 53]). Noorafza et al. [62] evaluate intermediate-stop operations and lower flight altitudes, examining the climate impact reduction potential of these operational measures. Even though their framework includes the climate impact objective, it only considers conventional kerosene aircraft and does not account for a mixed fleet with different aircraft and fuel types.

Research by Niklass et al. [60] examines the changes in climate impact and operating costs when rerouting aircraft to avoid climate-sensitive regions. Their research focuses on the change in climate impact when introducing penalties for certain geographical locations, and the results demonstrate a similar Pareto-distribution as shown in Figure 1 and also found by Dallara and Kroo [16].

As discussed in section 2.1.3, Teoh et al. [87] focus on the allocation of drop-in SAF to flights to mitigate the climate impact of those flights. They highlight the need for intelligent allocation of the scarce amounts of SAF in the future. These conclusions are in line with research from Burkhardt, Bock, and Bier [13], who found that only a small percentage of flights produce large-scale contrail cirrus outbreaks, which are responsible for a high percentage of the radiative forcing. They also argue that mitigating the climate impact of specifically those flights could reduce aviation's overall climate impact significantly.

3 Methodology

The proposed method integrates the climate assessment of varying aircraft types and fuels into airline fleet planning to find the optimal fleet allocation for profit and climate objectives. The method consists of three main parts: 1) the calculation of the climate impact per flight leg for different aircraft and fuel types for every departure time, 2) the calculation of the flight costs per flight leg, the acquisition costs and the objective formulation, and 3) the allocation of the fleet to a network for different objectives. The Extended Design Structure Matrix (XDSM) in Figure 2 provides an overview of the methodology discussed in this chapter and highlights these three main parts.

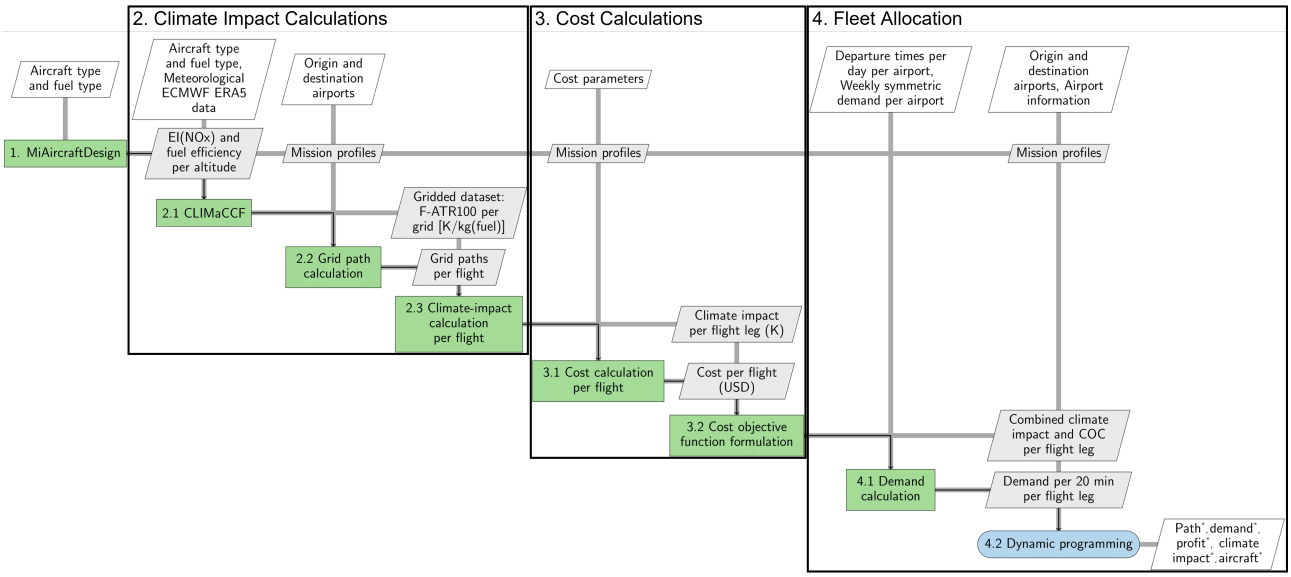

Figure 2: XDSM of set-up for the climate impact calculations, the cost calculations, and the fleet allocation. Figure made using pyXDSM from [49].

The chapter structure follows from the process shown in the XDSM: In section 3.1, the first step is discussed, depicted on the left of Figure 2 by the first green box. This step provides input to the three parts: the climate impact calculations, the cost calculations, and the fleet allocation, which are discussed in section 3.2, section 3.3, and section 3.4, respectively. The chapter continues with a description of the important decisions and assumptions, such as the fleet composition and network selection. These are discussed in section 3.5, and the chapter ends with a short description of the computational set-up in section 3.6.

3.1 MiAircraftDesign: Mission Profile Calculations

The mission profiles for every flight between the hub and spoke airports are calculated using the Python code from Proesmans [66]. It is a multidisciplinary design, analysis, and optimization framework that couples aerodynamics, propulsion, mass sizing, mission analysis, and cost/climate analysis. For each aircraft and fuel type, and every flight distance, the model generates a mission profile based on the aircraft's predefined cruise altitude and cruise Mach number.

These mission profiles are used in the calculations for the emission indices for NO_x and fuel efficiencies, as well as for the climate impact and cost calculations per flight. The files include data on the flight altitude, flown distance/range, the rate of fuel burn, the rate of emitted NO_x, and the velocity for every timestep of the mission (between 2 and 30 seconds).

This research considers three different fuel types: kerosene, SAF (50% blending ratio), and LH_2. However, for the method, it is chosen to only use kerosene aircraft and LH_2-combustion aircraft, because adding SAF to kerosene aircraft best represents the current situation. Therefore, the model assumes that the mission profiles for kerosene aircraft, fueled with kerosene or with a 50% SAF blend, are equivalent.

3.2 Climate Impact Calculations

For the eco-efficient fleet allocation, the climate impact of flights needs to be calculated. This depends on the altitude, geographical location, atmospheric conditions, time of emissions, fuel type, and aircraft design characteristics (e.g. [23, 66, 75]).

There are various approaches available in the literature to quantify the climate impacts of flights. For example, Grewe et al. [31] calculated the climate impact of transatlantic flights within the air traffic simulator (SAAM), for the EU FP7 Project REACT4C[3]. The authors used the European Centre HAMburg general circulation model (ECHAM)/Modular Earth Submodel System (MESSy) Atmospheric Chemistry (EMAC) model, which is a numerical chemistry-climate model system consisting of submodels describing various processes in the atmosphere and the interactions with oceans and land [41]. Grewe et al. [31] simulated the atmospheric reactions from different emissions, and the climate impact in terms of various climate indicators was calculated using five-dimensional climate change functions (CCFs).

These CCFs are computationally expensive, and therefore, the EU-project ATM4E developed approximate versions called algorithmic CCFs (aCCFs) [54]. Yin et al. [93] present the first version of the aCCF submodel

[3] `http://www.react4c.eu/`, accessed March 13th, 2025

called ACCF 1.0 for the EMAC model framework. They implement the aCCFs and elaborate on contrail aCCF development. The model can be used with a flight trajectory optimization model such as AirTraf 2.0 to assess changes in trajectories optimized for climate or cost objectives [92, 93].

Dietmüller et al. [18] present an open-source Python library called CLIMaCCF to calculate the climate impact of flights. The tool calculates the CO_2 aCCF, the individual non-CO_2 aCCFs, and the merged (non-) CO_2 aCCFs, given a geographical location and time-dependent meteorological input data. The authors argue that the tool is user-friendly and efficient compared to other models, such as EMAC, and that it is possible to estimate the climate impact as different physical climate metrics, such as pulse or future ATR, for various time horizons. The model uses meteorological input data, such as data from the European Centre for Medium-Range Weather Forecasts (ECMWF).

The CLIMaCCF model from Dietmüller et al. [18] is used in this research because of the above described reasons. It is designed for conventional aircraft, similarly to other available methods (e.g. [62, 79]), thus for the hydrogen and SAF flights, conversion factors are used to account for the difference in contrail characteristics and emission indices.

The climate impact is calculated for every flight using this model, for each aircraft type and fuel type, for different departure times, and for different days and years based on the input data. Moreover, the climate impact is expressed using the F-ATR_{100} climate metric, because of the following: Megill, Deck, and Grewe [57] study climate metrics and explore their suitability for existing aircraft as well as future aircraft using alternative fuels. They state that the ATR_H metric (average temperature response over H years) is suitable for calculating the climate impact of aircraft employing different fuels, defined according to Equation 1. A time horizon of at least 70 years would be most appropriate, as long-term climate effects need to be considered, such as long-term effects from CO_2 emissions. A 100-year time horizon is commonly used in the literature (e.g. [62, 66]), and is also compatible with the CLIMaCCF model. Furthermore, this model distinguishes between pulse (P-ATR) and future-ATR (F-ATR), and the latter is used because it is argued to be more adequate when focusing on the long-term effects of climate impact mitigation [26].

$$ATR_H = \frac{1}{\mathrm{H}} \int_{t_0}^{t_0+H} \Delta T(t) dt \tag{1}$$

This section describes the three parts of the climate impact calculations:

1. The CLIMaCCF model
2. The grid path calculations
3. The total climate impact calculations per flight leg

ERA5 reanalysis data from different pressure levels [33] and single levels [34] are used as input, containing the information as presented in Table 10. The data is downloaded as GRIB files and converted to netCDF files. This data contains information for a four-dimensional *grid* with the dimensions: latitude, longitude, pressure level, and time. The resolution of the data is per $0.25\,^\circ \times 0.25\,^\circ \times 25\ hPa \times 1\ hour$, which is referred to as a *grid cell*. The data is provided to the CLIMaCCF model, which calculates the aCCFs and determines the future average temperature response over 100 years (F-ATR_{100}) per grid cell (step 1). Consecutively, the grid path calculations provide the flight paths per origin-destination pair, in terms of grid cells, thus: a list of grid cells through which the flight passes (step 2). The aCCFs and the grid paths are then used by the climate impact calculations to determine the total climate impact per flight (step 3). The following sections describe each of these steps in more detail, and the process is also depicted in Figure 3.

3.2.1 The CLIMaCCF Model

The CLIMaCCF model [18] uses the meteorological input data to perform the climate impact calculations and saves the output to a netCDF file. This output file contains the merged aCCF, as well as the individual aCCFs, which include CO_2, O_3, CH_4, daytime contrails, and/or nighttime contrails, and H_2O. The aCCFs are calculated for the F-ATR_{100} climate metric, in Kelvin per kilogram fuel, for every grid cell in the dataset.

The CLIMaCCF model is run for every aircraft type (REG, SMR, LR) and fuel type (kerosene, SAF, LH_2), according to the aircraft and fuel-specific calorific values and emission indices (EI), and overall engine efficiencies. These values are presented in Table 1 and Table 2. For SAF and LH_2, scaling factors are introduced to adjust the CLIMaCCF model. These scaling factors apply to the change in emissions as well as climate impact from contrails, and convert the corresponding aCCF to a different fuel type. The values are presented in Table 3.

Table 1: Calorific values and emission indices ([17] as cited in [66])

	Kerosene	**SAF (50%)**	**LH_2**
LHV [MJ/kg]	43.0	43.6	120
EI H_2O [kg_{H_2O}/kg_{fuel}]	1.26	1.32	8.93

Table 2: Engines' overall efficiencies ([66])

	Kerosene		**LH_2**	
$\eta_{ov,cr}$	ATR_{100}	COC	ATR_{100}	COC
REG	32.1%	39.1%	35.7%	38.6%
SMR	32.6%	39.9%	34.8%	39.3%
LR	34.6%	40.8%	34.3%	39.4%

Table 3: Scaling factors to adjust CLIMaCCF model for SAF and LH_2 aircraft. For H_2O, the scaling factors remain 1; however, note that the emission indices in Table 1 are different for SAF and LH_2.

	Kerosene	**SAF (50%)**	**LH_2**
CO_2	1	0.5	0
O_3	1	1 [82]	0.14 [44]
CH_4	1	1 [82]	0.14 [44]
Contrails	1	0.79 [13]	0.50 [13]
H_2O	1	1	1

The model also uses NO_x emission profiles (note: different from the mission profiles described in section 3.1), and fuel efficiency [km/kg(fuel)] values. This data is provided as part of the CLIMaCCF model for regional, single-aisle, and wide-body aircraft for different altitudes. It is assumed that these three aircraft types correspond to the three types of aircraft used in this research (REG, SMR, and LR). The values contain the altitudes ranging between 20000 and 45000 feet, because the model is designed for these altitudes. Since the lowest cruise altitudes range just below 20000 ft, it is chosen to linearly extend the data slightly to include 18000 ft.

3.2.2 Grid Path Calculations

The flight paths are calculated assuming aircraft travel along the shortest path (according to the World Geodetic System 1984) and with an altitude, velocity, flight duration, and fuel burn according to the mission profile, which is calculated as described in section 3.1. These flight paths consist of waypoints (latitude, longitude), which are transformed to grid paths: a list of all the grids through which the flight path passes. For every grid, the flight altitude from the mission profile is converted to the nearest pressure level using the geopotential height from the ERA5 reanalysis data, and the flight duration is added to the departure time and rounded to the nearest hour. The result is a long list of four-dimensional coordinates for every grid cell in the flight path (latitude, longitude, pressure level, hour). These grid paths are used in the next calculation to transform the CLIMaCCF model output (F-ATR_{100}/kg(fuel) per grid) to F-ATR_{100} per flight. In Figure 3, the different steps towards the climate impact calculations per flight are visualized. The third figure represents the grid path, which is used to convert the results from the CLIMaCCF model (second figure) to the climate impact per flight (last figure).

The flight path is also used to calculate the distance and time the flight covers for every grid cell in the grid path. This is done through the linear interpolation of consecutive waypoints along the grid path. The total sum of these distances is verified and equals the length of the entire flight path with an error margin of less than 0.1%.

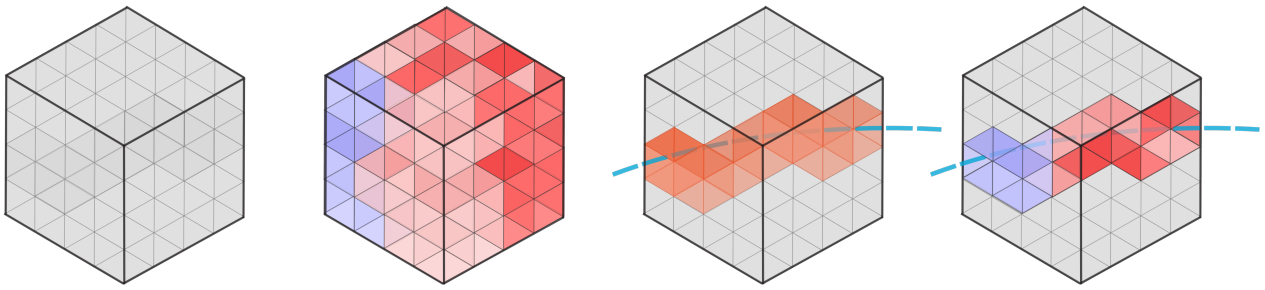

Figure 3: Visual representation of the climate impact calculations. The first figure represents the initial grid, which contains the ERA5 reanalysis data. The second figure depicts the climate impact calculations performed using the CLIMaCCF library. The third figure presents the grid path calculations as well as the flight path in blue, and the fourth figure presents the final climate impact calculation per flight (blue).

3.2.3 Climate Impact Formula

The total climate impact (F-ATR_{100}) can be calculated based on the grid path, the distance and time per grid cell, and the climate impact per grid cell. Next to this, the velocity, the flight time, and the amount of fuel burned (per second) corresponding with the traveled distance from the start location to the grid cells are retrieved from the mission profiles, for every grid cell in the grid path, per latitude (lat), longitude (lon), pressure level (p), and time (t). The formula for the climate impact calculation of one flight is presented by Equation 2.

$$\begin{aligned} \mathrm{aCCF}_{\mathrm{total}} &= \sum_{\text{Grid path}} aCCF(lat, lon, p, t) \times \dot{m}_{\mathrm{fuel}}(s(lat, lon, p)) \times \Delta t(lat, lon, p) \\ &+ \sum_{\text{rem. time}} (aCCF(lat, lon, p, t) \times \dot{m}_{\mathrm{fuel}}(t(lat, lon, p)) \times \Delta t(lat, lon, p) \end{aligned} \tag{2}$$

$aCCF_{\mathrm{total}}:$	$K\ (ATR_{100})$
$aCCF(lat, lon, p):$	K/kg_{fuel}
$\dot{m}_{\mathrm{fuel}}(lat, lon, p, t):$	kg_{fuel}/s
$s(lat, lon, p):$	km
$\Delta t(lat, lon, p, t), t(lat, lon, p, t):$	s

The second term in Equation 2 captures the small discrepancy in the difference in the distances from the mission profile and the shortest paths. The mission profiles are calculated for specified cruise ranges between airports, resulting in a mission profile that is too long, as it also includes the take-off, climb, descent, and landing. This is adjusted for by removing the overshoot from the middle of the profile, where the aircraft is in cruise. Because the mission profiles contain discrete data points, only a slight overestimation of the flight path length and minor jumps in altitude halfway through the mission are found. The latter is assumed not to influence the results, as the altitudes are fit to the nearest pressure levels in the grid path calculations. The small additional length of the mission profile, the remaining time (rem. time), is assumed to occur at the location of the arriving airport, and is thus captured by the second term in the formula.

3.3 Cost Calculations

The cost calculations in this research also consist of three parts: 1) the flight cost calculations, 2) the aircraft ownership cost calculations, and 3) the objective function formulation, which contains the flight and ownership costs, as well as the monetized costs for the climate impact of flights calculated in the previous section.

3.3.1 Flight Cost Calculations

The flight cost calculations for this research are based on the calculations described by Proesmans [66]. He uses direct operating costs for a dynamic programming model, and defines the costs per flight f as presented in Equation 3.

$$C_{\mathrm{f}} = C_{\mathrm{fuel/kg}} \times m_{\mathrm{fuel,kg}} + C_{\mathrm{hour}} \times t_{\mathrm{block}} + C_{\mathrm{landing}} \tag{3}$$

The block time t_{block} is defined as the flight time ($t_{\text{mission profile}}$) plus the ground maneuvering time (t_{gm}). Since the time covered for maneuvering is assumed to be incorporated in the mission profiles, only the length of the ground maneuvering time needs to be added, which is calculated by Equation 4, as described by Roskam [72]. MTOM stands for maximum takeoff mass, and OEM stands for operating empty mass. The turnaround times are not added explicitly; it is assumed to be covered by the time buffer created when the flight times and ground maneuvering times are rounded up to the nearest 20-minute interval during the fleet allocation.

$$t_{\mathrm{gm}} = 0.51 \times 10^{-6} \times \mathrm{MTOM} + 0.125 \tag{4}$$

The landing fee is defined as the landing costs per thousand pounds, as shown in Table 4. Additional input data for the cost calculations are presented in Table 4 and 5. The flight time, fuel mass, take-off thrust per engine ($T_{\mathrm{TO,eng}}$), and aircraft mass are retrieved from the mission profiles, as explained in section 3.1.

Table 4: Cost assumptions for the network, used for all airports/flights, from Reference [66]

Parameter	Value
Remain overnight parking cost (stay cost) [USD/hr]	48
Landing fee [USD/landing/thousand pounds]	7.8
Kerosene cost [USD/kg]	0.89*
SAF (HEFA 50-50 mixture) cost [USD/kg]	1.03**
Liquid hydrogen cost [USD/kg]	4.4***
Revenue per passenger-kilometer [USD/(pax km)]	0.148

* Based on 2.71 USD/US gallon (August 2021). Corrected for a 2% inflation to obtain an estimate for 2030.
** Forecast price in 2030, based on Reference [15] from 2020.
*** Forecast price in 2030, Based on Reference [65] from 2020.

Table 5: Input data for cost calculations for fleet allocation. Values retrieved from Reference [66]

Fuel	Range	COC			ATR		
		MTOM (10^3 kg)	**OEM** (10^3 kg)	**Cost/hr** (10^3 USD)	**MTOM** (10^3 kg)	**OEM** (10^3 kg)	**Cost/hr** (10^3 USD)
Kerosene	REG	35.2	20.6	2.10	33.2	19.0	2.01
	SMR	68.4	39.5	3.05	65.1	36.2	2.89
	LR	268	134	7.33	269	126	7.60
SAF	REG	35.2	20.6	2.10	33.2	19.0	2.01
	SMR	68.4	39.5	3.05	65.1	36.2	2.89
	LR	268	134	7.33	269	126	7.60
LH2	REG	33.7	22.3	2.16	32.8	21.2	2.11
	SMR	65.5	43.8	3.19	62.1	40.1	3.02
	LR	234	152	7.81	228	143	8.07

3.3.2 Aircraft Ownership Costs

The cost calculation presented by Jansen and Perez [40] estimates the weekly ownership costs of an aircraft k. The calculation is presented in Equation 5, where AFP stands for airframe purchase price and EPP stands for engine purchase price. This cost is included in the dynamic fleet allocation when a new aircraft is added to the fleet.

$$C_{\text{acq,week,k}} = 0.0835 \times \left(\text{AFP}_\text{k} + n_{\text{eng}} \times \text{EPP}_\text{k}\right)/52 \tag{5}$$

$$\text{AFP} = 0.0052 \cdot \text{OEM}^{0.927} \cdot 10^6 \tag{6}$$

$$\text{EPP} = 0.1604 \cdot T_{\text{TO,eng}}^{0.878} \cdot 10^6 \tag{7}$$

3.3.3 Cost Objective Function Formulation

The fleet allocation, discussed in the next section, is performed to maximize the profit objective. In order to include the climate impact in the objective function, the climate impact should be converted to a monetary value, which is done using a *climate impact tax*. This tax ($C_{\text{Climate impact, f}}$) is calculated for every flight (f): the climate impact (F-ATR$_{100}$, abbreviated to ATR) is multiplied by a conversion factor (χ), called the climate impact tax value. The formula is presented in Equation 8. The total cost of flight f ($C_{\text{(f + climate tax)}}$) is then the flight costs (C_f), as presented by Equation 3, plus the climate impact tax of flight f ($C_{\text{climate tax, f}}$).

$$C_{\text{climate tax, f}} = \text{ATR}_\text{f} \times \chi \tag{8}$$

$$C_{\text{(f + climate tax)}} = C_\text{f} + C_{\text{climate tax, f}} \tag{9}$$

The fleet allocation model, further elaborated on in the next section, calculates the weekly flights that aircraft k should fly to generate the highest profit. This list of flights in one week is referred to as the aircraft's path.

The total cost of this flight path for aircraft k is calculated using Equation 10. The overnight parking costs are included when aircraft are not parked at the hub overnight (see Table 4).

$$C_{\mathrm{k}} = \sum_{\mathrm{f} \in \text{ path}} (C_{(\mathrm{f} + \text{ climate tax}),k}) \quad + C_{\text{acq,week},k} + C_{\text{overnight parking,path},k} \tag{10}$$

The final objective function consists of the revenue calculation by multiplying the revenue per passenger-kilometer (R_{RPK}) with the flight distance (s_{f}) and the transported demand on flight f (D_{f}). The climate impact tax should only be imposed if the climate impact is positive (warming). Even though contrail avoidance is generally considered desirable, purposefully increasing cooling contrail coverage comes with a higher risk for harmful outcomes [59]. Therefore, the incentive to produce contrails, even though they are cooling, is undesirable, and an additional constraint is added. In Figure 30, an exemplary situation is depicted where the SMR COC-optimized hydrogen flight from Hartsfield-Jackson Atlanta International Airport (ATL) to Buffalo Niagara International Airport (BUF) produces significant (cooling) day-contrails, resulting in an overall negative climate impact. The resulting objective function is formulated as follows:

$$\max \text{ Profit} = \sum_{k \in \text{fleet}} \sum_{f \in \text{path}_k} \Big[\underbrace{(R_{\mathrm{RPK}} \times s_{\mathrm{f}} \times D_{\mathrm{f}})}_{\text{revenue}} - \underbrace{\left(C_{\mathrm{f},k} + \mathrm{ATR}_{\mathrm{f},k} \times \chi + C_{\text{acq,week},k} + C_{\text{overnight parking},k}\right)}_{\text{costs}} \Big] \tag{11}$$

$$\text{with } \mathrm{ATR}_{f,k} > 0, \text{ else } 0.$$

3.4 Fleet Allocation

Early work from Hane et al. [32] describes a basic fleet assignment model using a mixed-integer linear programming method (MILP). The model uses a given flight schedule and fleet, and therefore does not include the aircraft routing problem. Currently, more complex models are being examined and implemented in the aviation industry. Airlines face many logistical problems next to their fleet assignment: aircraft routing, crew pairing, crew rostering, and more [9, 47, 78]. Many of these problems are connected, and solving them simultaneously is unrealistic as the model becomes too complex and inefficient. Instead, a combination of a couple of problems can be solved to increase the optimality, but keep the model within a reasonable scope. A model that combines the aircraft routing and the fleet assignment is usually referred to as the fleet allocation. Based on the chosen network and demand, the goal is to research what routes should be performed with what aircraft type and fuel type (referring to Table 6), to reach the most optimal objective.

The fleet allocation is generally performed using either a mixed-integer linear programming (MILP) method or a dynamic programming method (e.g. [62, 73, 74]). The latter allows for non-linear calculations, which is the main reason this method is chosen. It uses a divide and conquer concept: the idea is to break down a large problem into incremental steps, which are recursively solved using a greedy policy.

The fleet allocation model is largely based on the method described in Reference [66]. It uses the Bellman-Ford algorithm and the solving method from Noorafza et al. [62], and (Álvarez [5] as cited in [66]). The approach is depicted in Figure 4. The main difference between the existing fleet allocation models and the fleet allocation model that is developed in this research, is the incorporation of the climate impact tax. The fleet allocation consists of two parts: 1) the demand calculation, and 2) the dynamic programming. These two parts are discussed below, in section 3.4.1 and section 3.4.2.

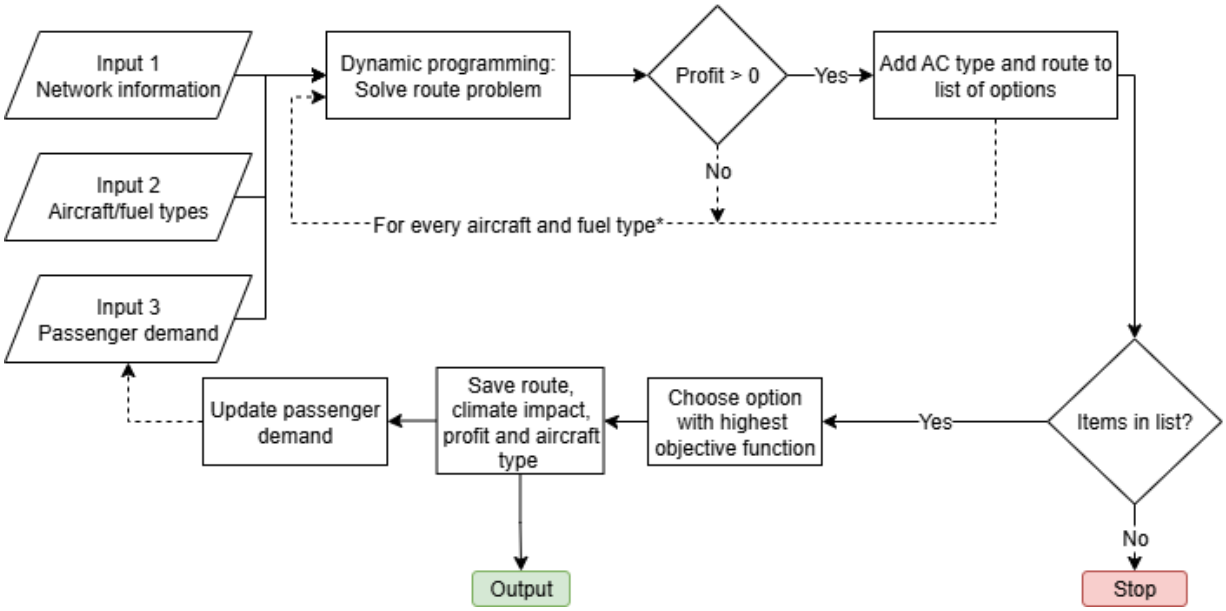

* For kerosene aircraft, for each departure time, flight leg, and climate impact tax value, SAF allocation is incorporated by checking whether a 50% SAF blend is *cheaper* than kerosene fuel. If this is true, the flight cost is updated to the cost using SAF.

Figure 4: Block diagram of the dynamic programming model used to solve the fleet allocation problem. Diagram adapted from [74], and ([5] as cited in [66])

3.4.1 Demand Calculation

To perform the fleet allocation, the demand data first needs to be processed. The initial weekly demand is presented in Table 9, obtained from Reference [66]. The data was originally presented by Jansen and Perez [40], and obtained from the Bureau of Transportation Studies for the year 2011. The total weekly demand is divided by the number of flights throughout the week and subsequently normally distributed around the scheduled departure times for the first week of August for 2025[4]. A 20-minute interval is introduced, and for the normal distribution, a 95% confidence interval of $\pm$ 1.5 hours is assumed. The weekly demand for the flight leg Atlanta (ATL) $\rightarrow$ Rome (FCO) is plotted in Figure 5. The time difference is taken into consideration, and all departure times are converted to Atlanta local time (UTC-4). More elaboration on the demand calculation is provided in Appendix B.

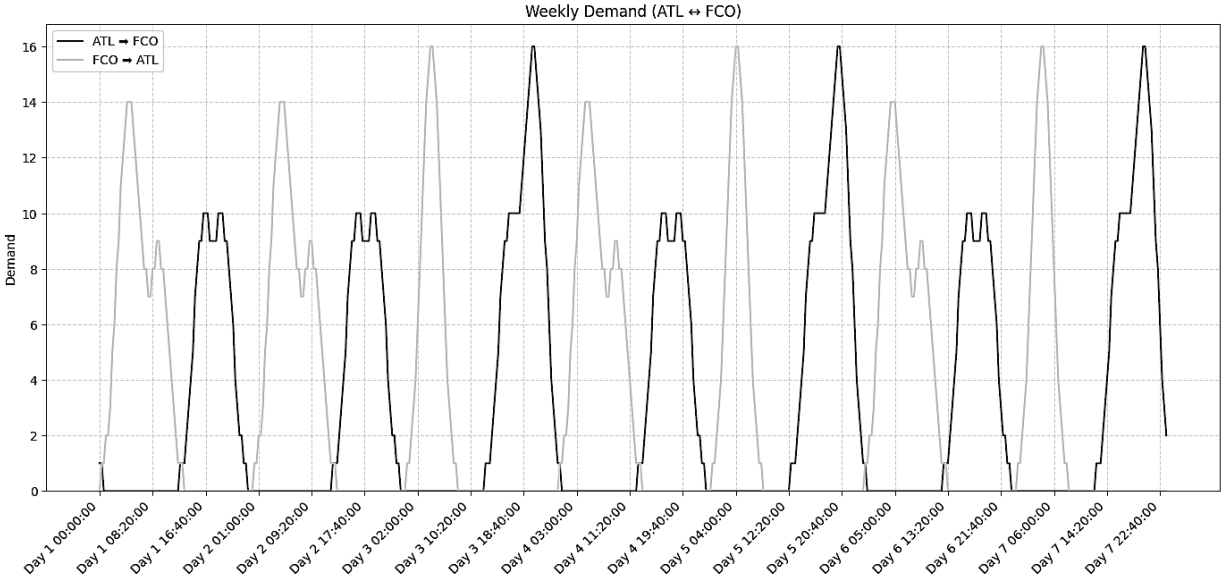

Figure 5: Results from demand calculation for the symmetric weekly demand between Atlanta (ATL) and Rome (FCO). Atlanta local time is used: UTC-4.

[4] `https://www.delta.com/flightsearch/book-a-flight` accessed March 18th, 2025

3.4.2 Dynamic Programming

The fleet allocation is conducted as depicted in Figure 4, using dynamic programming. The dynamic programming starts with calculating the optimal flight paths for aircraft. When the path calculation is performed for all aircraft types, the aircraft type with the path resulting in the highest total profit, if larger than zero, is added to the fleet. The corresponding transported demand is subtracted from the demand, and the process continues until no path can be found that leads to a positive profit value.

The time differences between the airports are accounted for by converting all the times to Atlanta local time (UTC-4). The climate impacts of the flights are calculated for UTC and therefore also converted to UTC-4.

The path calculation is performed on a profit matrix. The profit matrix consists of the airports and the time intervals of the dataset. For every *node* (airport, time), a profit value is found. The process is depicted in Figure 6, and performed as follows:

(a) The profit is calculated for each flight.

Example: Flight departing from airport 1 at 02:00 generates a profit value of 20.

(b) The nodes that violate constraints are removed (see section 3.5.6).

Example: At the start and end of the time duration (in figure 3 hours, but in dataset 1 week), the aircraft should be at the hub. This eliminates certain flights, which are removed. These nodes are depicted in red; see airport 1 at 2:20.

(c) Through backward iteration, starting on the right, the flight costs (and overnight parking costs) are used to calculate the maximum profit value for every node. The resulting value per node is the maximum value an aircraft could have obtained in that particular node (from right to left). For every hub node, from right to left, the flight path responsible for the profit value at the hub node (hub or other node) is documented. These are presented in the top row and is referred to as the guide (see Figure 6c and 6d).

Example: Airport 3 has at 2:20 a profit value of 8, which is the maximum value from all possible flight paths from the hub to that node (03:00 to 2:20). In this case, there are 2 possible paths: 1) flight to hub at 02:20, and remaining at hub between 02:40 and 03:00, or 2) staying at hub until 2:40 (thus paying parking costs) and flying to the hub at 2:40.

(d) The guide is then used to find the optimal path. Starting at the hub on the left side of the matrix, the airport in the guide shows which path should be taken. The total profit of the path is the value of the profit matrix at time step zero at the hub.

Example: On the left, the guide shows value 3, referring to airport 3, thus this flight is selected. At airport 3, the decision is to stay at airport 3, or to fly back to the hub. If the next node at airport 3 equals the profit minus parking costs, then the aircraft stays at airport 3, otherwise, it flies back to the hub. This process continues until the end of the matrix. The resulting final path can then be found, and the total profit of the path is 100.

As depicted in Figure 6, the flight durations are incorporated in the model, shown by the gray lines, and these include the ground maneuvering and turnaround times.

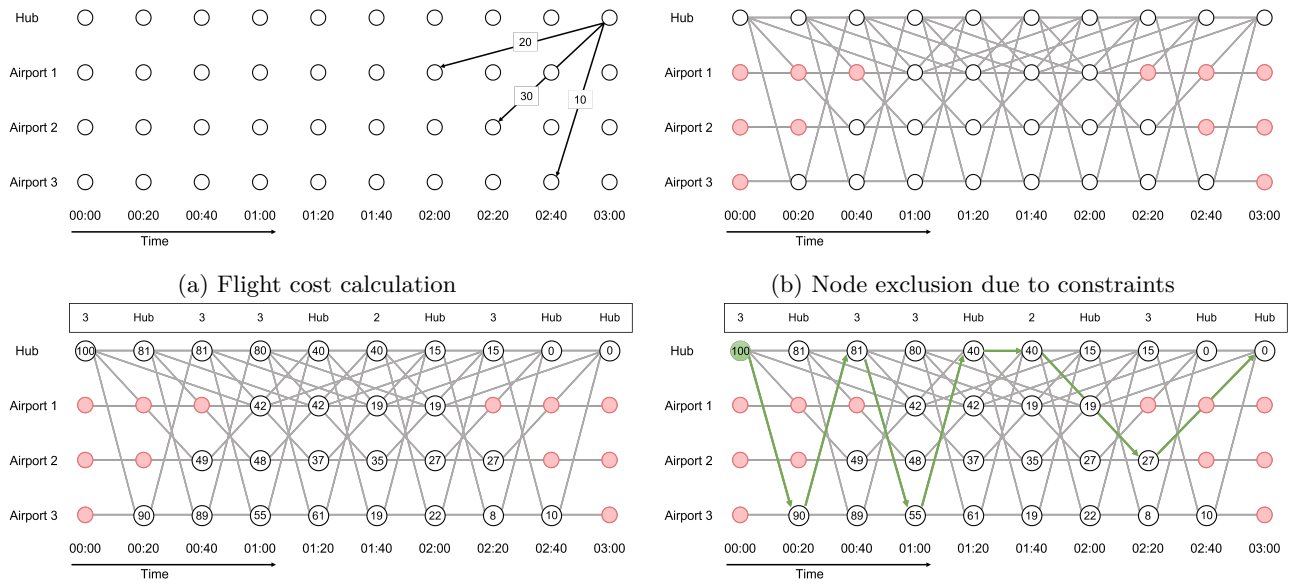

(a) Flight cost calculation

(b) Node exclusion due to constraints

(c) Profit matrix and guide calculation

(d) Flight path generation

Figure 6: Representation of the profit matrix and path calculation for aircraft. Matrix is simplified, and images are based on Reference [74].

3.5 Decisions and Assumptions

Various decisions and assumptions are made for this research. The most important ones are discussed in chronological order in this section:

1. the Delta-network used by Proesmans [66]
2. the use of twelve different aircraft, from Proesmans and Vos [67], including the use of SAF
3. the conversion factors for the CLIMaCCF model for the climate impact of contrails from hydrogen and SAF
4. the exclusion of H_2O and NO_x at lower altitudes
5. the scope, which contains the first week of August for five consecutive years (2020-2024)
6. the constraints for the fleet allocation

3.5.1 Network Selection

The passenger demand network used by Proesmans [66] is selected for this research. This network provides a weekly symmetric demand for a hub-and-spoke network with 1 hub, representing Delta Airlines in Atlanta. This network is chosen because of five reasons: it contains short- to long-haul flights, making it suitable for the three aircraft types (REG, SMR, LR); it is positioned around the North Atlantic, which is necessary for the CLIMaCCF tool; it is a hub-and-spoke network, which means the fleet allocation is flexible as aircraft can be assigned to different flight legs throughout the week; the passenger demand assumes no transfer passengers; and it contains only 1 hub. The last two limit the complexity of the fleet allocation model, which is necessary for the scope of this research.

A few adjustments are made to the network. Dietmüller et al. [18] highlight that the CLIMaCCF tool is not appropriate for tropical regions due to the aCCF algorithms being designed around the North Atlantic corridor. Therefore, the five southernmost flights from Atlanta (ATL) to Latin America are removed. Additionally, the Manchester-Boston regional airport (MHT) is removed from the dataset, because Delta Airlines has discontinued its flights from ATL to this airport since the COVID-19 pandemic[5]. The remaining network and demand are presented in Table 9.

[5] `https://www.flymanchester.com/flights-airlines/airlines-serving-mht/`, accessed March 24th, 2025

3.5.2 Fleet Selection

As discussed before, Proesmans and Vos [67] designed kerosene, SAF, and LH_2-powered aircraft for cost-optimal (COC) and climate-optimal (ATR) objectives, as well as a multi-objective (MO) combining cost, climate, and fuel consumption. These aircraft form the basis of this research. The MO aircraft are ignored in this research because the MO blurs the distinction between COC-optimized and ATR-optimized aircraft.

As a reminder, there is an important distinction made between aircraft specifically designed for SAF (SAF aircraft) and kerosene aircraft employing SAF fuel. SAF aircraft are not included in this research; however, it is assumed that SAF (fuel) can be allocated to kerosene aircraft (ATR and/or COC-optimized), because of the following three arguments: the SAF aircraft are very similar to kerosene aircraft; current (kerosene) aircraft need hardly any adjustments to use drop-in SAF [4]; and it best represents the current situation: SAF is blended with kerosene and allocated to conventional aircraft. Therefore, the possibility of allocating SAF is included, but aircraft specifically optimized for the use of drop-in SAF are not. The SAF allocation is included in the fleet allocation by comparing the total flight cost (including the climate impact tax) for SAF and kerosene. If SAF results in a lower flight cost, SAF is allocated to that flight. A parallel file keeps track of these cases and is later used to determine the fuel type for each flight leg. Table 6 shows the final selection of aircraft types used in this research: 12 aircraft types, all designed by Proesmans and Vos [67].

Table 6: The aircraft types selected for this research, from Reference [67].

Aircraft type (Fuel type)	**Kerosene Aircraft** (Kerosene, SAF)			**SAF Aircraft** (SAF)			**LH_2 Aircraft** (LH_2)		
Design objective	**ATR**	**COC**	**MO**	**ATR**	**COC**	**MO**	**ATR**	**COC**	**MO**
REG	✓	✓	-	-	-	-	✓	✓	-
SMR	✓	✓	-	-	-	-	✓	✓	-
LR	✓	✓	-	-	-	-	✓	✓	-

LR LH_2 aircraft are included in the fleet as shown in the table, even though the use of hydrogen aircraft is expected to occur for short- to medium-range aircraft first [43], because this forecast is expected to be reflected in the results of this research. As can be seen in results from Proesmans [66] in Figure 22, the relative network profit for all three LR LH_2 aircraft is very low compared to REG and SMR LH_2 aircraft and kerosene aircraft. It is therefore expected that LR LH_2 aircraft are used only in the fleet allocation when the climate objective dominates the cost objective.

3.5.3 Conversion Factors for Contrails

The CLIMaCCF model is developed for kerosene flights, and therefore needs to be modified to include SAF and hydrogen fuel. For contrails, conversion factors for the different fuel types are necessary. In section 2.1, the differences in contrail properties from kerosene, LH_2, and SAF aircraft are presented.

Burkhardt, Bock, and Bier [13] discuss the influence of the number of ice crystals on the contrail cirrus net radiative forcing. They argue that the net radiative forcing of contrail cirrus decreases by 50% when the ice particle number decreases by 80%. This is shown in Figure 7. Bier et al. [10] show that ice crystal numbers in contrails from LH_2 combustion decrease by around 80-90% compared to kerosene combustion. These two findings support the assumption that contrail cirrus from hydrogen aircraft leads to an 80% reduction in ice crystal number, and consequently to 50% less net radiative forcing, compared to kerosene aircraft. Therefore, a conversion factor of 0.5 is introduced. The aCCFs for contrails are multiplied by these conversion factors to account for the change in climate impact due to changes in contrail properties and subsequent changes in radiative forcing.

Moreover, Burkhardt, Bock, and Bier [13] argue that by reducing the number of ice crystals by 50% through the use of a 50% SAF blending ratio, a reduction of 21% in the net radiative forcing from contrail cirrus can be achieved. Therefore, a conversion factor of 0.79 is used for the climate impact of contrails from aircraft employing 50% drop-in SAF. Since different blending ratios could affect the conversion factor, it is chosen to simplify the SAF allocation by allowing only a 50% blending ratio for SAF. Moreover, the same SAF type used by Proesmans [66], a synthetic SAF called HEFA (hydroprocessed esters and fatty acids), is assumed in this research.

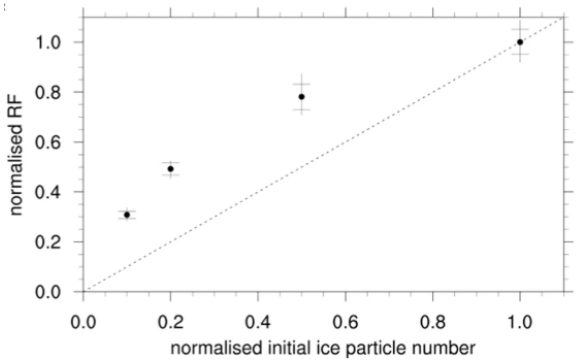

Figure 7: The global net radiative forcing from contrail cirrus, normalized to present day soot numbers, versus the initial ice particle number concentration of contrails, from Reference [13]

3.5.4 CLIMaCCF at Lower Altitudes

An intermediate verification step is performed to examine whether extending the CLIMaCCF model to include NO_x emissions from cruise range down to 0 ft altitude could be justified. The verification concludes that it is not possible to extend the model, since the results are not in line with existing literature. However, because the model starts at an altitude of 20000 ft, it is chosen to linearly extend the model only to 18000 ft, such that the lowest cruise altitudes from climate-optimized aircraft would still be included in the results. The impact of NO_x and H_2O is found to be much lower at lower altitudes ([22, 48], [85], respectively), and therefore it is assumed that the climate impact of NO_x and H_2O below 18000 ft is insignificant to the overall climate impact of flights. Thus, for these lower altitudes, the climate impact of these emissions is set to zero.

Moreover, the climate impacts in K/kg(NO_x) from O_3 are found to be in contrast to the available literature for lower cruise altitudes (pressures between 250 hPa and 550 hPa). Köhler et al. [46] present the radiative forcing of NO_x as a function of altitude, and demonstrate that it decreases with lower altitudes, which is in line with References [22, 27, 30, 48]. It is therefore that the scaling factors, presented in Table 7, are introduced. Similar to the scaling factors for contrails, the scaling factors for O_3 are multiplied with the aCCF for O_3, depending on the pressure level. Based on Figure 40, the linear decrease in radiative forcing and the relative size of the forcing factors are used to derive these scaling factors. The trend (decreasing magnitude for decreasing altitude) corresponds to Reference [27], but the sizes of the scaling factors need to be verified using a high-fidelity climate model. The resulting climate impact from O_3 and NO_x as a function of altitude are presented in Figure 8. The climate impact is averaged over the full geographical scale of the data (see Table 10). The scaling factors are only applied to O_3, and not to CH_4, as the O_3 emissions dominate the effect from NO_x on the climate. The original climate impacts from NO_x at different altitudes without the scaling factors are presented in Figure 32.

Table 7: Scaling factors for O_3 at different pressure levels

Pressure (hPa)	250	300	350	400	450	500	550
Scaling factor	0.94	0.81	0.59	0.41	0.28	0.20	0.15

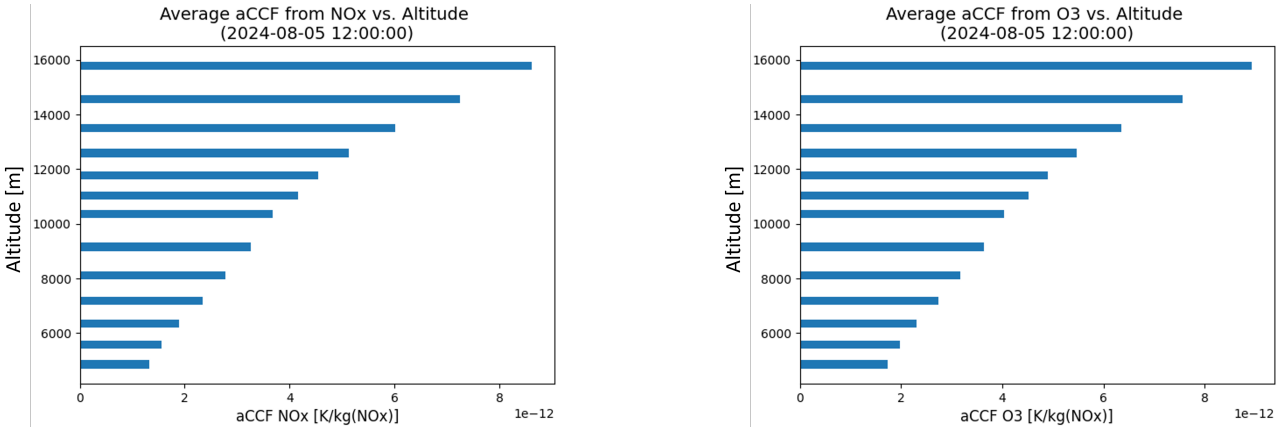

Figure 8: Results from the climate impact with the applied scaling factors, from NO_x (left) and O_3 (right) for different altitudes (F-ATR_{100}) in [K/kg(NO_x)]. The values represent the average climate impact for the full geographical scale (64°N/13°E/25°S/-123°W) for different altitudes. Results for August 5th, 2024, at 12:00 UTC.

3.5.5 Week Selection

Grewe et al. [29] study a climate-optimized routing strategy for trans-Atlantic flights, during summer and winter days, and they find that for summer days, the variability and the climate-reduction potential are the highest. It is therefore that the summer season is chosen.

Additionally, Irvine et al. [39] found that the strength of the North Atlantic jet stream is generally weaker for summer compared to winter. The influence of the jet stream on fuel usage and daily costs for North-Atlantic flights has been researched by Grewe et al. [29], who investigated the feasibility of climate-optimized routing for trans-Atlantic flights. They demonstrated that, if possible, the use of the jet-stream tailwind is preferred for all eastbound flights, since leaving the jet stream results in large penalties on fuel burn, emissions, and flight duration. As the jet stream is found to be generally weaker during summer, and because the network is a hub-and-spoke network and aircraft are assumed to be flying there-and-back, the presence of the jet stream is neglected during this research.

As the summer season lasts from June to September, the first week of August is selected because it falls in the middle of the season. The same week is used for five consecutive years to gather a representative dataset for the summer weather conditions (2020-2024). The network demand (1-week duration) remains the same across all years.

3.5.6 Constraints

Besides the decisions described above, assumptions are made that lead to certain constraints. These constraints influence the fleet allocation, but also the dynamic programming, as particular nodes and flights are eliminated. The curfew hours, for example, influence the nodes, which are described in section 3.4.2. The constraints are as follows:

- The REG, SMR, and LR aircraft can fly to the same airports as specified by Proesmans [66].
- Departure and arrival times should remain within 6:00 and 23:00. This is a general assumption, based on the classification of Night Flights by the European Union, which fall between 23:00 and 6:00. It is assumed that even though some airports do not to impose a curfew on flights, airlines still try to avoid night-time flights for noise abatement and also for cost reduction, as personnel costs are higher during night hours.
- The time difference between the airport locations is considered, as well as the ERA5 reanalysis data (UTC). All times are converted to Atlanta local time (UTC-4).
- Aircraft must start and end the week at the hub airport.
- The attraction band for passengers is between ±2 hours from their desired departure time.
- Overnight parking costs are applied when aircraft are parked between 23:00 and 6:00 at airports other than the hub airport.

3.6 Computational Set-Up

All the computations are performed using the Linux-server from the Operations and Environment department of the Aerospace Engineering Faculty at the TU Delft (128 cores/256 threads, and 503 GiB of RAM). The code is developed in Python 3.10, and the CLIMaCCF library is used.

The downloaded ERA5 reanalysis data contains large files, as is described in Table 10. The conversion from these input files to the calculated climate impact per grid cell (section 3.2.1) takes a couple of minutes, resulting in 30 files of around 7.9 GB each. The calculations are run separately based on fuel type (kerosene, SAF, hydrogen) and year (2020-2024), resulting in 15 runs, and for each run, the distinction is made between the COC and ATR-optimized aircraft, therefore creating 30 output files.

The next steps, the grid path calculations and the climate impact calculations per flight (section 3.2.2 and section 3.2.3), are combined into one code. This code uses the output files from the previous step. The code performs the calculations for both the COC and ATR-optimized aircraft as well as the aircraft categories (REG/SMR/LR). Therefore, the code runs 15 times, for each fuel type and year, taking around 8 hours per run. The results are saved to 15 CSV files, which are in turn used for the fleet allocation calculations.

The fleet allocation uses the climate impact calculations, as well as the cost calculations. The computational time of the cost calculations is short, taking less than a minute. The fleet allocation, however, takes a little longer. This code runs for each climate impact tax value. Starting at low climate impact tax values, the running time is between 30 and 40 minutes; however, for higher taxes, fewer aircraft are allocated to the fleet, resulting in a shorter runtime.

4 Results

The results of this thesis are discussed below. The chapter starts with a short explanation of the results from the climate impact calculations (section 4.1). Thereafter, in section 4.2, the results from the cost calculations are presented. The climate impact calculations and the cost calculations are performed independently from the fleet allocation model, and the results from these calculations are used as input for the fleet allocation model. The final results from the fleet allocation are presented in section 4.3 and are used to address the research questions posed in section 1.

4.1 Results: Climate Impact of Flights

The climate impact of flights are calculated for the different aircraft types, fuel types, and design objectives (see Table 6). This is done for each flight leg (hub↔spoke), for each year, and for each possible departure hour of the week. The climate impact results are presented below, and thereafter, in section 4.1.1, the verification and validation of the results are explained.

In Figure 9, the results are shown for COC and ATR-optimized aircraft. The climate impacts of flights are compared based on their aircraft type (REG, SMR, LR), fuel type (kerosene, SAF, LH_2), and design objective (COC, ATR). The destinations are grouped by flight distance from the hub to the spoke airports, resulting in 7 groups, of which the average values are taken. The climate impacts from different emissions are visualized, per aircraft type, fuel type, and design objective. The results show that the LR-kerosene and -SAF aircraft have the largest climate impacts. As expected, the total climate impact for ATR-optimized aircraft is smaller compared to COC-optimized aircraft.

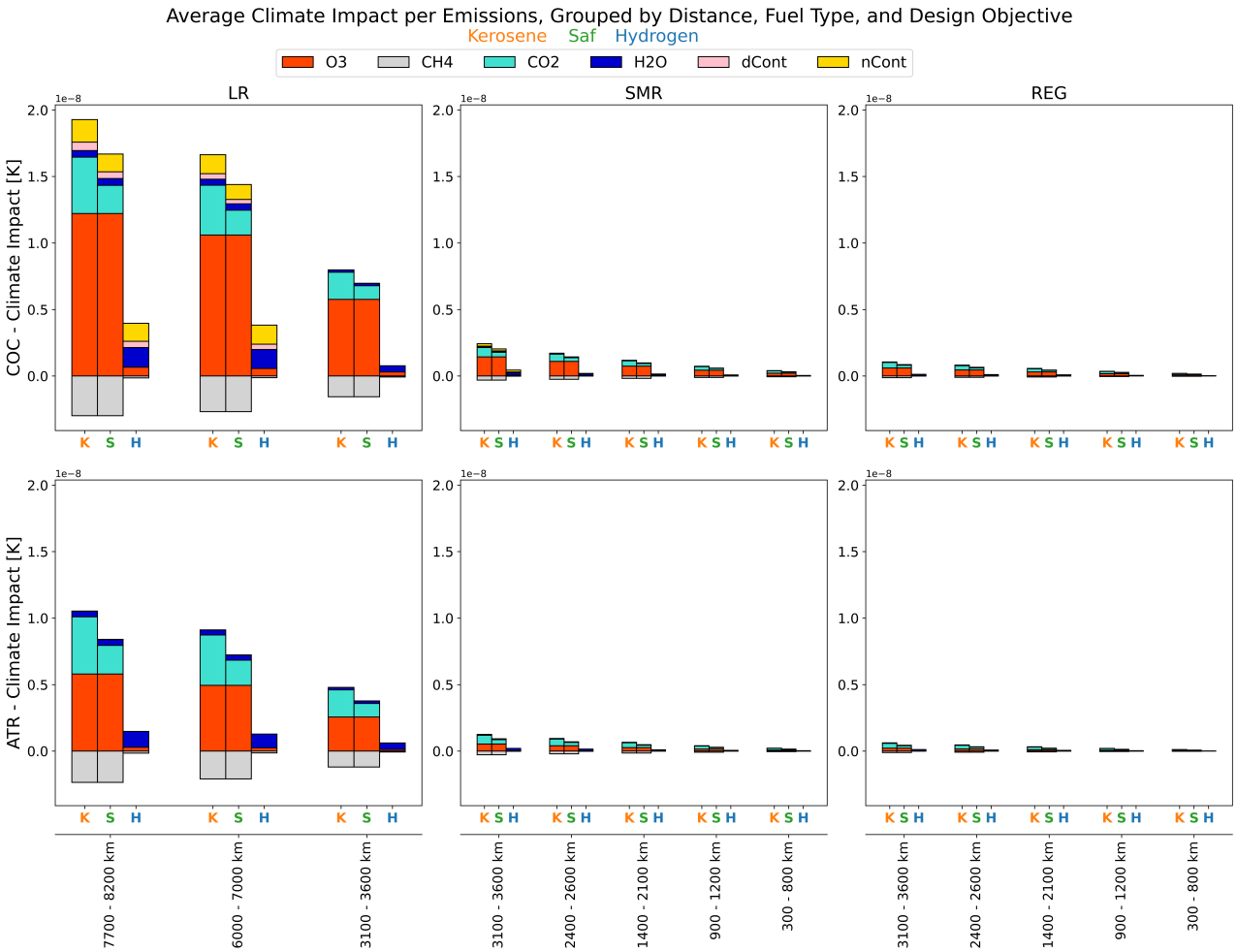

Figure 9: Climate impact per emission, fuel type, distance group, and design objective (COC/ATR). The top three plots are for COC-optimized aircraft, and the bottom three are for ATR-optimized aircraft. The climate impact contributions from the different emissions are stacked. The values in this plot are averaged over the years, departure times, and flight legs.

In Figure 10, the variability in climate impact is plotted for one day. Note: it does not present the uncertainty; it presents the changes in the climate impact of flights during 24 hours. The large variability is mostly caused by the changes in climate impact from contrail formation. The difference between the contrail formation for the LR flight and the SMR flight to Seattle Airport (SEA) is deliberately shown: For the SMR flight, a significant variation is observed for the total climate impact, whereas this is not the case for the LR flight. This is explained by the difference in flight altitude between the two aircraft types, resulting in the LR aircraft avoiding the persistent contrail formation areas (PCFAs). The PCFAs are mapped for 250 hPa and 300 hPa, presented in Figure 31.

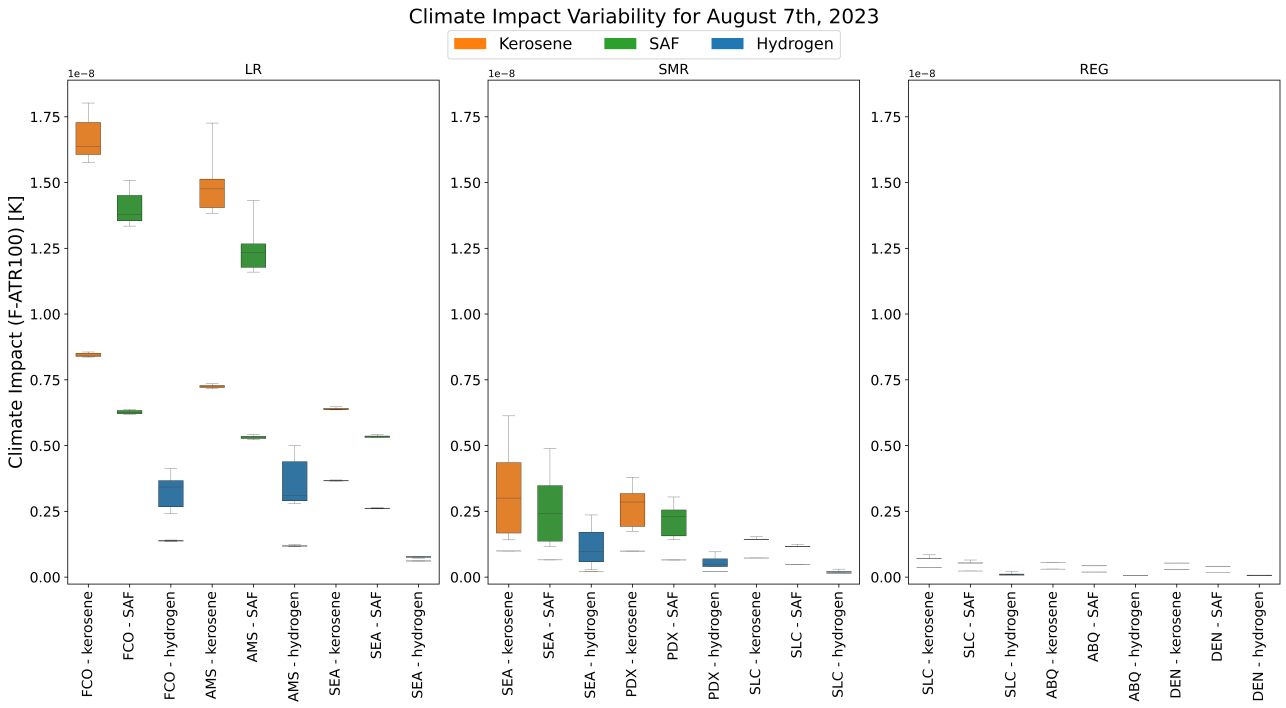

Figure 10: The variability in the climate impact of flights from ATL to airports is plotted for one day. Each subplot represents a different aircraft type (LR, SMR, REG), and the colors refer to the fuel type. Every category on the x-axis corresponds to two box plots; the upper box corresponds to the COC-optimized aircraft, and the lower box to the ATR-optimized aircraft. The values are plotted for Monday, August 7th, 2023.

4.1.1 Verification and Validation of the Climate Impact of Flights

The verification and validation are explained in this section. The verification compares the relative size of the emissions with existing literature to assess the individual emission calculations. The validation compares the magnitude of the calculated climate impact, in terms of K/kg(fuel), to evaluate whether results align with available literature.

The climate impact calculations of the individual flights in this thesis are compared with the results from the climate impact calculation of 85 European flights by Yin et al. [93]. They examine the difference in climate impact between flights with optimized trajectories that minimize costs and those that minimize the climate impact of NO_x. The authors used a subset of 85 European Flights flown with an A320 aircraft and a CFM56 engine model. The trajectories are simulated using MESSy submodels AirTraf 2.0 coupled with the ACCF 1.0 ([92, 93]). In Figure 11, the results from Yin et al. [93] are compared with the results from the climate impact calculations performed in this research. Both results are normalized because of the difference in magnitude, and these values allow for the comparison of the relative size of the climate impact from different emissions. The top figure presents the relative climate impacts of H_2O, O_3, CH_4, CO_2, and contrails. From the figure, it is apparent that the climate impact from CO_2 is bigger compared to the results from Yin et al. [93]. This is expected, because Yin et al. [93] considers en-route emissions during cruise, while in this research the CO_2 emissions also include the take-off, climb, descent, and landing, resulting in a relatively higher impact from CO_2 emissions. Additionally, it has been demonstrated that there is high variability in climate impact (see Figure 10) due to changes in contrail formation. Therefore, the larger contribution from CO_2 and contrails to the total climate impact does not raise concern. By removing CO_2 and contrails from the plot, the relative size between H_2O, O_3, and CH_4 can more clearly be compared (see Figure 11). Based on the bottom image, it can be concluded that the relative contribution of these emissions is in line with results from Yin et al. [93].

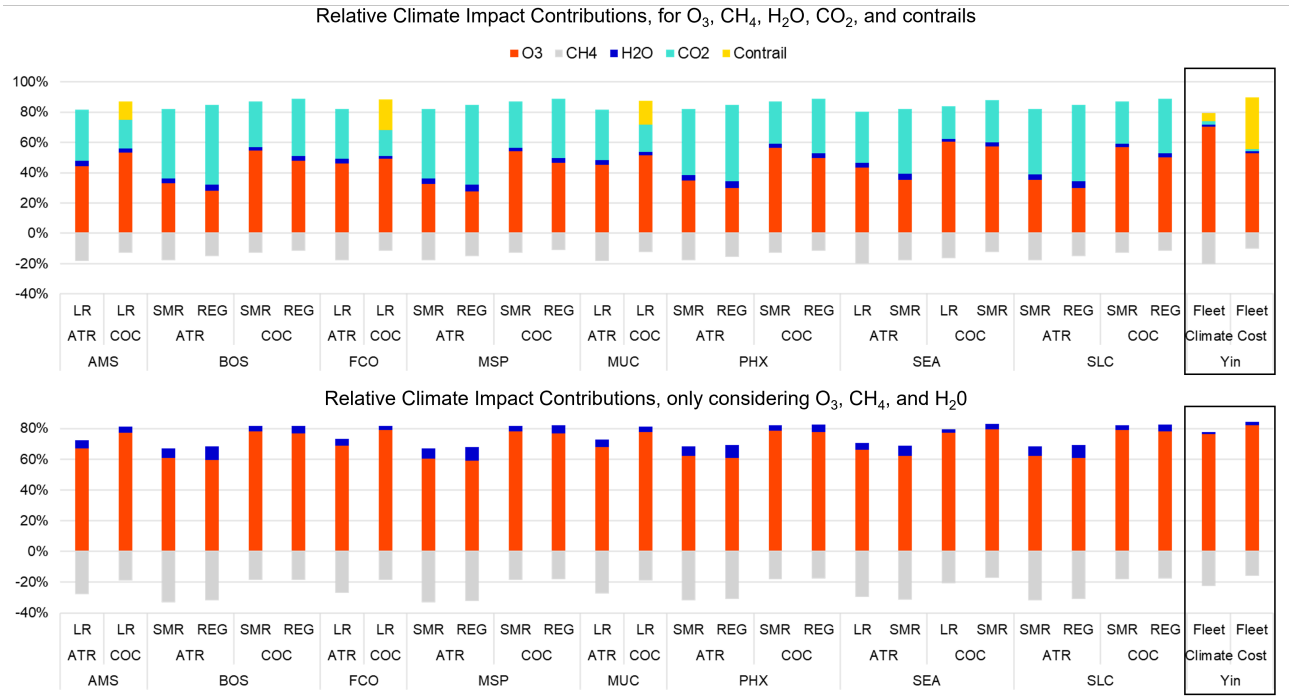

Figure 11: Relative contribution to the total climate impact, per emissions. Data from Reference [93] is used in the figure, on the right depicted by the box. A randomly selected set of flights from August 8th, 2024, at 22:00 UTC is presented, and the values are all for F-ATR$_{20}$.

The results are validated for the LR COC-optimized kerosene aircraft in Figure 12, by comparing the results with Figure B2 in Dietmüller et al. [18]. The order of magnitude of the climate impact is in line with the results found in this paper (10^{-13} K/k(fuel)). Moreover, as can be seen in the figure, the model captures the expected spatial patterns: the climate-sensitive regions are calculated with the CLIMaCCF model shown by the darker-red regions in Figure 12.

Overall, the verification confirms the relative contributions from different emissions, and the validation shows that the magnitude and spatial patterns align with existing literature. Nevertheless, this research conducts off-design use of the CLIMaCCF model by, for example, using different fuel types and aircraft types, which limits the validation. Therefore, future validation of the results using a high-fidelity climate impact model (e.g. EMAC) is recommended.

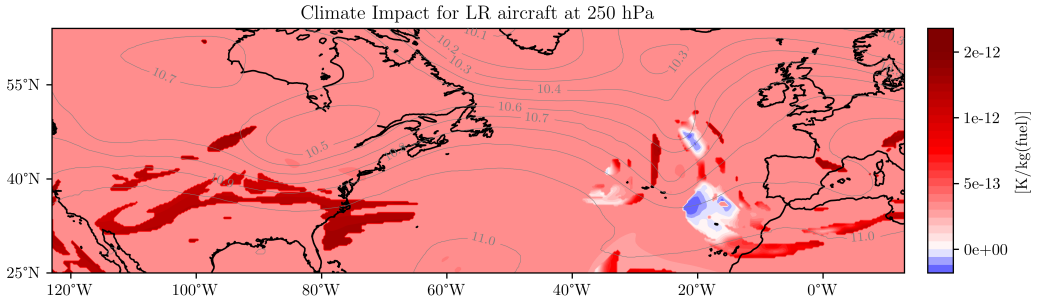

Figure 12: The total climate impact (merged aCCF) at 250 hPa for LR COC-optimized kerosene aircraft in [K/kg(fuel)], on August 5th 2024 at 12:00 UTC.

4.2 Results: Cost Calculations

For the cost calculations, the flight costs and the aircraft ownership costs are determined. Results for the flight cost calculations are presented in Figure 26, 27, and 28. Flight costs for kerosene aircraft are consistently lower compared to SAF and hydrogen flights, with the latter resulting in the highest flight costs. For ownership costs, commercial aircraft are typically designed for a 30-plus-year operational lifetime[6]. The calculated acquisition costs per week are presented in Table 8.

[6] `https://www.airbus.com/en/products-services/commercial-aircraft/the-life-cycle-of-an-aircraft/operating-life`, accessed May 23rd, 2025.

Table 8: Aircraft acquisition costs per week

Fuel	Range	Acquisition Cost/Week COC [10^3 USD]	ATR [10^3 USD]
Kerosene/ SAF	REG	118	107
	SMR	212	193
	LR	654	612
LH_2	REG	122	116
	SMR	222	204
	LR	681	644

The results for the climate impact tax are used in the dynamic programming model for the fleet allocation. The average monetary value considered per aircraft type and fuel type is presented in Figure 29 for different levels of climate impact taxes. The values presented in the plot are the averages over all years, departure hours, and destinations.

4.3 Results: Fleet Allocation

This section starts with the verification of the fleet allocation in section 4.3.1. Thereafter, the results of the fleet allocation are presented. They are split into two parts, corresponding to the two sub-questions posed in section 1: the effect of the climate impact tax on the network, and the trade-off between profit and climate impact, in section 4.3.2 and section 4.3.3, respectively.

4.3.1 Verification of the Fleet Allocation

The verification of the fleet allocation model is performed for the model with zero climate impact tax (χ=0 USD/K), by plotting the cumulative profit against the selected aircraft and the transported demand per aircraft, shown in Figure 13. The shape of the curve in the left image is similar to Figure 7.5 in Reference [66]; however, as can be seen in the figure, the SMR COC-optimized kerosene aircraft are selected first, which is contrary to the results from Proesmans [66] where the LR aircraft are selected first. This difference could be explained by the difference in the attraction bands (4 hours vs. 6 hours) and curfew hours (23:00-6:00 vs. 23:00-5:00). As for the total transported demand, over 70% is served, which is reasonable considering the model does not include changes in the ticket prices or flexible curfew hours. Realistically, this percentage might be too low for airlines, as they aim to maximize their profit; however, they also often consider their market share [90]. The latter is not included in the fleet allocation in this paper. Moreover, the fleet allocation has an optimality gap, which is further elaborated upon in section 5.3. The shapes of the curves are according to expectation, as the most profitable aircraft are selected first.

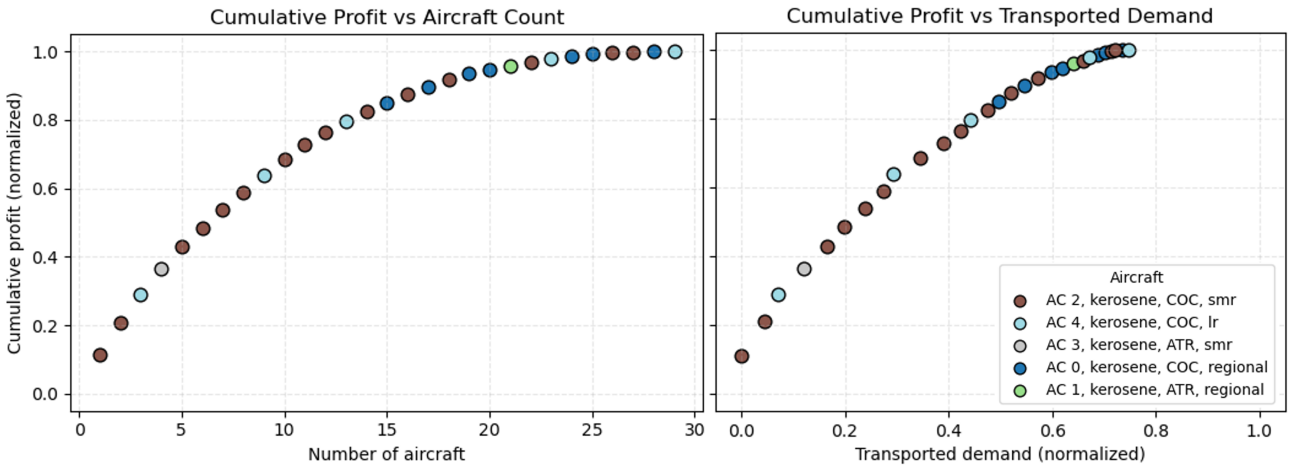

Figure 13: Results of the fleet allocation without climate impact tax. The figures demonstrate which aircraft are selected and how the cumulative profit and transported demand increase for each selected aircraft type.

4.3.2 Fleet Allocation Network

This section aims to answer the first sub-question of this research: *To what extent do the fuel and aircraft type affect the fleet composition, the satisfied demand, the flight frequencies, and the flight routes when reducing the overall climate impact?* This question covers four aspects, which are discussed in chronological order: fleet composition, satisfied demand, flight frequencies, and flight routes.

Fleet Composition: For the different climate impact tax values, the results of the fleet allocation in terms of aircraft type and fuel usage are presented in Figure 14. The figure presents the average aircraft types and fuel types for the 5 years. For the SAF allocation, it is important to note that the bars are turned green if SAF is used for **any** of the flights performed by the aircraft during the entire week.

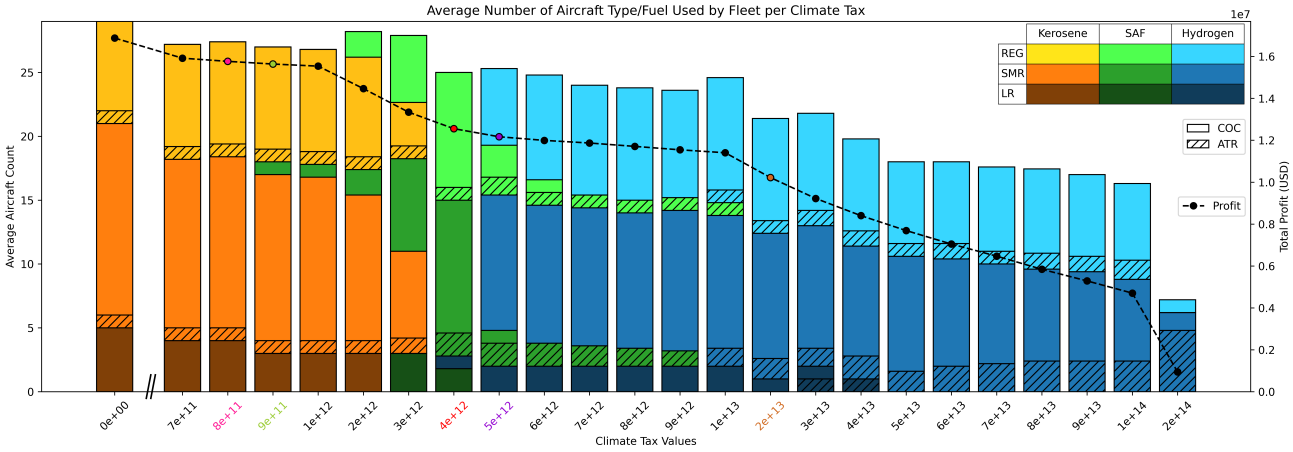

Figure 14: Stacked bar plot for the average number of aircraft used by the fleet, for different levels of climate impact tax. The bars are colored based on aircraft type and fuel type. All values are averaged over the 5 years. No change in aircraft count or aircraft types is measured until 1e+11 USD/K, after which it remains constant until 7e+11 USD/K.

From the figure, it becomes apparent for which climate tax values changes in the fleet composition occur. Until 8e+11 USD/K, the fleet composition remains rather constant. When looking at the fuel types, only kerosene is used up to that point, with minimal profit loss. At 9e+11 USD/K, the first flights are performed with SAF instead of full kerosene. The number of SAF-fueled aircraft increases until 4e+12 USD/K, which is the turning point at which (almost) the entire fleet uses SAF instead of kerosene. For LR aircraft, the first hydrogen aircraft are allocated. The tax value thereafter, 5e+12 USD/K, is the first for which REG and SMR hydrogen aircraft are used. SAF-fueled kerosene aircraft are replaced with hydrogen aircraft, until 2e+13 USD/K, when all aircraft are hydrogen-powered. At this point, there is a decline in the number of aircraft and profit, until there are no profitable flights left.

Considering the types of aircraft, the COC-optimized designs are dominant. Only for higher climate impact tax values, the ATR-optimized hydrogen aircraft become attractive. It should be noted that even without any climate impact tax, two ATR-optimized aircraft (1xREG, 1xSMR) are allocated. This is caused by the flight cost calculations, where the flight costs for ATR-optimized aircraft are found to be lower or close to those of COC-optimized aircraft, for flights to/from SAV, MSY, and CMH. The mission analysis tool assumes a fixed flight altitude and does not consider the flight distance, meaning very short COC-optimized flights climb to 10 km altitude, only to start descending immediately after, which is not realistic. This discrepancy is assumed to only apply to very short flights, resulting in a low amount of additional selected ATR-optimized aircraft. Future researchers are recommended to explore the mitigation of this issue, for example, by using a different mission analysis tool for the shorter flight distances.

The shift to a different fuel type is preferred over the switch to a different design objective (COC/ATR), as can be seen in Figure 14. This is because changes in the flight durations impact the airline's profit. The increase in flight time, by using an ATR-optimized aircraft, could affect the personnel costs, as well as the number of flight legs covered per day, and thus the number of transported passengers and the acquired revenue. Realistically, there are only a couple of flight legs within the airline's schedule where there is room to decrease the flight speed without significant harm to the airline's profit[7].

The latter implies the necessary flexibility: if only a couple of flights in an airline's schedule have the room to fly slower, designing *slow* ATR-optimized aircraft may not be desirable, but instead *fast* COC-optimized aircraft could be scheduled to fly slower (and lower). For future research, it is recommended to consider this

[7] According to an expert from an undisclosed airline, discussed on July 7th, 2025.

possibility in the fleet allocation, to examine how often this takes place and how much impact these decisions could have on the climate impact. Elaboration on this topic is provided in section 8.

As for the changes in fuel types, a gradual shift from kerosene to SAF, and then to hydrogen, is observed. For LR aircraft, the shift is less gradual compared to REG and SMR aircraft: between 2+e12 and 5e+12 USD/K, all LR aircraft change from kerosene fuel to SAF fuel, and then to hydrogen aircraft. Additionally, beyond the 4e+13 USD/K climate impact tax, no LR aircraft are selected by the fleet. For low-cost airline carriers, this might not necessarily be as big of an issue as they generally fly fewer long-haul flights, and they could more easily drop those flights; however, for big hub-and-spoke airlines, this may be a problem. Their business model is built around those long-haul flights: connecting passengers through their regional and short flights to further destinations using long-haul flights. By optimizing transfer times and transfer services, they aim to capture those passengers. Hub-and-spoke airlines would have to compete with low-cost carriers without those long-haul flights. Therefore, future implementation of such a climate impact reduction scheme should consider how the airlines and the aviation industry are affected.

Satisfied Demand: Various key performance indicators (KPIs) are plotted in Figure 15. It can be seen that the satisfied demand decreases similarly to the revenue passenger kilometers (RPK) and average seat kilometers (ASK), however, the load factor increases. This means that when fewer flights are allocated, the satisfied demand decreases and the seat utilization increases, because emptier flights become more expensive to operate with increased climate impact tax.

Flight Frequency: Similarly, the number of unique destinations stays up to 21 until 2e+13 USD/K, while the total number of flights decreases. This aligns with the above: a higher climate impact tax means a lower flight frequency between airports, and a higher average seat utilization.

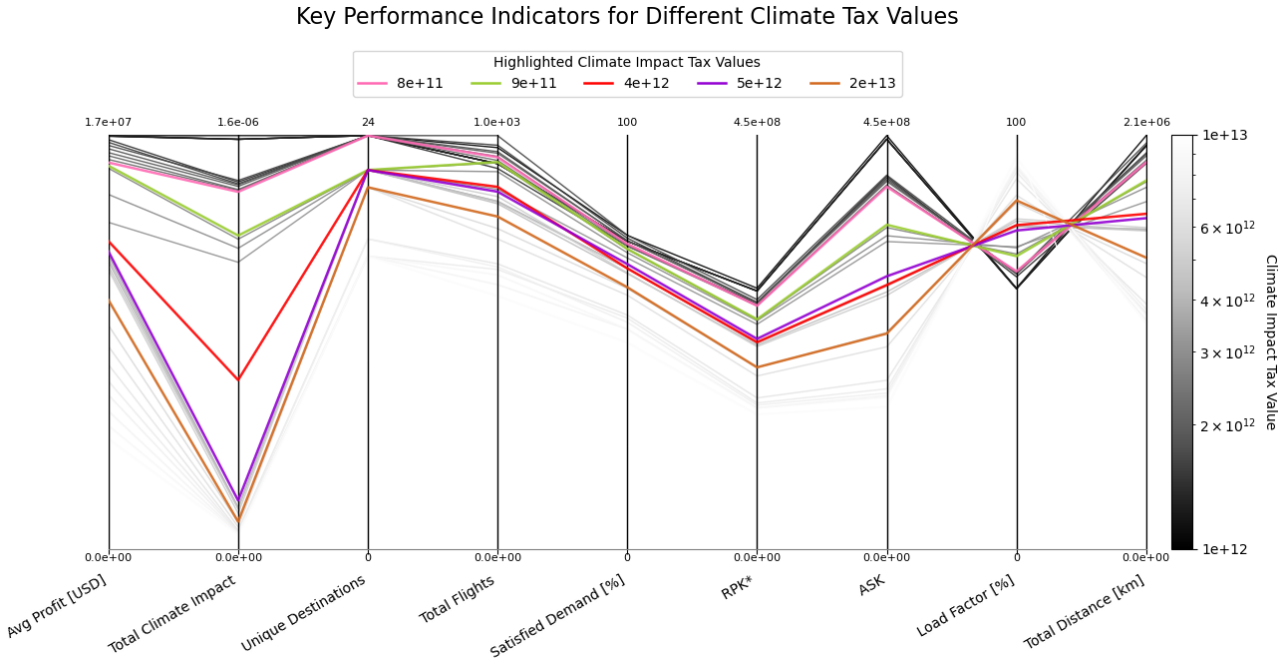

Figure 15: Key performance indicator plot. All values are averaged over the 5 years. *The RPK is calculated as the total amount of passengers served during the week multiplied by the total flight distance during the week. The RPK is therefore an approximation and not an exact calculation.

Flight Routes: As is depicted in Figure 14, the SAF allocation occurs between 9e+11 and 2e+13 USD/K. Since there is a gradual change between the fuel types, it is observed whether patterns could be found in the SAF allocation. The flight paths are plotted for the different years for the climate impact tax value of 3e+12 USD/K, because the SAF allocation varies the most for this tax. The plots can be found in Figure 33. While changes in fleet composition and flight frequency are observed above, no clear pattern in the fuel allocation is found when looking at the latitude, longitude, and flight distance to the spoke airports, besides the consistent use of SAF for the transatlantic flights.

Nevertheless, the SAF used per spoke-airport is evaluated to explore possibilities for lowering the pressure on the SAF supply chain. In Figure 16, it is shown that the SAF usage differs per airport. The aircraft locations are also plotted with the corresponding colors in Figure 34, and the airports further away from the hub airport

show higher SAF amounts. This is due to a combination of interdependent factors, including the higher amounts of fuel burn, climate impact, flight distance, and aircraft size. This suggests that the SAF could be allocated to larger airports with (more) long-range flights, instead of uniformly distributing it among all airports. This could possibly lower the pressure on the supply chain. Various recommendations based on these findings are developed, which can be found in section 8.

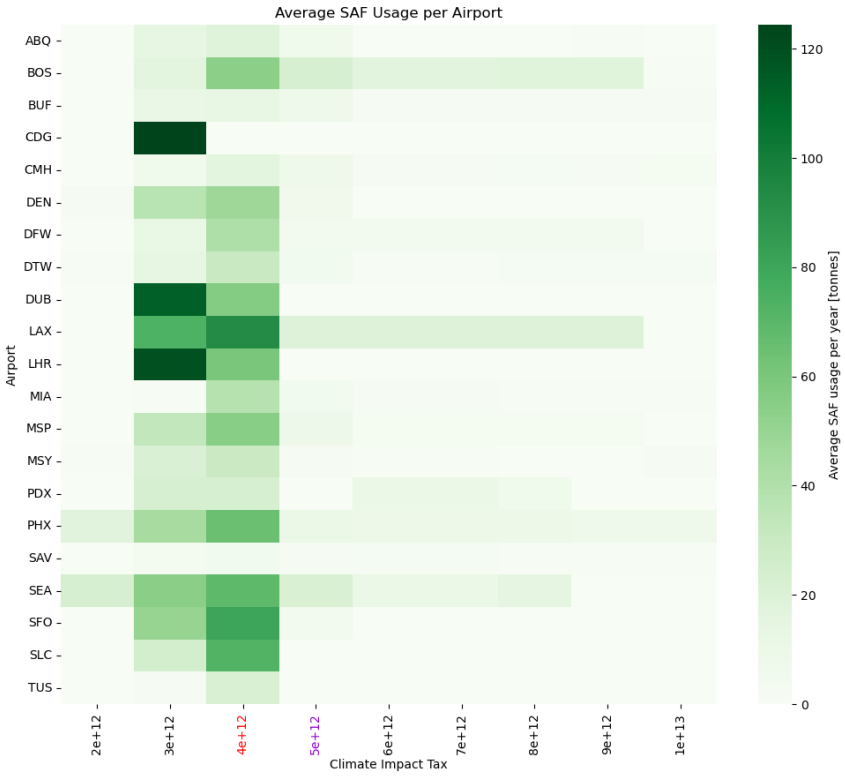

Figure 16: The amount of SAF used per airport for varying levels of climate impact tax. The values are averaged over the 5 years, and the SAF usage is expressed in terms of tonnes of 100% SAF (which blended with the same amount of kerosene results in a 50% blend). As can be seen in this figure, as well as in Figure 34, no flights using SAF take place to AMS, FCO, and MUC, because the demand is too low at these airports, and the flights do not generate profit at these tax levels.

These results presented above demonstrate that climate impact taxes could stimulate the transition to more sustainable fuel types and aircraft types. This results in a mixed fleet with an increased number of aircraft types, which should not be an issue for big hub-and-spoke airlines, as they use up to around 10 different aircraft types[7].

Low-cost carriers, on the other hand, generally use very few aircraft types[8,9]. Their business model is built around the cost savings from lower maintenance costs and uniformity benefits such as minimal pilot training and airport infrastructure. These airlines could face difficulties when forced to broaden their fleet with more aircraft types. It is expected that more COC-optimized SAF aircraft will be used compared to ATR-optimized aircraft, since this would avoid those additional costs. Moreover, as low-cost carriers generally have a point-to-point network structure, there is less flexibility in the allocation of aircraft/fuel types, and therefore, the expectation is that the transition between aircraft types and fuel types is less gradual.

Lastly, the transition from kerosene to other aircraft and fuel types, due to the increasing climate impact tax, varies between REG, SMR, and LR aircraft. This raises the question of whether a fleet-wide climate impact tax would be appropriate. Policymakers should consider the differences between these types when implementing a climate reduction incentive. For example, taxes could create (dis)advantages between airlines (hub-and-spoke vs. low-cost carriers); regional flights could compete with ground transport such as cars, which do not automatically result in a lower climate impact per passenger [89]; and the implementation of a tax without considering the availability of the required resources to mitigate those taxes could result in increased costs without the desired sustainable transition, such as the scarcity of SAF and hydrogen.

[8] `https://www.easyjet.com/en/help/boarding-and-flying/our-fleet`, accessed July 9th, 2025.
[9] `https://corporate.ryanair.com/about-us/our-fleet/`, accessed July 9th, 2025.

4.3.3 Trade-Off between Profit and Climate Impact

The second sub-question in this research investigates the trade-off between the profit and the climate impact of the fleet: *What is the trade-off between climate impact and profit for the allocation of different aircraft types, sizes, fuels, and combinations thereof in a network?* In Figure 17, this trade-off is presented. For 8e+11 and 9e+11 USD/K, some climate impact reduction is found. Between 9e+11 and 4e+12 USD/K, a significant reduction in climate impact is achieved (25-35%) with a profit reduction of 20-25%, and between 4e+12 and 5e+12 USD/K, the largest reduction in climate impact can be achieved for a minimal profit loss (20-30% vs 5%). Beyond 2e+13 USD/K, the climate impact tax does not contribute to significant climate impact reduction; instead, it rapidly reduces the profit value and number of flights (see Figure 15).

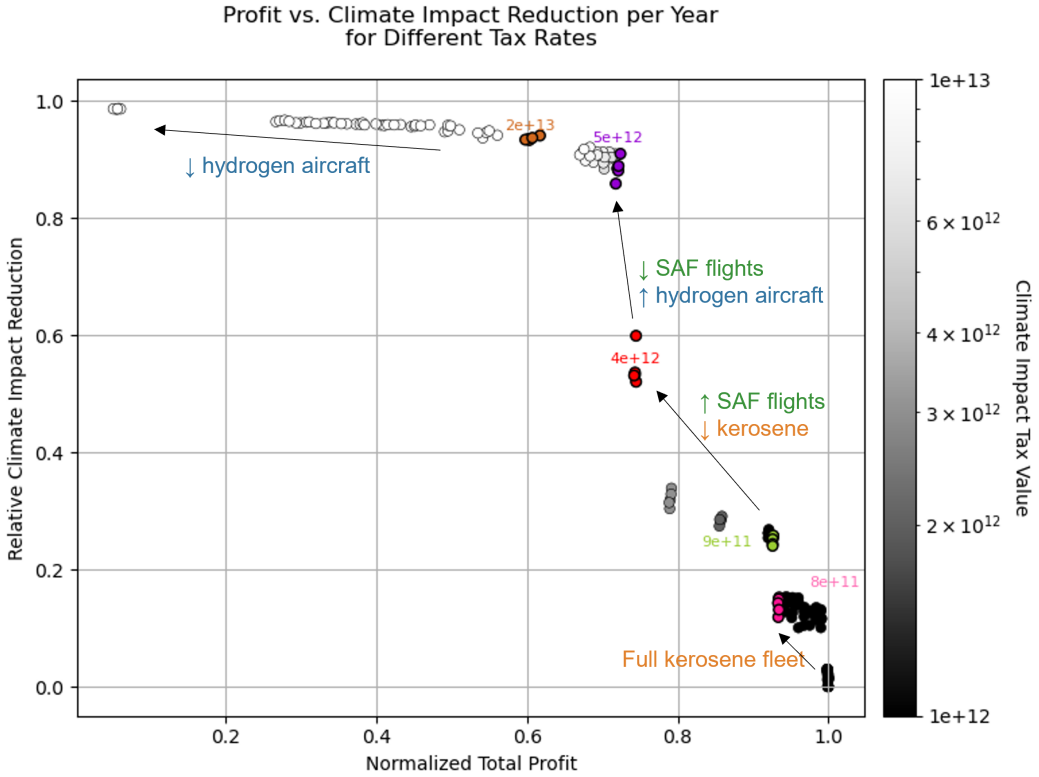

Figure 17: Eco-efficient distribution between the normalized total profit and relative climate impact reduction for the fleet allocation for different levels of climate impact tax. The fuel usage is depicted, where kerosene, SAF, and hydrogen are represented in orange, green, and blue, respectively. The colors and arrows describe the fuel transition, which corresponds to Figure 14.

At 4e+12 USD/K, all flights are flown using SAF or hydrogen, resulting in a 50-60% climate impact reduction. In turn, a 20-30% profit loss is expected. With 1% profit loss, according to Figure 17, a maximum of around 10-15% climate impact reduction could be achieved.

This raises the following question: how much should the climate impact of the aviation industry be reduced? As argued by The Guardian, the term *climate change* is not an accurate description of the current state of the world; instead, *climate crisis* is used as it covers the urgency and gravity. With a 3.8% yearly projected growth in passenger demand [37], the climate impact from the aviation sector is expected to keep growing. To instigate global change to mitigate this crisis, the industry should drastically reduce its impact, for which global policy/coordination is required (e.g. [45, 57]).

5 Sensitivity Analyses and Uncertainties

In this chapter, two sensitivity studies are performed on the fleet allocation model. The first study researches how changes in the climate impact of NO_x influence the fleet allocation, and the second examines the influence of fuel prices on the results (section 5.1 and section 5.2, respectively). Thereafter, the chapter continues by describing the optimality gap of the fleet allocation in section 5.3, and the uncertainties in the climate impact calculations in section 5.4.

5.1 Sensitivity Analysis: NO_x

Manen and Grewe [54] present the uncertainties of aCCF in comparison with CCF, and argue that the quality of the algorithm for O_3 is low, and is expected to have the largest impact on the results of the climate impact calculations. They argue that the spatial pattern can be captured, but that the higher frequency variability is not represented in the algorithm. Whether this higher frequency variability is incorrectly captured with the CCF or with the aCCF is unknown. Additionally, since various assumptions on the NO_x emissions are made in this paper, a sensitivity analysis is performed, examining the influence of the climate impact of NO_x calculated using the aCCF on the results of the fleet allocation.

The flight path climate impact calculations are performed using the following scaling factors for the aCCFs from O_3 and CH_4: 0.6, 0.8, 1.2, and 1.4. The fleet allocation is executed for the new climate impacts, to compare the results with the baseline (1.0). The sensitivity analysis is limited to the year 2020.

The resulting profit vs. climate impact reduction trade-off is presented in Figure 18. For lower climate impact tax values and higher NO_x scaling factors, the trade-off moves downward, whereas for climate impact tax values above 2e+13 USD/K, only a small leftward shift in the normalized total profit is observed. The changes in fleet composition are plotted (see Figure 35). As expected, the NO_x scaling factors do not influence the climate impact tax value for which SAF is introduced, because kerosene and SAF produce an equal amount of NO_x. Hydrogen, however, is used by the fleet for lower tax levels when the scaling factors are higher. Similarly, more ATR-optimized aircraft are used for higher scaling factors, which is expected, because the climate impact previously mitigated using SAF fuel remains, and some of this is now mitigated using the ATR-optimized aircraft.

Moreover, as shown in Figure 18, the lines move mostly vertically, and the locations of the points for 8e+11, 9e+11, 2e+13 USD/K, hardly change. Only for 4e+12 and 5e+12 USD/K, the points are further apart horizontally, which corresponds to the transition from SAF to hydrogen. With this being said, and looking at Figure 35, the NO_x climate impact calculations are observed to have the biggest impact on the transition from SAF to hydrogen, and on the amount of ATR-optimized aircraft. Higher NO_x is expected to positively influence the allocation of ATR-optimized aircraft and hydrogen aircraft, and negatively influence the amount of allocated SAF.

The flight paths for each scaling factor are plotted in Figure 36 for tax value 3e+12 USD/K. In practice, the transition to sustainable fuels and aircraft also depends on the availability of these resources. This analysis shows how changes or future developments in the climate impact calculations could influence the results, but it also implies that future research could investigate how different taxation schemes influence the transition. Future research could investigate different taxes, for example: taxes based on flight altitude, fuel burn, CO_2 emissions, NO_x emissions, fuel type, or flight distance.

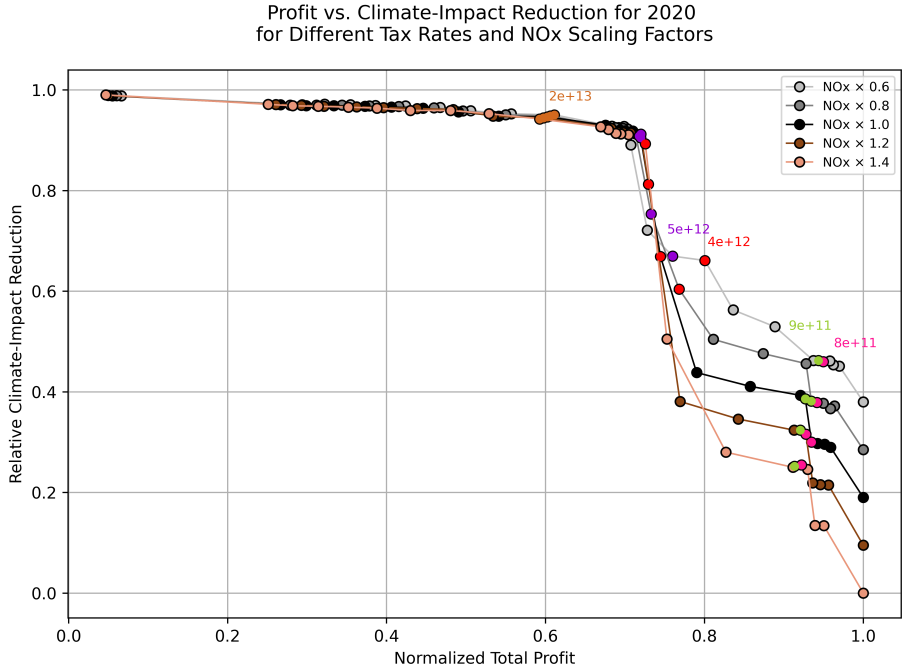

Figure 18: Sensitivity analysis for the eco-efficient distribution between the normalized total profit and relative climate impact reduction for the fleet allocation for different levels of climate impact tax. The graph presents the trade-off for 5 different NO_x scaling factors.

5.2 Sensitivity Analysis: Fuel Costs

This sensitivity analysis examines whether different fuel prices affect the results. The considered fuel prices for kerosene and SAF (HEFA) are: 0.94 USD/kg (0.80 EU/kg) for kerosene, and 2.34 USD/kg (2.0 EU/kg) for a 50% SAF blend[7]. For LH_2, the price is found to be 8.14 USD/kg (6.96 EU/kg)[10]. Since these fuel cost values vary from the values presented in Table 4, it is decided to perform this analysis.

The results for the fuel sensitivity analysis are presented in Figure 19. The following observations are found: No SAF allocation takes place; ATR-optimized aircraft are used more; the profit declines more rapidly compared to Figure 14; there is a sharp transition to hydrogen aircraft, and the LR hydrogen aircraft are not used.

These observations mean that the increased SAF price is too expensive in comparison to the other fuels; thus, ATR-optimized kerosene aircraft in combination with higher climate impact taxes from kerosene fuel are preferred over SAF fuel usage. At 2e+13 USD/K, the fleet shifts almost completely to hydrogen aircraft, and no LR aircraft are allocated.

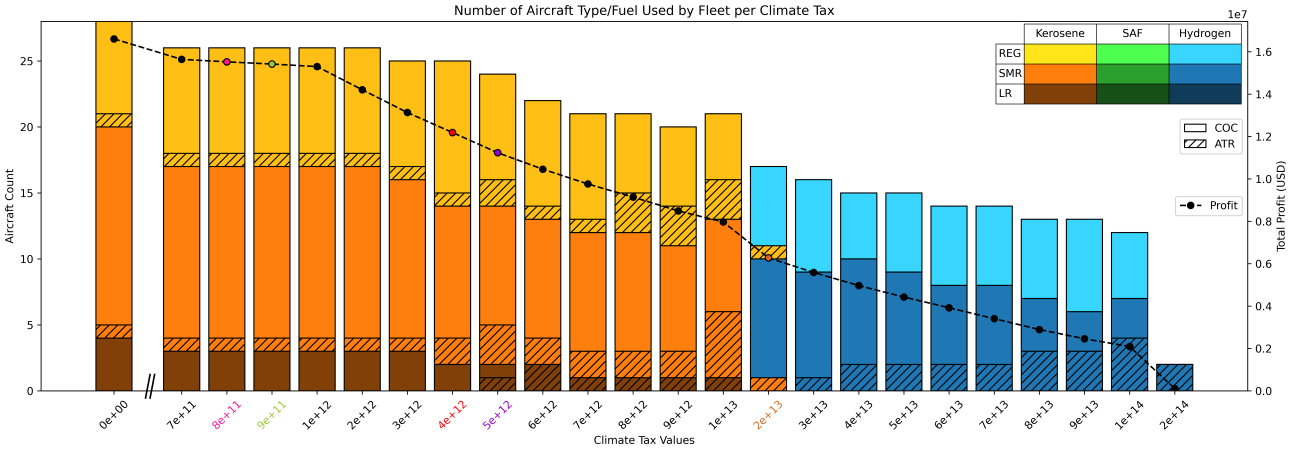

Figure 19: Sensitivity analysis with the different fuel prices. The stacked bar plot shows the number of aircraft used by the fleet for different levels of climate impact tax. The Values are only for 2020.

Currently, a 2% SAF blend is mandated; however, by 2050 this will increase to 70% [71]. This means airlines could face serious profit losses if 1) the SAF price is not mandated, or 2) the competitive field is not level across airlines, for example, when local policies regarding SAF are used, instead of continent-wide regulations. Firstly, if the goal is to persuade airlines to use more sustainable fuels and aircraft, the effectiveness of a climate impact tax depends on the fuel costs, because these significantly influence the profit margins. Similarly, the climate impact reduction potential is affected by the change in fuel price, which can be seen in the profit vs. climate impact reduction trade-off in Figure 20. The trade-off for the increased fuel price presents a flatter, linear line, which falls left and below the baseline trade-off curve for the initial fuel prices, which is expected as the climate impact mitigation through SAF usage does not take place, resulting in fewer climate impact reductions and corresponding profit savings. Without the tools for airlines to mitigate the tax levels through the adoption of sustainable practices, the sustainable transition could be harmed, as it takes away the airlines' profit margins and simultaneously their capacity to invest in sustainable practices. Secondly, airlines advocate for climate impact reduction schemes, but emphasize that local policy undermines their business strategy[11]. For high SAF prices and Refuel EU regulations, airlines would need a continent-wide SAF price (or an alternative incentive) when the goal is to transition from kerosene to SAF.

Moreover, these results highlight the importance of specific and stable climate reduction plans. Airlines need time to order and invest in new aircraft, and if the climate tax or the fuel prices change, different aircraft designs could become more or less attractive.

[10] `https://h2v.eu/analysis/statistics/financing/hydrogen-cost-and-sales-prices`, accessed July 7th 2025.

[11] `https://news.klm.com/klms-response-to-the-european-commissions-fitfor55-proposals-green-deal`, accessed July 28th, 2025

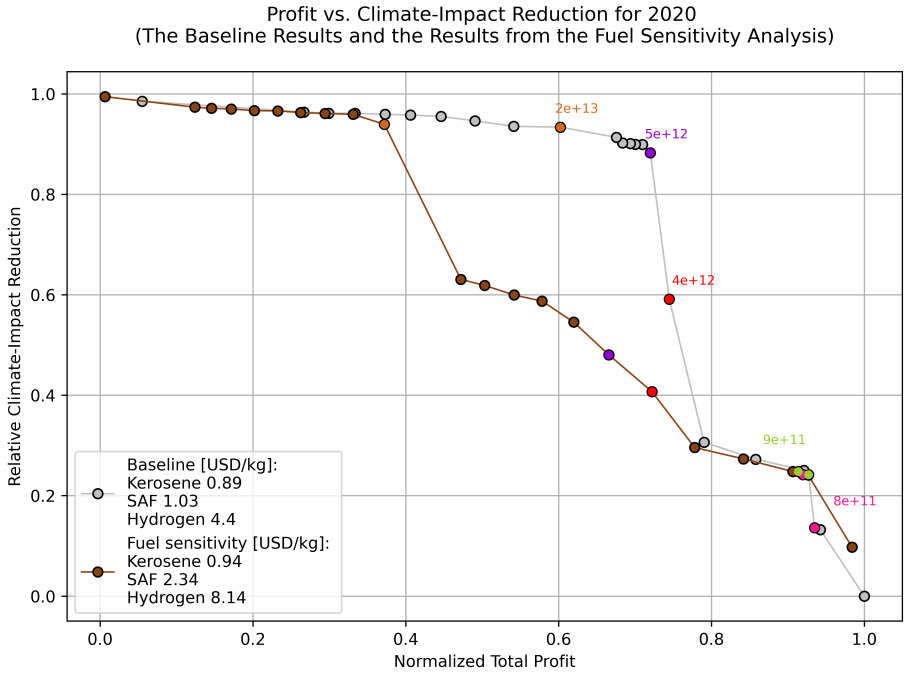

Figure 20: Sensitivity analysis with different fuel prices for the eco-efficient distribution between the normalized total profit and the relative climate impact reduction for the fleet allocation for different levels of climate impact tax. The two lines represent the case with the baseline fuel prices and the sensitivity case with the new fuel prices.

5.3 Optimality Gap Fleet Allocation

The path calculations performed in the fleet allocation model are solved using dynamic programming. The optimality of dynamic programming relies on the optimality of the substructure. With an optimal substructure, the global optimal solution can be found by combining the optimal solutions to the subproblems. The path calculation consists of an optimal structure and therefore finds the optimal paths that generate the highest profits[12,13].

However, for the overall network profit, these optimal paths are combined to solve the global solution: the maximum network profit. This global solution does not necessarily equal the global optimum. Specifically, due to overlapping passenger demand and the iterative structure, optimality may be obstructed. Each iteration optimizes for the path generation, but it does not take into consideration that other aircraft may be allocated later. Airlines should be aware, when using such a fleet allocation approach, that there could be an optimality gap between the calculated network profit and the maximum network profit.

5.4 Uncertainties

The CCFs, developed by Grewe et al. [28], contain various uncertainties, and aCCFs build upon those and aggregate the uncertainties. Manen and Grewe [54] compare the CCFs and aCCFs, and present Table 11. As can be seen in the table, the quality of the aCCF for CH_4 is low; however, the authors argue that the variability in methane captured with the CCF is much lower (order of magnitude) compared to O_3. They argue that it is therefore less important that these spatial patterns are captured by the aCCF, as they are expected not to significantly influence the results. Rao et al. [69] perform a case study to validate the O_3-aCCF for climate-optimized flight planning. They conclude that the aCCFs provide a reasonable estimate of the climate impact of NO_x induced O_3, yet the large simplification of the prediction of the climate impact is emphasized. Because the inaccuracies of the O_3-aCCFs are expected to have a much bigger impact on the results, a sensitivity analysis is conducted in section 5.1. The analysis shows that the magnitude of the climate impacts from NO_x emissions influences the transition to more sustainable aircraft and fuels. This is in line with various other literature on the aCCFs (e.g. [54, 69]), that highlight the road-map presented by Grewe et al. [29]. This consists of steps towards the practical implementation of climate-optimized flight planning and acknowledges the required investigation of uncertainties and robustness of the aCCFs.

Furthermore, Dietmüller et al. [18] advise against the off-design use of aCCF, and emphasize that the use of aCCF in tropical regions could lead to unreliable results. They implemented the ability to add different versions

[12] `https://web.stanford.edu/class/archive/cs/cs161/cs161.1172/CS161Lecture12.pdf`, accessed July 31st, 2025
[13] `https://courses.csail.mit.edu/6.006/fall10/lectures/lecture15.pdf`, accessed July 31st, 2025

of the aCCF in the CLIMaCCF model, and they highlight that development of the aCCF is ongoing, and new versions of the aCCFs will be added to the model once published. Moreover, they argue that more studies need to be conducted on the impact of the radiative forcings (RF) of emissions on the temperature response model, to more accurately define the efficacies (Table 4 from [18]). Not only the efficacies, which are based on RF factors, but also the RF factors themselves come with some uncertainties. The radiative forcings from contrail cirrus and short-term O_3 contain the largest uncertainties (≈70% and ≈36-56%, respectively) [50].

Moreover, the ATR climate metric used to express the climate impact results could lead to some uncertainties. However, compared to other climate metrics, ATR covers more climatic processes and leads to a more accurate assessment of the climate impact for existing and future aircraft and fuels [57].

In the case where the spatial pattern or the magnitude of the climate impact calculations from the different emissions are under- or overestimated, results are expected to change as follows. When the magnitude changes, the transition to different aircraft and fuel types is expected to change, similar to the results presented in section 5.1. Specifically, when the magnitude of the climate impact due to contrail formation changes, the allocation of SAF, hydrogen, and ATR-optimized aircraft is expected to change similarly, as these produce contrails with a net lower radiative forcing factor (see Table 3) and have a lower formation probability, respectively. In the situation where forecasts become reliable enough to calculate accurate spatial patterns, flight trajectory rerouting might become attainable. This could be an alternative solution to the fleet allocation presented in this paper. Future research could investigate how robust trajectory rerouting (e.g. [29, 80]) could be combined with eco-efficient fleet allocation to decrease the climate impact while maximizing the profit margins.

Next to the climate impact calculations, the reliability of the input data should also be considered. The ERA5 reanalysis data provides an ensemble spread that depends on the observational coverage. Since the North Atlantic region has a dense observation system, the ensemble spread is small (on August 5th 2024 at 12:00 UTC at 250hPa, the average standard deviation for the geopotential and the temperature is <0.1%, for the relative humidity it is 9%, for the potential vorticity it is 6%, and for the top of atmosphere net thermal radiation it is 2%). It is therefore, that uncertainties in the results due to the random analysis error are assumed insignificant. The ensemble spread does however not cover systematic model bias. Hersbach et al. [35] outline the known bias issues in ERA5 reanalysis data, which include temperature bias for high altitudes starting at the stratosphere; small discrepancies between the hourly data, which could result in systematic jumps between hours; and at some locations (infrequent and mostly found in Africa) ERA5 reanalysis data contains unrealistically high amounts of precipitation. Nevertheless, these issues do not apply to the data and the application used in this paper, and therefore, it is concluded that ERA5 reanalysis data provides a reliable and accurate dataset.

6 Discussion

This chapter focuses on the higher-level aspects of this research, as the discussion of the results was already provided in section 4. It starts with a concise discussion, followed by a summary of the key limitations.

The research in this paper has been conducted using ERA5 reanalysis data. Forecast data will have to be used instead, if the calculation of the climate impact of flights is conducted in real-time. The ECMWF forecast system continuously updates its forecast quality, and at the time of writing, different experimental machine learning forecast models for upper-air parameters are compared [33]. For the geopotential at 500 hPa, all models lose between 5-10% accuracy in pattern detection within a 5-day forecast period, and between 18-28% accuracy within a 7-day forecast period. Without accurate pattern detection, the climate impact calculations come with great uncertainties, and airlines generally plan the final operational decisions, such as matching specific flights with specific aircraft, 2 weeks in advance. The practicality of the fleet allocation presented in this paper, thus, depends on the forecast accuracy and the flexibility in the operational plans of airlines to make last-minute decisions on aircraft types or fuel types.

Another option would be to use climate-optimal trajectory rerouting. In this case, air traffic control is expected to grant airlines greater flexibility in their route planning [84]. Similarly, without significant improvement in the accuracy of weather forecasts, it would be difficult to implement this. Moreover, researchers have shown that trajectory rerouting does not always lead to significant climate impact reduction potential. For the North-Atlantic flight corridor, little reduction potential was found [29], because the fuel savings by using (eastern) or avoiding (western) the jet-stream outweigh the climate reduction potential by rerouting around the climate-sensitive regions.

When meteorological-forecast uncertainty remains considerable, future researchers could investigate whether the combination of fleet allocation and trajectory optimization would improve robustness: assigning sustainable aircraft and fuels, while also attempting to fly around climate-sensitive regions. The expectation is that this would make the climate impact mitigation more resilient.

Besides the climate impact calculations, the fleet allocation methodology should be discussed. Other methods, such as MILP optimizations, could reduce the optimality gap and provide a higher profit margin. Using MILP, researchers have shown that the ticket pricing and demand variations could also be included [11], which

would further improve the accuracy of the results.

Furthermore, the fleet allocation assumes the availability of resources when optimizing the model for different tax levels. Resource scarcity and/or competition (e.g. [36]) impose a timeline on the transition to sustainable practices. Implementing this in the model could provide realistic time frames for the aviation industry's sustainable transition.

Besides the technical assessment, it is important to address the practical aspects of the implementation of a climate impact tax: 1) by whom the climate impact tax is imposed, 2) how it is monitored and collected, and 3) how it would change current operations. First, a climate impact tax should be imposed by a large operational authority, such as the ICAO, the FAA, or the EU. As is explained in section 5.2, local policies could lead to adverse climate effects, because additional flight distances and fuel consumption may result from airlines avoiding certain areas subject to those policies. Although not covered in this paper, another important consideration for the implementation is that the climate impact of persistent contrails is the largest for the first aircraft flying through a particular region and decreases with each additional aircraft due to saturation effects. While one airline might try to avoid this region, as it is subject to a climate impact tax, another airline not subject to this tax might fly straight through it, diminishing the collective benefit [59]. It is therefore that a broad coordinated policy is required. Second, the monitoring and collection of taxes might be performed using the current Emissions Trading System (ETS) in the EU. This system could potentially be extended to include non-CO_2 emissions and climate effects. Niklass et al. [59] investigate the impact of non-CO_2 pricing on routing and ticket fares, through the incorporation of non-CO_2 emissions in the ETS based on equivalent CO_2 emissions. They argue that climate impact mitigation policies should be simplified and in line with existing policies (e.g. ETS or CORSIA) in order to facilitate monitoring and compliance. They point to the North Atlantic Track System for the first tests, as the operational complexity is low, but the climate impact mitigation potential is high. Instead of a climate tax imposed and spent by operational authorities, another method would be to obligate airlines to invest a mandatory percentage of their profit in sustainable development. This percentage could, for example, be based on the magnitude of their climate impact, and would refute the argument of airlines that climate impact taxes lower their profits and take away their ability to invest in sustainable developments. This percentage could be based on the magnitude of their climate impact. Third, climate impact taxes may lead to changes in the network and covered flight paths and frequencies, as also shown in the results of this paper, which could influence the airspace. In reality, airlines might compete for certain departure times when the climate impact and subsequent tax are lower, or fly around climate-sensitive areas. This could put increased pressure on the airspace, which could lead to additional consequences, such as noise nuisance, and limit the mitigation possibilities, as the European airspace is already saturated according to Eurocontrol[14]. Similarly, airport facilities and infrastructure may also be affected. These considerations show that beyond the technical design of a climate impact tax, the implementation and operational consequences must be taken into account.

6.1 Limitations

This research does not include demand fluctuations, changes in ticket prices, and/or market effects. These are interconnected and could influence the results presented in this paper. For example, the demand for certain destinations or departure times could change, affecting the profit margins; the ticket prices may rise with increased demand, as airlines try to maximize their ticket price as well as their load factors; and market effects such as the gate occupation, ticket price competition, or resource competition, such as SAF acquisition, could influence the profits. In the scenario with sufficient demand, and where a climate impact tax is imposed on all flights ensuring a level playing field, there may be other options for airlines besides switching to more sustainable practices, such as increasing the ticket price and paying the climate taxes without changing to more sustainable aircraft or fuel types. Next to this, this research considers a constant demand across the five years, and does not account for the expected growth in passenger demand [37].

Moreover, it is decided not to include COC-optimized aircraft that fly lower and slower (similar to the ATR-optimized aircraft) from the analysis. For future research, this could be considered in the fleet allocation, as this requires no additional aircraft investments from airlines, and could therefore be more appealing than ATR-optimized aircraft. Specifically, flexibility in the flight schedules of individual flights could be used to reduce the climate impact of aircraft, without influencing the total transported demand or the number of flights. The results are expected to change, such that much more COC-optimized aircraft fly lower and slower for specific flight paths, as significant mitigation could be obtained using these COC-optimized aircraft.

The mission profiles calculated using MiAircraftDesign are unrealistic for the shortest distances. This has been explained in section 4.3.2. This limits the accuracy and validity of the research, because the comparison between COC and ATR-optimized aircraft is inaccurate for the shortest distances. The flight altitude and the fuel burn for REG COC-optimized aircraft are likely overestimated for the shortest distances, which influences both the flight costs and the climate impact calculations of those flight legs.

[14] `https://www.eurocontrol.int/summer-2025`, accessed September 2nd, 2025.

Furthermore, the cost calculations in this research are continuous linear equations using general values for operating costs per hour. In reality, airlines are subject to strict regulations, and their operating costs are usually discretized functions. For example, at specific flight durations, more crew members are legally required in the cockpit [19]. Depending on the flight, there may be more or less room to lower the flight speed and increase the flight time, without adding the additional costs of an extra crew member. Currently, airlines fly faster for a few flight legs in their daily schedule to avoid those costs[7]. This linear assumption limits the results as it could over- or underestimate the cost penalties associated with the flight speed.

Lastly, various scaling factors have been used in this paper, see Table 3 and Table 7. Assumptions on these scaling factors come with some uncertainties. There is stronger scientific evidence necessary to prove the validity of these scaling factors, in particular the scaling factors for the radiative forcing from contrails and from O_3. The radiative forcing from contrails contains very high levels of uncertainty [51], and while there is continuous development in the research on the differences in contrail properties for different fuel types, there are still quite some unknowns, such as the significance of the formation of ultrafine volatile particles such as volatile ammonium nitrate and their effect on contrails [10]; the aerosol concentration in the ambient atmosphere [10]; or assuming uniform mixing of particles across the exhaust plume cross-section [55]. Bier et al. [10] find a 80% decrease in ice particles from hydrogen contrails, corresponding to a 50% decrease in radiative forcing [13], while Ortuno et al. [64] use a value of 69% corresponding to a 90% decrease in ice particles. Similarly, for scaling factors of O_3 from NO_x emissions, Khan et al. [44] argue a 86% reduction in NO_x emissions, and Ortuno et al. [64] argue a 76% reduction in the emission index for NO_x. There is a possibility that the scaling factors over- or underestimate the radiative forcing differences, which impacts the climate impact calculations as well as the fleet allocation. Future updated values could be implemented in the CLIMaCCF application in this research. It is expected that the climate costs change, and subsequently, the profitability of the fuel types and the overall profit margin.

7 Conclusion

The goal of this research is to examine changes in the fleet, the allocation of SAF, and the overall profit and climate impact by allocating different types of aircraft employing different fuels to a network. To achieve this, a fleet allocation model is developed using dynamic programming. The climate impact is incorporated as a monetary climate impact tax, based on the climate impacts of flights calculated using CLIMaCCF. The model employs twelve different aircraft, and the SAF allocation is included through the possibility of using a 50% SAF blend in kerosene aircraft. This research addresses the following research question:

> **To what extent can a future airline reduce its climate impact while considering changes in operating costs by allocating climate-optimized aircraft and alternative fuels in its fleet?**

This research presents the following key findings, which answer the above question:

First, the results indicate that a future airline can reduce its climate impact by 50-60% at the expense of a 20-30% profit loss, when incentivized by a climate impact tax. This would mean the fleet consists fully of kerosene aircraft employing a 50% SAF blend and LH_2 aircraft. For a profit loss of 1%, a future airline could reduce its climate impact by 10-15%. In this case, the flight frequency reduces, while the number of airports and the satisfied demand remain high. Also, the fuel type remains kerosene (thus no SAF blend). Subsequently, higher profit losses are expected when using a tax to incentivize airlines to adopt a 50% SAF blend, ATR-optimized aircraft, or LH_2 aircraft.

When increasing the climate impact tax levels, the profitability of the LR aircraft is found to decrease more rapidly compared to REG and SMR aircraft, and switch to LH_2 more quickly. Moreover, the ATR-optimized REG and SMR aircraft are allocated only in low amounts (with no LR ATR-optimized aircraft allocated), due to their increased flight time and higher flight costs. This emphasizes the importance of considering the potential revenue generation of aircraft, and not just the flight costs.

Additionally, the analysis of the trade-off between the climate impact reduction and the overall profit shows a Pareto front. This corresponds to the transition from a full kerosene fleet, through the use of SAF, to predominantly LH_2 aircraft. Beyond very high levels of climate impact tax, the fleet fully consists of LH_2 aircraft. At this point, the profit reduces much more rapidly compared to the overall climate impact, and hardly any climate impact reduction potential remains.

The fuel sensitivity analysis shows how this trade-off changes for different fuel costs. For higher SAF costs, the profitability of the fuel deteriorates, which affects the trade-off, showing fewer climate impact mitigation possibilities. Moreover, the NO_x sensitivity analysis shows that for different NO_x scaling factors, the trade-off moves up or down, but that the transition to SAF remained relatively constant. On the other hand, the introduction of LH_2 aircraft started with lower climate impact tax values for higher NO_x scaling factors.

The findings in this research contribute to the existing knowledge on sustainable aviation, providing insights into the effect of using sustainable fuels and aircraft in a future fleet using an eco-efficient fleet allocation model. The overall profit and climate impact are examined, as well as the changes in the fleet composition, the satisfied demand, and the flight routes. These insights are relevant for airlines, aircraft manufacturers, and policymakers; they highlight the importance of understanding the operational feasibility of sustainable measures when minimizing the climate impact. Nevertheless, the approach used in this research entails quite some uncertainties, especially regarding the climate impact calculations and assumptions about fuel costs. Policymakers should acknowledge these uncertainties and carefully consider the most appropriate climate impact reduction incentive and its effects on airlines. Future research could validate the results using high-fidelity climate models and explore the effectiveness and robustness of eco-efficient fleet allocation alongside trajectory optimizations. While the model simplifies certain real-world complexities such as constant ticket prices and resource availability, this research can support the navigation toward a more sustainable aviation industry.

8 Recommendations

The research on climate impact mitigation possibilities for the aviation industry remains ongoing. Various topics include the accuracy of the aCCFs, the development of different aircraft types and their prospects on the market, and the acquisition and influence of fuel and fuel prices on the industry. Therefore, the following seven recommendations are formulated, which apply directly to this research. Additional research areas, priorities, and steps necessary for the sustainable transition can be found in the road-map presented by Grewe et al. [29].

1) Future researchers are recommended to include the passengers' willingness to contribute to sustainable initiatives, such as the willingness to pay extra for their tickets. KLM Royal Dutch Airlines, for example, currently offers passengers the option to pay extra for their ticket, which is used to add more SAF to the airport fuel systems[15]. The airline is also starting a trial experiment in September 2025, where they test passengers' willingness to pay extra for 2 specific flights. The ticket price covers the flight costs if flown with 100% SAF, and this additional revenue is fully invested in the acquisition of SAF, which is added to the fuel systems to increase the average SAF blending ratio at the airport. If the experiment is successful, it could indicate the viability of a sustainability-focused business model, showing additional possibilities to incentivize the adoption of sustainable aircraft and fuels. When implemented in this model, the revenues could change, and this would directly influence the calculated profit.

2) It is recommended to perform an additional validation step on the climate impact calculations. To validate the climate impact calculations, researchers could compare the results with a high-fidelity climate impact model (e.g. EMAC). Such a model simulates atmospheric chemical processes, which would more accurately assess the climate impacts.

3) As explained in section 6.1, COC-optimized aircraft flying slower and lower are excluded from this research. In the future, researchers could use MiAircraftDesign and implement a different mission of interest to calculate the mission profiles. They could modify the cruise altitude and speed, and run the calculations accordingly. Results are expected to change when introducing this option in the fleet, as this could provide an additional climate impact mitigation measure.

4) Similar to the above, researchers are recommended to include electric (or hybrid-electric) aircraft. These have not been used in this research, as electric aircraft do not emit in-flight emissions; however, it has been established that mineral resources for electric aircraft (used for the batteries) have a greater climate impact than conventional aircraft (e.g. [7, 8]). When incorporating electric aircraft in the fleet allocation, a careful assessment of the climate impacts from the full life-cycles of the aircraft needs to be considered, including the battery lifetime and the origin of the electricity used by the electric aircraft.

5) Future studies could extend the analysis of the SAF allocation by looking into the following aspects: Researchers could explore the SAF volume used per airport by performing the analysis on more extensive networks. Alternatively, they could research whether allocating SAF to specific airports would significantly influence the overall climate impact, compared to allocating it to specific flights. Moreover, researchers could examine whether SAF usage is almost directly linked to PCFAs, and whether robust planning (e.g. [80]) of those areas could facilitate the allocation when applied to forecast data. Lastly, researchers could study whether the allocation of different fuels (kerosene vs. 50% SAF) is realistic for airports. Currently, the available SAF is added to the fuel systems at airports and provided to all aircraft[16]. However, this research assumes that airports can support more than one fuel type.

6) Researchers could investigate how continent-wide taxation implementations could affect the global aviation market and the transition to sustainable practices. Taxes would lower the profit margins, which could have other negative effects on the sustainable transition. For example, KLM Royal Dutch Airlines has expressed concerns about taxes that harm its profit margins, as this takes away its ability to invest in sustainable initiatives and

[15] `https://www.klm.nl/information/sustainability/saf#contributing-to-saf`, accessed July 17th, 2025

[16] `https://skynrg.com/fly-with-saf/saf-for-airlines/supply-chain/`, accessed September 2nd, 2025.

developments[11]. Future research could investigate the effect of taxes on airlines and other industries in the global market, and possibly whether taxation schemes could be combined with compensation initiatives to avoid losing profit margins. This would provide insights into the expected global market changes.

7) Results show that the transition from kerosene to other aircraft and fuels differs per aircraft category (REG/SMR/LR). This means that tax levels could create (dis)advantages between airlines operating different aircraft categories. For example, regional flights may face more competition from ground transportation (which does not necessarily lead to a lower climate impact). Future researchers and policymakers should be aware of these differences, and they could examine adequate tax values that account for different airline characteristics, alternative modes of ground transport, and resource availability across the different categories.

References

[1] E. J. Adler and J. R. R. A. Martins. "Hydrogen-powered aircraft: Fundamental concepts, key technologies, and environmental impacts". In: *Elsevier: Progress in Aerospace Sciences* 141 (2023). DOI: 10.1016/j.paerosci.2023.100922.

[2] European Union Aviation Safety Agency. *Sustainable Aviation Fuels*. 2025. URL: https://www.easa.europa.eu/en/domains/environment/eaer/sustainable-aviation-fuels.

[3] E. E. de Almeida and A. V. M. Oliveira. "An econometric analysis for the determinants of flight speed in the air transport of passengers". In: *Scientific Reports* 13 (1 Dec. 2023). ISSN: 20452322. DOI: 10.1038/s41598-023-30703-y.

[4] *Alternative Fuels Data Center: Sustainable Aviation Fuel*. URL: https://afdc.energy.gov/fuels/sustainable-aviation-fuel.

[5] M. Seaone Álvarez. "Assessment of Climate Impact Mitigation Potential of Intermediate Stop Operations". MA thesis. Delft University of Technology, 2021.

[6] H. Appleman. "The Formation of Exhaust Condensation Trails by Jet Aircraft". In: *Bull. Am. Meteorol* 34 (1953), pp. 14–20.

[7] R. Arvidsson, A. Nordelöf, and S. Brynolf. "Life cycle assessment of a two-seater all-electric aircraft". In: *International Journal of Life Cycle Assessment* 29 (2 Feb. 2024), pp. 240–254. ISSN: 16147502. DOI: 10.1007/s11367-023-02244-z.

[8] A. Barke et al. "Life cycle sustainability assessment of potential battery systems for electric aircraft". In: *Procedia CIRP*. Vol. 98. Elsevier B.V., 2021, pp. 660–665. DOI: 10.1016/j.procir.2021.01.171.

[9] C. Barnhart, T. S. Kniker, and M. Lohatepanont. "Itinerary-based airline fleet assignment". In: *Transportation Science* 36 (2 2002), pp. 199–217. ISSN: 00411655. DOI: 10.1287/trsc.36.2.199.566.

[10] A. Bier et al. "Contrail formation on ambient aerosol particles for aircraft with hydrogen combustion: a box model trajectory study". In: *Atmospheric Chemistry and Physics* 24 (2024), pp. 2319–2344. DOI: 10.5194/acp-24-2319-2024.

[11] S. Birolini et al. "Integrated flight scheduling and fleet assignment with improved supply-demand interactions". In: *Transportation Research Part B: Methodological* 149 (July 2021), pp. 162–180. ISSN: 01912615. DOI: 10.1016/j.trb.2021.05.001.

[12] N. Brown and A. Oldani. *Sustainable Aviation Fuel*. 2022. URL: https://www.faa.gov/media/74261.

[13] U. Burkhardt, L. Bock, and A. Bier. "Mitigating the contrail cirrus climate impact by reducing aircraft soot number emissions". In: *npj Climate and Atmospheric Science* 1 (1 Dec. 2018). ISSN: 23973722. DOI: 10.1038/s41612-018-0046-4.

[14] E. Cabrera and J. M. Melo de Sousa. "Use of Sustainable Fuels in AviationA Review". In: *Energies* 15 (7 Apr. 2022). ISSN: 19961073. DOI: 10.3390/en15072440.

[15] *Clean Skies for Tomorrow -Sustainable Aviation Fuels as a Pathway to Net-Zero Aviation*. Tech. rep. World Economic Forum, 2020.

[16] E. S. Dallara and I. M. Kroo. "Aircraft Design for Reduced Climate Impact". In: American Institute of Aeronautics and Astronautics (AIAA), Jan. 2011. DOI: 10.2514/6.2011-265.

[17] E. S. Dallara, I. M. Kroo, and I. A. Waitz. "Metric for comparing lifetime average climate impact of aircraft". In: *AIAA Journal* 49 (8 Aug. 2011), pp. 1600–1613. ISSN: 00011452. DOI: 10.2514/1.J050763.

[18] S. Dietmüller et al. "A Python library for computing individual and merged non-CO2 algorithmic climate change functions: CLIMaCCF V1.0". In: *Geoscientific Model Development* 16 (15 Aug. 2023), pp. 4405–4425. ISSN: 19919603. DOI: 10.5194/gmd-16-4405-2023.

[19] *Easy Access Rules for Aircrew (Regulation (EU) No 1178/2011)*. Tech. rep. EASA, 2011. URL: http://eur-lex.europa.eu/.

[20] *Electric and Hybrid Aircraft Platform for Innovation*. URL: https://www.icao.int/environmental-protection/Pages/electric-aircraft.aspx.

[21] Eurocontrol. *EUROCONTROL Data Snapshot #11 on regulation and focused logistics unlocking the availability of sustainable aviation fuels (SAF)*. 2021. URL: https://www.eurocontrol.int/publication/eurocontrol-data-snapshot-11-saf-airports.

[22] C. Fichter. "Climate Impact of Air Traffic Emissions in Dependency of the Emission Location and Altitude". PhD thesis. DLR, 2009.

[23] C. Frömming et al. "Aviation-induced radiative forcing and surface temperature change in dependency of the emission altitude". In: *Journal of Geophysical Research Atmospheres* 117 (19 2012). ISSN: 01480227. DOI: 10.1029/2012JD018204.

[24] V. Grewe. *Climate Impact of Air Traffic Part 1*. Lecture. 2023.

[25] V. Grewe. *Climate Impact of Air Traffic Part 3*. Lecture. 2023.

[26] V. Grewe and K. Dahlmann. "How ambiguous are climate metrics? And are we prepared to assess and compare the climate impact of new air trafc technologies?" In: *Atmospheric Environment* (37 2015). DOI: 10.1016/j.atmosenv.2015.02.039.

[27] V. Grewe and A. Stenke. *AirClim: an efficient tool for climate evaluation of aircraft technology*. Tech. rep. 2008, pp. 4621–4639. DOI: 10.5194/acp-8-4621-2008. URL: www.atmos-chem-phys.net/8/4621/2008/.

[28] V. Grewe et al. "Aircraft routing with minimal climate impact: The REACT4C climate cost function modelling approach (V1.0)". In: *Geoscientific Model Development* 7 (1 Jan. 2014), pp. 175–201. ISSN: 1991959X. DOI: 10.5194/gmd-7-175-2014.

[29] V. Grewe et al. "Feasibility of climate-optimized air traffic routing for trans-Atlantic flights". In: *Environmental Research Letters* 12.3 (2017). DOI: 10.1088/1748-9326/aa5ba0.

[30] V. Grewe et al. "Impact of aircraft NOx emissions. Part 2: Effects of lowering the flight altitude". In: *Meteorologische Zeitschrift* 11 (3 2002), pp. 197–205. ISSN: 09412948. DOI: 10.1127/0941-2948/2002/0011-0197.

[31] V. Grewe et al. "Reduction of the air traffic's contribution to climate change: A REACT4C case study". In: *Atmospheric Environment* 94 (2014), pp. 616–625. ISSN: 18732844. DOI: 10.1016/j.atmosenv.2014.05.059.

[32] C. A. Hane et al. *The fleet assignment problem: 1 solving a large-scale integer program*. 1995.

[33] H. Hersbach et al. *ERA5 hourly data on pressure levels from 1940 to present*. Copernicus Climate Change Service (C3S) Climate Data Store (CDS). 2023. DOI: 10.24381/cds.bd0915c6.

[34] H. Hersbach et al. *ERA5 hourly data on single levels from 1940 to present*. Copernicus Climate Change Service (C3S) Climate Data Store (CDS). 2023. DOI: 10.24381/cds.adbb2d47.

[35] H. Hersbach et al. "The ERA5 global reanalysis". In: *Quarterly Journal of the Royal Meteorological Society* 146 (730 July 2020), pp. 1999–2049. ISSN: 1477870X. DOI: 10.1002/qj.3803.

[36] *Hydrogen for aviation: A future decarbonization solution for air travel?* Tech. rep. IATA, 2025.

[37] IATA. "Global Outlook for Air Transport: Deep Change". In: *IATA Sustainability and Economics* (June 2024). URL: https://www.iata.org/en/iata-repository/publications/economic-reports/global-outlook-for-air-transport-june-2024-report/.

[38] ICAO. *ICAO document - CORSIA Sustainability Criteria for CORSIA Eligible Fuels*. Nov. 2022. URL: https://www.icao.int/environmental-protection/CORSIA/Documents/CORSIA_Eligible_Fuels/ICAO%20document%2005%20-%20Sustainability%20Criteria%20-%20November%202022.pdf.

[39] E. A. Irvine et al. "Characterizing North Atlantic weather patterns for climate-optimal aircraft routing". In: *Meteorological Applications* 20 (1 2013), pp. 80–93. ISSN: 14698080. DOI: 10.1002/met.1291.

[40] P. W. Jansen and R. E. Perez. *Coupled optimization of aircraft design and fleet allocation with uncertain passenger demand*. 2013. DOI: 10.2514/6.2013-4392.

[41] P. Jöckel et al. "Development cycle 2 of the Modular Earth Submodel System (MESSy2)". In: *Geoscientific Model Development* 3 (2 2010), pp. 717–752. ISSN: 1991959X. DOI: 10.5194/gmd-3-717-2010.

[42] M. E. Kahn and J. Nickelsburg. "An Economic Analysis of U.S Airline Fuel Economy Dynamics from 1991 to 2015". In: *National Bureau of Economic Research* (2016). URL: http://www.nber.org/papers/w22830.

[43] S. Kaufmann, R. Dischl, and C. Voigt. "Regional and seasonal impact of hydrogen propulsion systems on potential contrail cirrus cover". In: *Atmospheric Environment: X* 24 (Dec. 2024). ISSN: 25901621. DOI: 10.1016/j.aeaoa.2024.100298.

[44] M. A. H. Khan et al. "The Emissions of Water Vapour and NOx from Modelled Hydrogen-Fuelled Aircraft and the Impact of NOx Reduction on Climate Compared with Kerosene-Fuelled Aircraft". In: *Atmosphere* 13 (10 Oct. 2022). ISSN: 20734433. DOI: 10.3390/atmos13101660.

[45] M. Klöwer et al. "Quantifying aviation's contribution to global warming". In: *Environmental Research Letters* 16 (10 Oct. 2021). ISSN: 17489326. DOI: 10.1088/1748-9326/ac286e.

[46] M. O. Köhler et al. "Impact of perturbations to nitrogen oxide emissions from global aviation". In: *Journal of Geophysical Research Atmospheres* 113 (11 June 2008). ISSN: 01480227. DOI: 10.1029/2007JD009140.

[47] M. Kühlen et al. "An explanatory approach to modeling the fleet assignment in the global air transportation system". In: *CEAS Aeronautical Journal* 14 (2022), pp. 255–269. ISSN: 18695590. DOI: 10.1007/s13272-022-00622-1.

[48] A. A. Lacis, D. J. Wuebbles, and J. A. Logan. *Radiative Forcing of Climate by Changes in the Vertical Distribution of Ozone*. Tech. rep. 1990. DOI: 10.1029/JD095iD07p09971.

[49] A. B. Lambe and J. R. R. A. Martins. "Extensions to the Design Structure Matrix for the Description of Multidisciplinary Design, Analysis, and Optimization Processes". In: *Structural and Multidisciplinary Optimization* 46 (2012), pp. 273–284. DOI: 10.1007/s00158-012-0763-y.

[50] D. S. Lee et al. "The contribution of global aviation to anthropogenic climate forcing for 2000 to 2018". In: *Atmospheric Environment* 244 (Jan. 2021). ISSN: 18732844. DOI: 10.1016/j.atmosenv.2020.117834.

[51] D. S. Lee et al. "Transport impacts on atmosphere and climate: Aviation". In: *Atmospheric Environment* 44 (1352-2310 2010), pp. 4678–4734. DOI: 10.1016/j.atmosenv.2009.06.005.

[52] R. Lindsey. *Climate Change: Atmospheric Carbon Dioxide*. 2024.

[53] M. Liu et al. "Green Airline-Fleet Assignment with Uncertain Passenger Demand and Fuel Price". In: *Sustainability (Switzerland)* 15 (2 Jan. 2023). ISSN: 20711050. DOI: 10.3390/su15020899.

[54] J. van Manen and V. Grewe. "Algorithmic climate change functions for the use in eco-efficient flight planning". In: *Transportation Research Part D: Transport and Environment* 67 (Feb. 2019), pp. 388–405. ISSN: 13619209. DOI: 10.1016/j.trd.2018.12.016.

[55] R. S. Märkl et al. "Powering aircraft with 100% sustainable aviation fuel reduces ice crystals in contrails". In: *Atmospheric Chemistry and Physics* 24 (2024), pp. 3813–3837. DOI: 10.5194/acp-24-3813-2024.

[56] S. Matthes et al. "Climate-optimized trajectories and robust mitigation potential: Flying atm4e". In: *Aerospace* 7 (11 Nov. 2020), pp. 1–15. ISSN: 22264310. DOI: 10.3390/aerospace7110156.

[57] L. Megill, K. Deck, and V. Grewe. "Alternative climate metrics to the Global Warming Potential are more suitable for assessing aviation non-CO2 effects". In: *Communications Earth and Environment* 5 (1 2024). ISSN: 26624435. DOI: 10.1038/s43247-024-01423-6.

[58] L. Megill and V. Grewe. "Investigating the limiting aircraft design-dependent and environmental factors of persistent contrail formation". Preprint. Nov. 2024. DOI: 10.5194/egusphere-2024-3398.

[59] M. Niklass et al. *Impact of Non-CO 2 Pricing on Routing and Ticket Fares in Aviation: Strategies to Address Uncertainties in Climate Policies*. Preprint submitted to Transport Policy. 2025. DOI: 10.5281/zenodo.15438171.

[60] M. Niklass et al. "Implementation of eco-efficient procedures to mitigate the climate impact of non-CO2 effects." In: *Proceedings of the 31st Congress of the International Council of the Aeronautical Sciences* (2018).

[61] H. Nojoumi, I. Dincer, and G. F. Naterer. "Greenhouse gas emissions assessment of hydrogen and kerosene-fueled aircraft propulsion". In: *International Journal of Hydrogen Energy* 34 (3 Feb. 2009), pp. 1363–1369. ISSN: 03603199. DOI: 10.1016/j.ijhydene.2008.11.017.

[62] M. Noorafza et al. "Airline Network Planning Considering Climate Impact: Assessing New Operational Improvements". In: *Applied Sciences (Switzerland)* 13 (11 June 2023). ISSN: 20763417. DOI: 10.3390/app13116722.

[63] *Operating Life*. 2025. URL: https://www.airbus.com/en/products-services/commercial-aircraft/the-life-cycle-of-an-aircraft/operating-life.

[64] M. S. Ortuno et al. "Climate Assessment of Hydrogen Combustion Aircraft: Towards a Green Aviation Sector". In: *AIAA SciTech Forum and Exposition, 2023*. American Institute of Aeronautics and Astronautics Inc, AIAA, 2023. ISBN: 9781624106996. DOI: 10.2514/6.2023-2513.

[65] *Path to hydrogen competitiveness - A cost perspective*. Tech. rep. Hydrogen Council, 2020. URL: www.hydrogencouncil.com..

[66] P. Proesmans. "Climate-Optimal Aircraft Design and Fleet Allocation: Evaluating the Impact of Sustainable Aviation Fuels". Dissertation at TU Delft, Delft University of Technology. PhD thesis. Delft University of Technology, 2024. DOI: 10.4233/uuid:295a037d-02ef-4bb9-bd4e-c6e346f0fefa.

[67] P. Proesmans and R. Vos. "Airplane Design Optimization for Minimal Global Warming Impact". In: *Journal of Aircraft* 59 (5 Sept. 2022), pp. 1363–1381. ISSN: 15333868. DOI: 10.2514/1.C036529.

[68] K. Ranasinghe et al. "Review of advanced low-emission technologies for sustainable aviation". In: *Energy* 188 (Dec. 2019). ISSN: 03605442. DOI: 10.1016/j.energy.2019.115945.

[69] P. Rao et al. "Case Study for Testing the Validity of NOx-Ozone Algorithmic Climate Change Functions for Optimising Flight Trajectories". In: *Aerospace* 9 (5 May 2022). ISSN: 22264310. DOI: 10.3390/aerospace9050231.

[70] A. Rap et al. "The climate impact of contrails from hydrogen combustion and fuel cell aircraft". In: *EGU General Assembly 2023*. Apr. 2023. DOI: 10.5194/egusphere-egu23-5520.

[71] "Regulation (EU) 2023/2405 of the European Parliament and of the Council on ensuring a level playing field for sustainable air transport (ReFuelEU Aviation)". In: *Official Journal of the European Union* (32023R2405 2023). URL: http://data.europa.eu/eli/reg/2023/2405/oj.

[72] J. Roskam. *Airplane Design. Part VIII: Airplane Cost Estimation: Design, Development, Manufacturing and Operating*. DARcorporation, 1985.

[73] J. J. Salazar-González. "Approaches to solve the fleet-assignment, aircraft-routing, crew-pairing and crew-rostering problems of a regional carrier". In: *Omega (United Kingdom)* 43 (2014), pp. 71–82. ISSN: 03050483. DOI: 10.1016/j.omega.2013.06.006.

[74] B. F. Santos. *AE4423 Lect 6.2 Aircraft Routing Dynamic Programming*. 2022. URL: https://www.youtube.com/watch?v=bUiaxFiHtmU.

[75] R. Sausen et al. "A Diagnostic Study of the Global Distribution of Contrails Part I: Present Day Climate Ã". In: *Springer: Theoretical and Applied Climatology* (61 1998), pp. 127–141.

[76] E. Schmidt. "Die Entstehung von Eisnebel aus den Auspuffgasen von Flugmotoren". In: *Schriften der Deutschen Akademie der Luftfahrtforschung* 44 (1941), pp. 1–15.

[77] U. Schumann. "On conditions for contrail formation from aircraft exhaust". In: *Meteorol Zeitschrift* 5 (1996), pp. 4–23.

[78] H. D. Sherali, E. K. Bish, and X. Zhu. "Airline fleet assignment concepts, models, and algorithms". In: *European Journal of Operational Research* 172 (1 July 2006), pp. 1–30. ISSN: 03772217. DOI: 10.1016/j.ejor.2005.01.056.

[79] A. Simorgh et al. *A Comprehensive Survey on Climate Optimal Aircraft Trajectory Planning*. Mar. 2022. DOI: 10.3390/aerospace9030146.

[80] A. Simorgh et al. "Concept of robust climate-friendly flight planning under multiple climate impact estimates". In: *Transportation Research Part D: Transport and Environment* 131 (June 2024). ISSN: 13619209. DOI: 10.1016/j.trd.2024.104215.

[81] S. Solomon et al. *Irreversible climate change due to carbon dioxide emissions*. 2009. URL: www.pnas.org/cgi/content/full/.

[82] Z. Song, Z. Li, and Z. Liu. *Comparison of Emission Properties of Sustainable Aviation Fuels and Conventional Aviation Fuels: A Review*. July 2024. DOI: 10.3390/app14135484.

[83] L. Ström and K. Gierens. "First simulations of cryoplane contrails". In: *Journal of Geophysical Research Atmospheres* 107 (18 2002), AAC 2-1-AAC 2–13. ISSN: 01480227. DOI: 10.1029/2001JD000838.

[84] J. Sun and X. Olive. "Contrail, or not contrail, that is the question: the "feasibility" of climate-optimal routing". In: (Apr. 2025). URL: http://arxiv.org/abs/2504.13907.

[85] F. Svensson, A. Hasselrot, and J. Moldanova. "Reduced environmental impact by lowered cruise altitude for liquid hydrogen-fuelled aircraft". In: *Elsevier: Aerospace Science and Technology* 8 (2004), pp. 307–320. DOI: 10.1016/j.ast.2004.02.004.

[86] R. Teoh et al. "Aviation contrail climate effects in the North Atlantic from 2016-2021". In: *Atmospheric Chemistry and Physics* 22 (2022), pp. 10919–10935. DOI: 10.5194/acp-22-10919-2022.

[87] R. Teoh et al. "Targeted Use of Sustainable Aviation Fuel to Maximize Climate Benefits". In: *Environmental Science and Technology* 56 (23 Dec. 2022), pp. 17246–17255. ISSN: 15205851. DOI: 10.1021/acs.est.2c05781.

[88] *The Clean Future of Flight.* URL: https://zeroavia.com/.

[89] *Transport and environment report 2020: Train or plane?* Tech. rep. European Environment Agency, 2020.

[90] Y. Wang et al. "Optimization model and algorithm design for airline fleet planning in a multiairline competitive environment". In: *Mathematical Problems in Engineering* 2015 (2015). ISSN: 15635147. DOI: 10.1155/2015/783917.

[91] K. Wolf, N. Bellouin, and O. Boucher. "Sensitivity of cirrus and contrail radiative effect on cloud microphysical and environmental parameters". In: Copernicus Publications (on behalf of the European Geosciences Union), Nov. 2023. Chap. 23, pp. 14003–14037. DOI: 10.5194/acp-23-14003-2023.

[92] H. Yamashita et al. "Newly developed aircraft routing options for air traffic simulation in the chemistryclimate model EMAC 2.53: AirTraf 2.0". In: *Geoscientific Model Development* 13 (10 Oct. 2020), pp. 4869–4890. ISSN: 19919603. DOI: 10.5194/gmd-13-4869-2020.

[93] F. Yin et al. "Predicting the climate impact of aviation for en-route emissions: the algorithmic climate change function submodel ACCF 1.0 of EMAC 2.53". In: *Geoscientific Model Development* 16 (11 June 2023), pp. 3313–3334. ISSN: 19919603. DOI: 10.5194/gmd-16-3313-2023.

Appendices

A Network and Input Data

Table 9: Network for weekly passenger demand data, adopted from Reference [66]

Origin Airport	Destination Airport	Destination Country	Demand
Atlanta (ATL)	Los Angeles (LAX)	USA	6442
Atlanta (ATL)	Minneapolis (MSP)	USA	5849
Atlanta (ATL)	Boston (BOS)	USA	5280
Atlanta (ATL)	Dallas (DFW)	USA	4908
Atlanta (ATL)	Miami (MIA)	USA	4760
Atlanta (ATL)	Salt Lake City (SLC)	USA	4611
Atlanta (ATL)	San Francisco (SFO)	USA	4212
Atlanta (ATL)	New Orleans (MSY)	USA	4193
Atlanta (ATL)	Detroit (DTW)	USA	3932
Atlanta (ATL)	Denver (DEN)	USA	3658
Atlanta (ATL)	Seattle (SEA)	USA	3528
Atlanta (ATL)	Phoenix (PHX)	USA	3406
Atlanta (ATL)	Columbus (CMH)	USA	2508
Atlanta (ATL)	Savannah (SAV)	USA	2273
Atlanta (ATL)	Buffalo (BUF)	USA	1943
Atlanta (ATL)	Portland (PDX)	USA	1577
Atlanta (ATL)	Albuquerque (ABQ)	USA	1327
Atlanta (ATL)	Tucson (TUS)	USA	984
Atlanta (ATL)	Amsterdam (AMS)	The Netherlands	1860
Atlanta (ATL)	Dublin (DUB)	Ireland	2084
Atlanta (ATL)	Rome (FCO)	Italy	1689
Atlanta (ATL)	London (LHR)	UK	2896
Atlanta (ATL)	Paris (CDG)	France	3438
Atlanta (ATL)	Munich (MUC)	Germany	1289

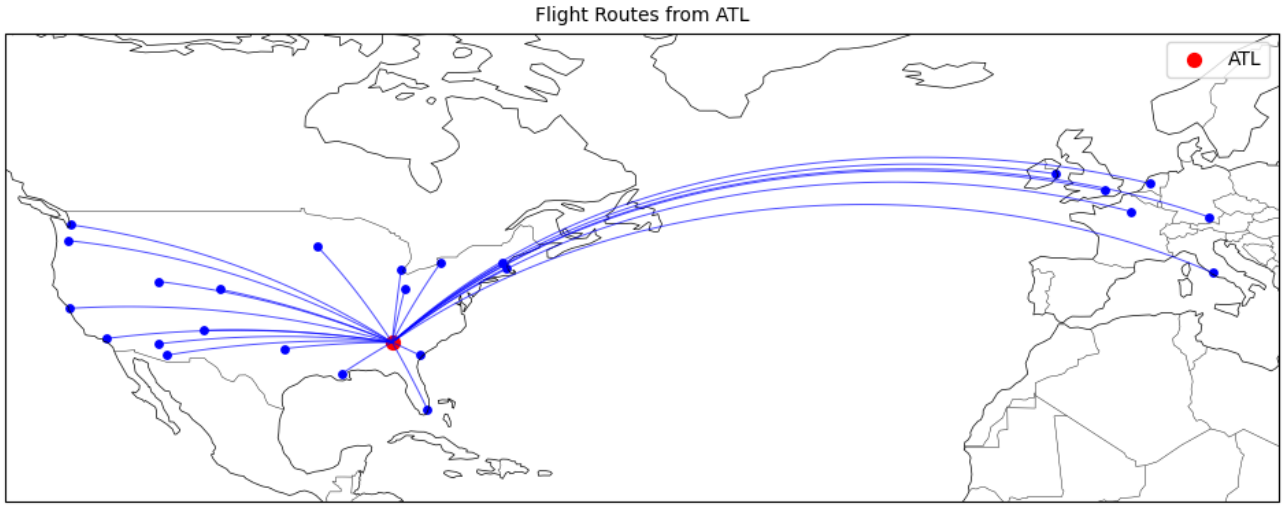

Figure 21: Flight legs from network to/from ATL. Flight paths for the shortest path according to the World Geodetic System 1984.

Table 10: ECMWF data: ERA5 hourly data from 1940 to present

Data	**Pressure levels [33]**	**Single levels [34]**
Product type	Reanalysis data from ERA5	Reanalysis data from ERA5
Variables	Geopotential, Potential vorticity, Relative humidity, Specific humidity, Temperature, U- and V-components of wind	TOA incident solar radiation, Top net thermal radiation
Years	2020, 2021, 2022, 2023, 2024	2020, 2021, 2022, 2023, 2024
Month	August	August
Days	2020: 3-9 2021: 2-9 2022: 1-7 2023: 7-13 2024: 5-11	2020: 3-9 2021: 2-9 2022: 1-7 2023: 7-13 2024: 5-11
Time	Every hour from 00:00 to 23:00	Every hour from 00:00 to 23:00
Pressure levels	100 - 1000 hPa (steps of 25 hPa)	-
Geographical area	N: 64N/13E/25S/-123W	N: 64N/13E/25S/-123W
Data format	NetCDF	NetCDF
File size	10.6 GB (1 file for each year)	112 MB (1 file for each year)

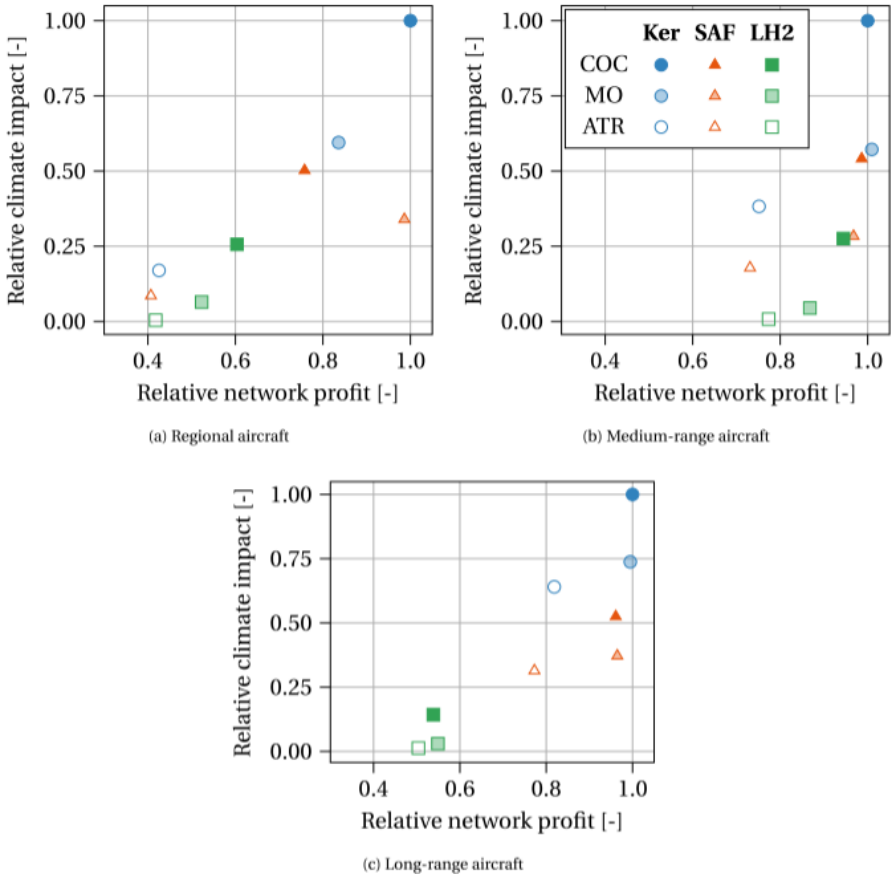

Figure 22: Relative climate impact vs. relative network profit for REG, SMR, and LR aircraft, from Reference [66].

B Demand Calculation

The initial weekly demand presented in Table 9 is obtained from Reference [66]. The data is originally presented by Jansen and Perez [40], retrieved from the Bureau of Transportation Studies for the year 2011. This demand is taken, and no growth factor has been used. Therefore, the demand remains constant for all five years (2020-2024). This section describes the steps performed to process the demand data.

Step 1: The total weekly demand is divided by the number of flights throughout the week. The first week

of August is used, and therefore the scheduled departure times for 2025 are retrieved from the Delta Airlines website[17]. In Figure 23, the demand peaks at various departure times are presented. The figures are developed for illustrative purposes and are not based on the actual demand data. An example of the final demand from Atlanta (ATL) → Rome (FCO) is plotted in Figure 5.

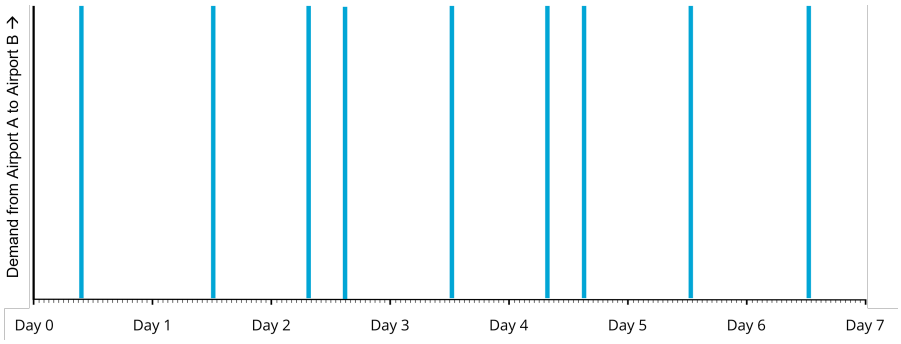

Figure 23: Weekly demand from Airport A to Airport B divided among the scheduled departure times.

Step 2: The demand peaks are normally distributed around the scheduled departure times. The demand is spread over a ±1.5 time period, with a 95% confidence interval. The step is visualized in Figure 24.

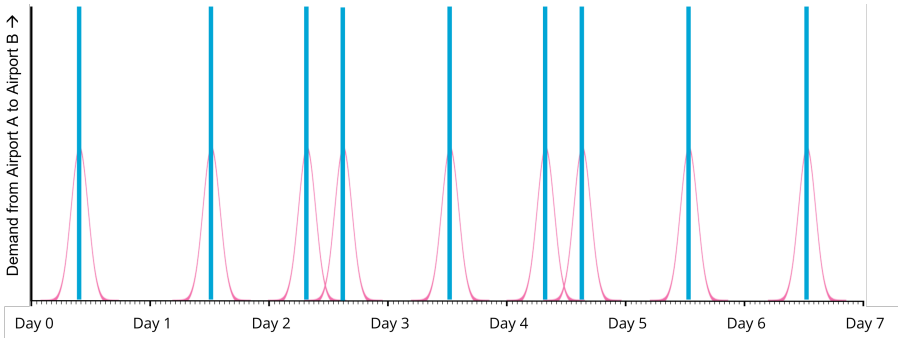

Figure 24: Demand peaks are normally distributed around the departure times, with ±1.5 hours with a 95% confidence interval.

Step 3: The overlapping demand curves are summed together, and the data is discretized into 20-minute time intervals and rounded to whole passengers, as can be seen in Figure 25. If the demand continues into the next day at the end of the week (from Sunday to Monday), it is added to the first day of the week (Monday). Subsequently, the time difference is taken into consideration, and all departure times are converted to Atlanta local time (UTC-4).

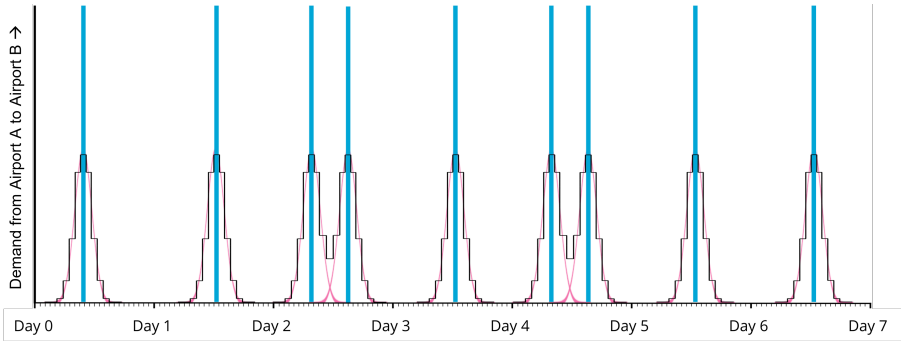

Figure 25: Demand is discretized into 20-minute intervals and rounded to whole passengers. The overlapping curves are combined, showing the total sum.

[17] `https://www.delta.com/flightsearch/book-a-flight` accessed March 18th, 2025

C Flight Costs and Climate Impact Taxes

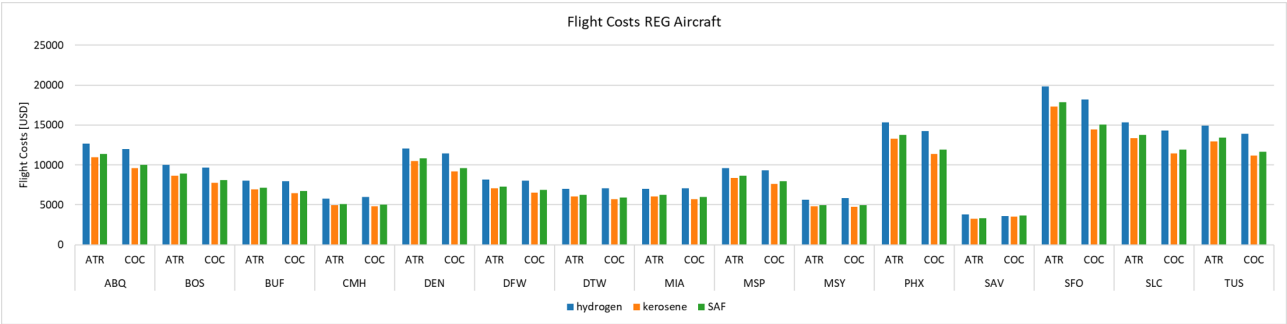

Figure 26: Flight costs for REG aircraft.

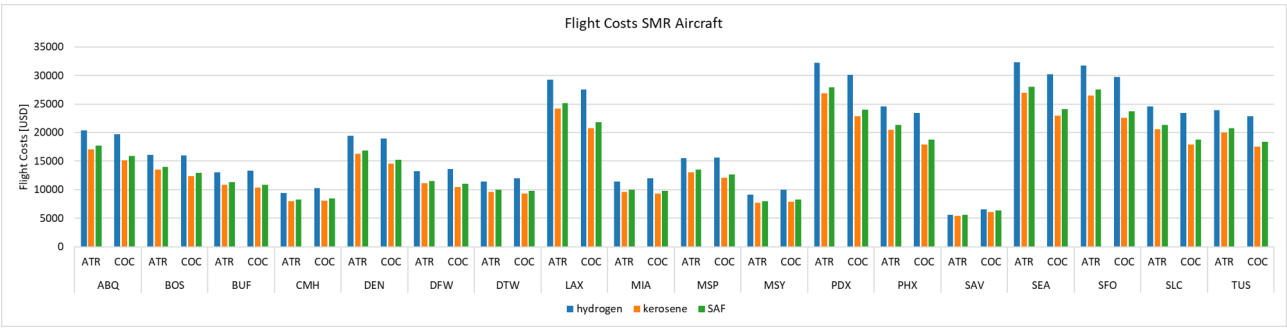

Figure 27: Flight costs for SMR aircraft.

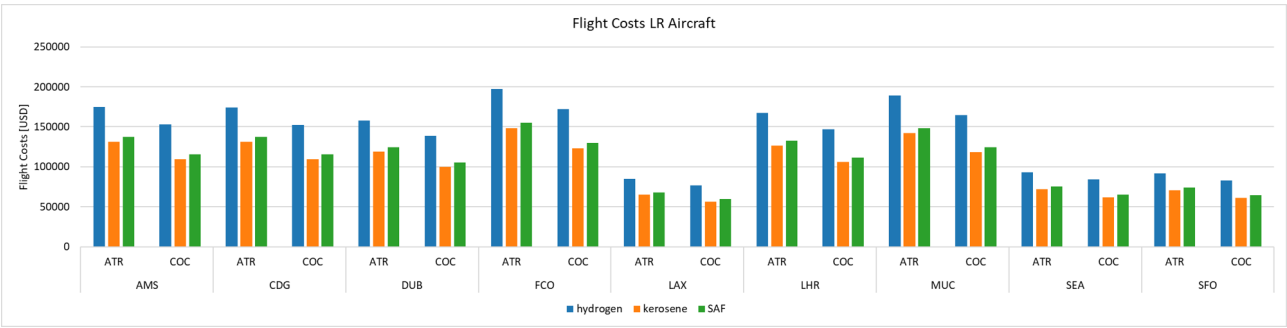

Figure 28: Flight costs for LR aircraft.

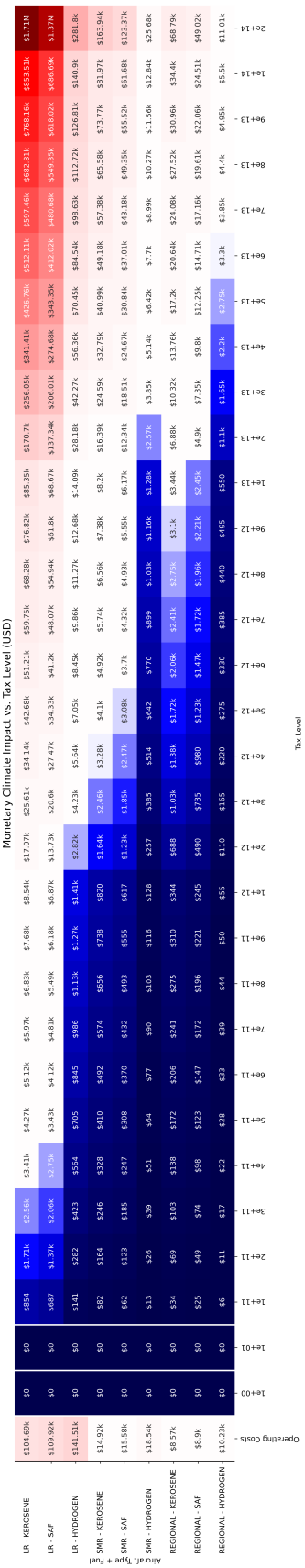

Figure 29: Average monetary values for the different aircraft types and fuel types. The climate impact is averaged over the destinations covered per aircraft type, for each year, departure hour, and optimization (COC and ATR). On the left, the average operating costs without climate tax are presented, to allow for visual magnitude comparison between the operating costs and climate impact tax for different tax values.

D Climate Impact Plots

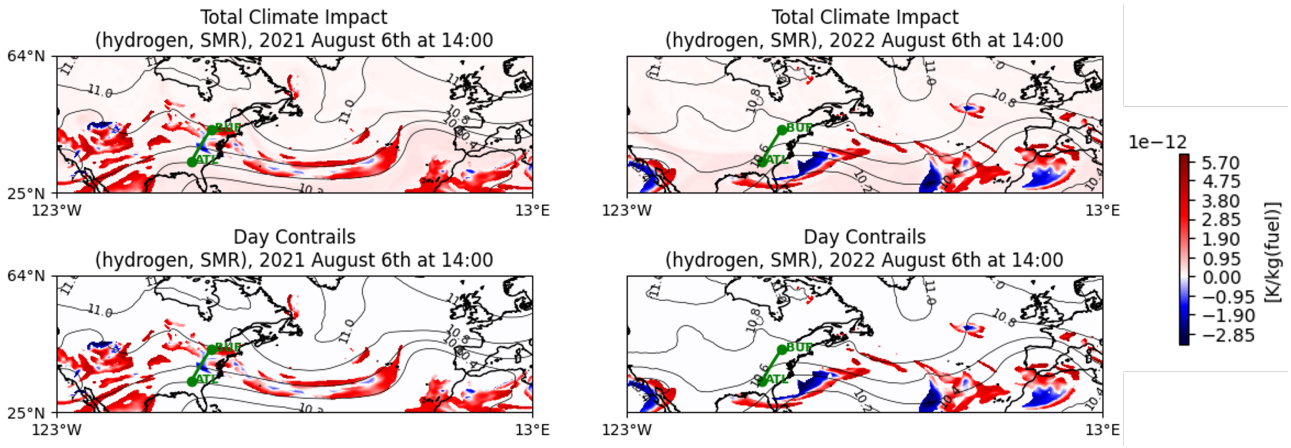

Figure 30: The total climate impact (upper) and the climate impact from day contrails (lower) are presented. On the left, the situation on August 6th at 14:00 UTC for 2021 is presented, and on the right, the same situation for 2022 is presented. The flight from ATL to BUF is visualized to show that the flight leg in 2021 passes through blue (cooling), which results in an overall negative (cooling) climate impact.

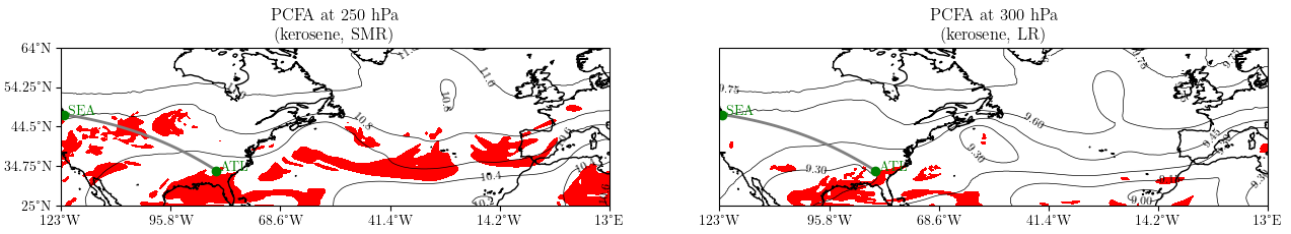

Figure 31: Persistent Contrail Formation Areas (PCFAs) are plotted for the LR and SMR kerosene flight from ATL to SEA, on August 7th 2023, at 04:00 UTC.

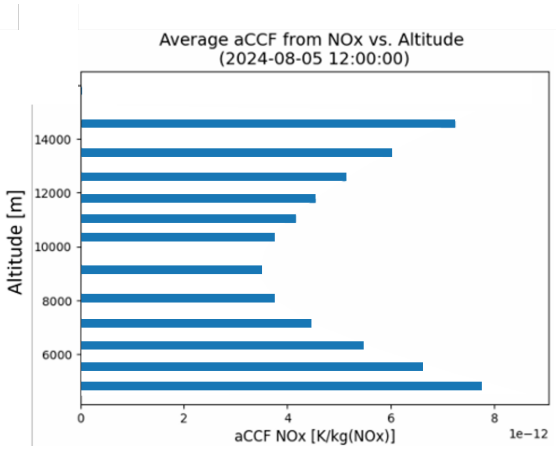

Figure 32: Average climate impact (F-ATR$_{20}$) from NO_x at different pressure levels in [K/kg(NO_x)], before multiplication with O_3 scaling factors. August 5th, 2024, at 12:00 UTC.

E Flight Paths with Climate Impact Tax Value of 3e+12 USD/K

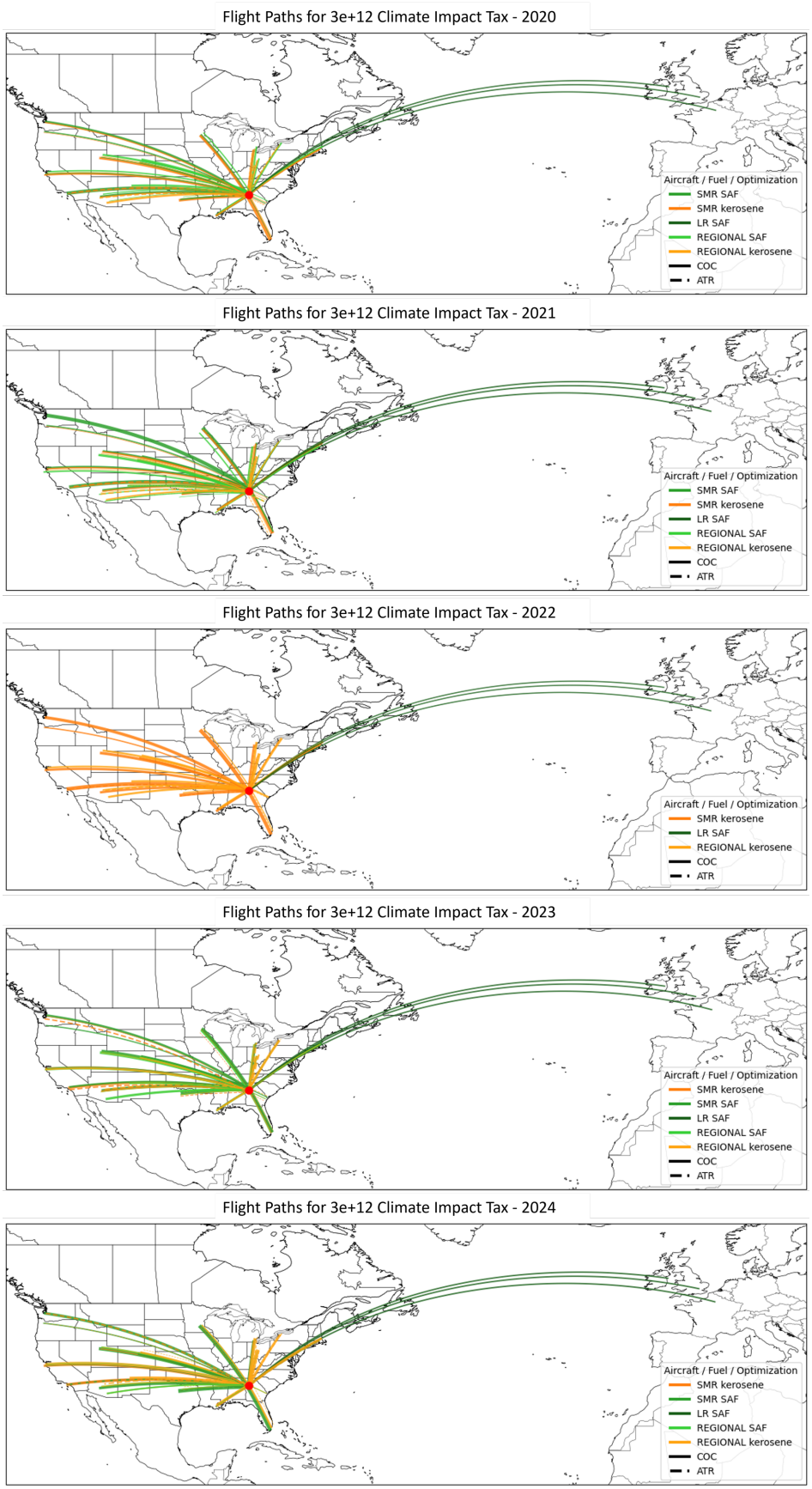

Figure 33: Visualization of the kerosene and SAF flight legs, for years 2020-2024, for climate impact tax value 3e+12 USD/K.

F SAF Usage per Airport

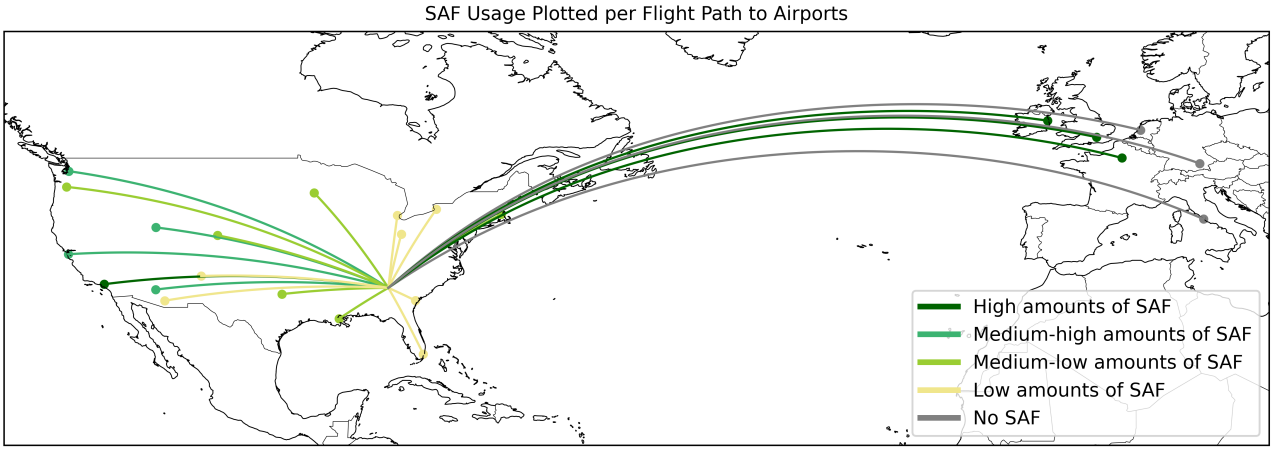

Figure 34: The SAF usage per airport. The categories are generalized based on Figure 16.

G Sensitivity Analysis for Effect of NO_x Calculations in the Fleet Allocation

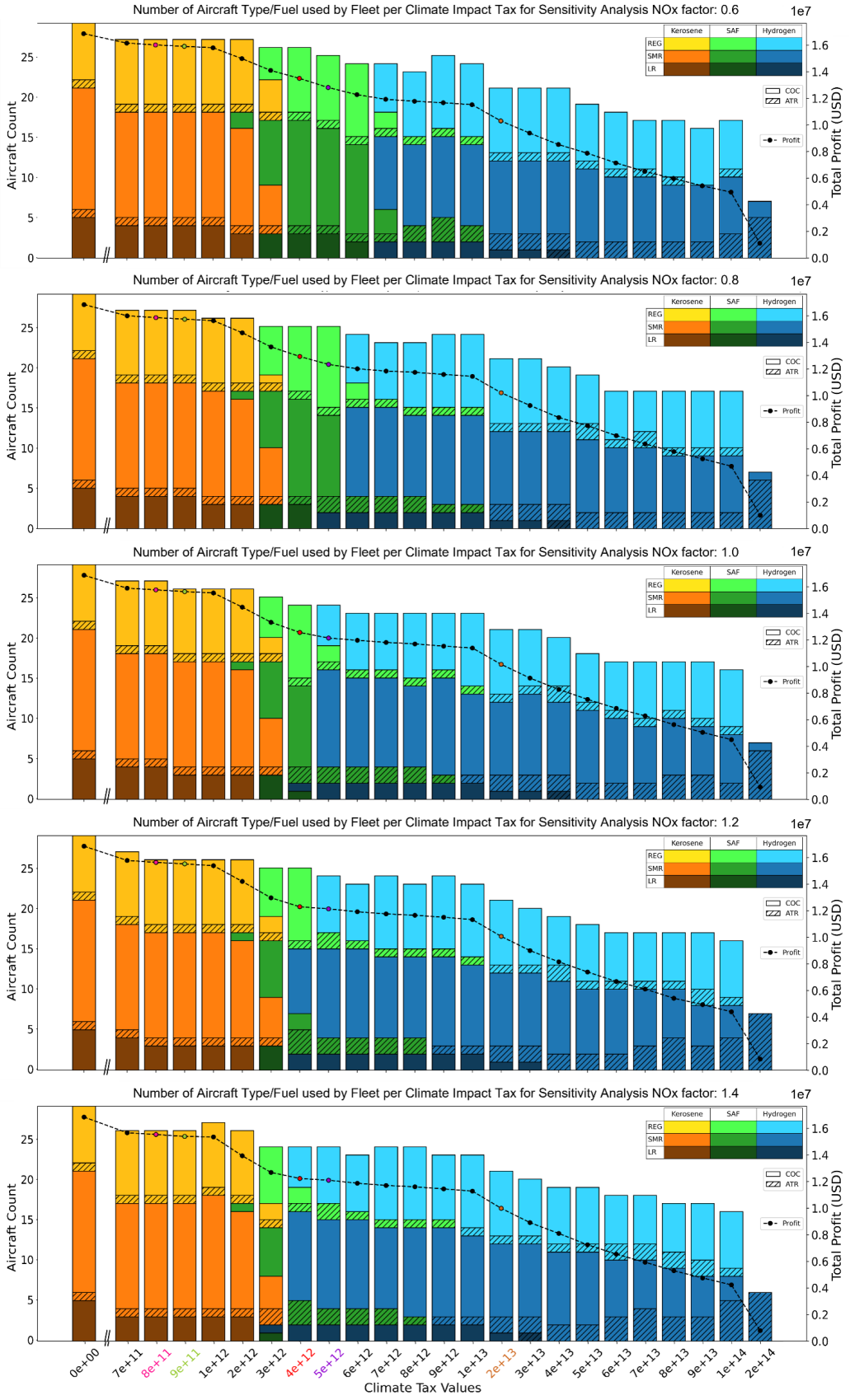

Figure 35: Sensitivity analysis for the different NO_x scaling factors. Stacked bar plots for the fleet composition in 2020 for different climate impact tax values.

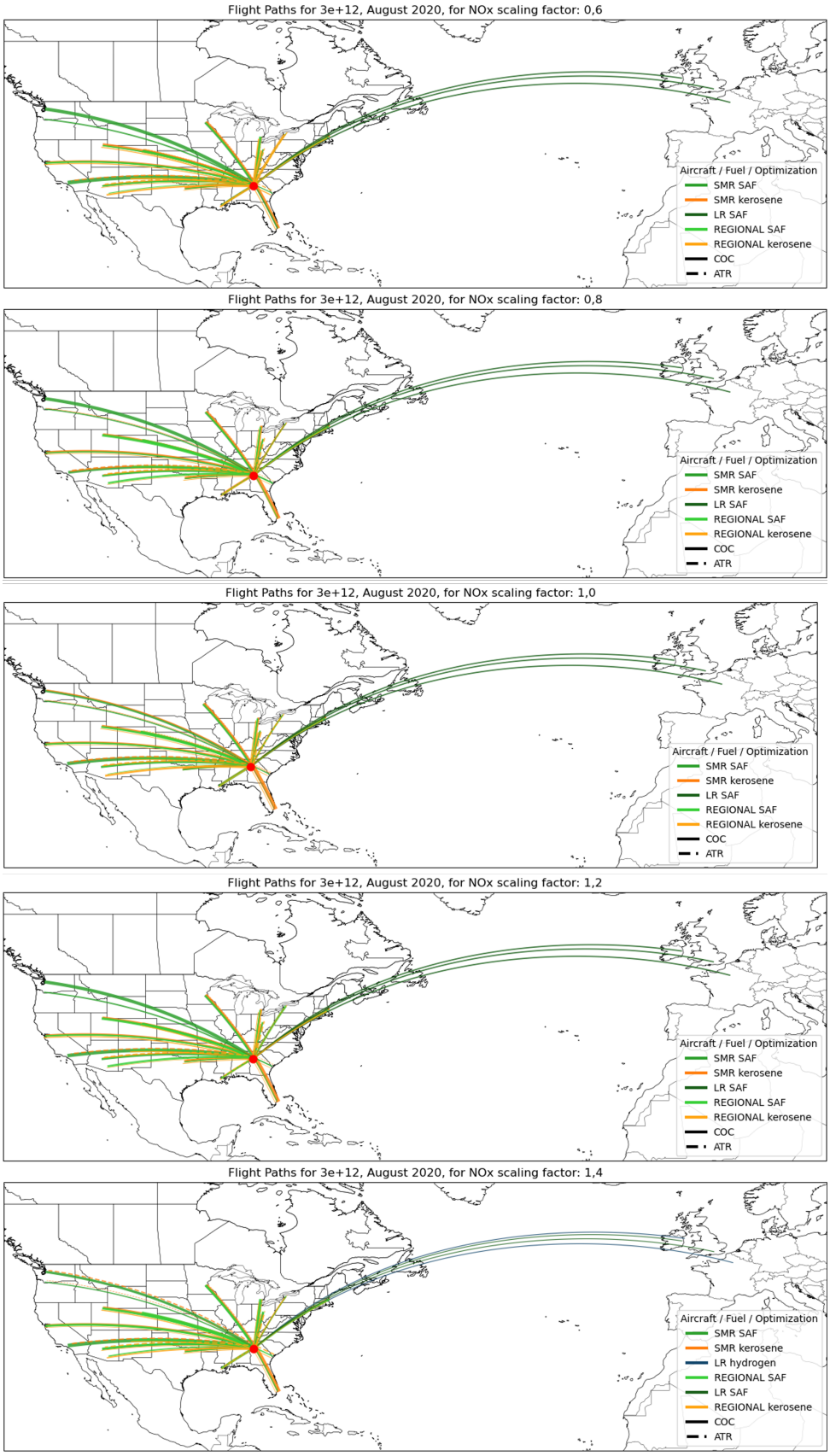

Figure 36: Sensitivity analysis for the different NO_x scaling factors. The flight paths for climate impact tax 3e+12 USD/K are plotted.

H Flight Costs for Increased Fuel Prices for the Sensitivity Analysis

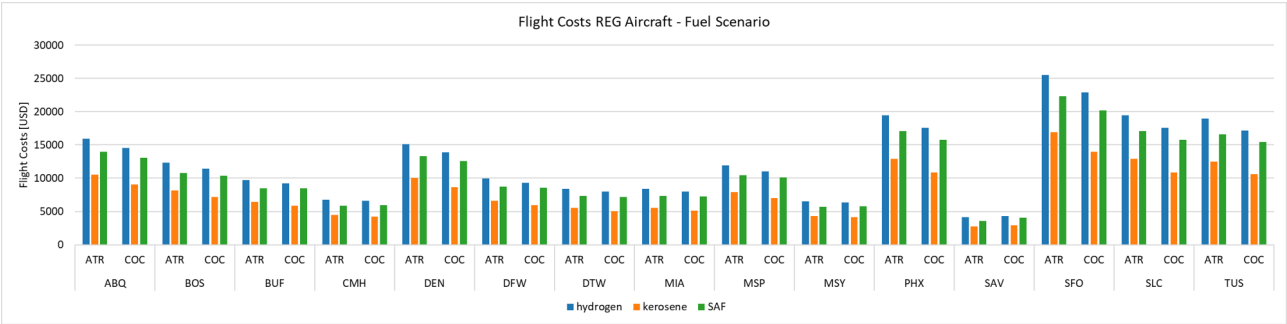

Figure 37: Flight costs for REG aircraft for fuel sensitivity analysis.

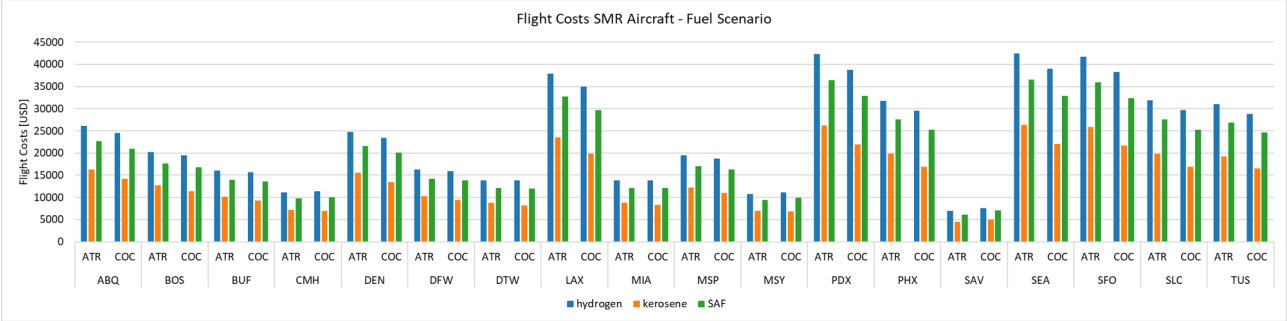

Figure 38: Flight costs for SMR aircraft for fuel sensitivity analysis.

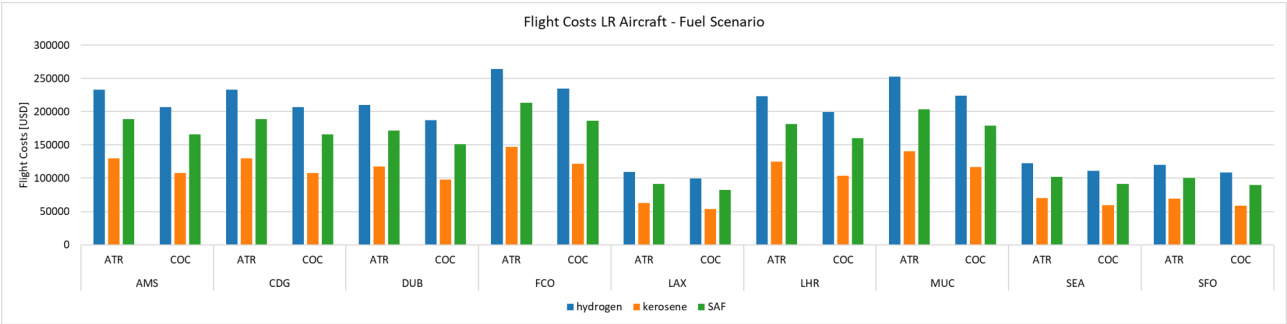

Figure 39: Flight costs for LR aircraft for fuel sensitivity analysis.

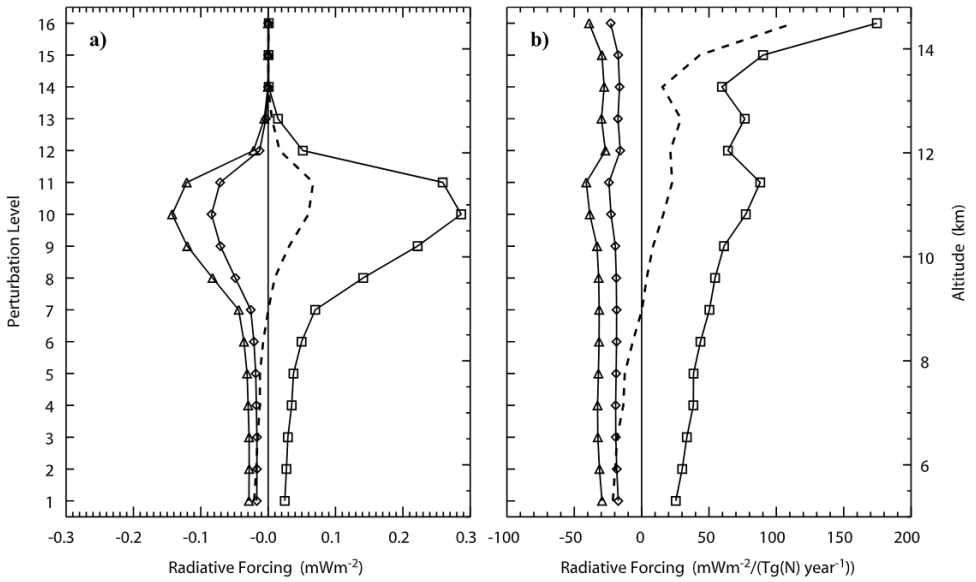

Figure 40: Radiative forcings due to changes in NO_x emissions. O_3 is represented with squares; CH_4 with triangles; PMO with diamonds; net forcing from NO_x with dashed line. Figure from Reference [46].

Table 11: Comparison of the characteristics of CCFs and aCCFs. Table from Reference [54].

	CCF	**aCCF**
Characteristics		
Meteorology	8 specific simulated days	Arbitrary days
Horizontal coverage	North Atlantic	30°N 90°N
Implementation	Unflexible fixed dataset	Easily implemented in numerical weather prediction models
Extension	Large computational effort with limited applicability to the chosen date or area	Large computational effort and additional work to derive new algorithms for other areas; once established, highly flexible in application
Verification	Comparison of general patterns with literature	Dedicated numerical simulation with a climatechemistry model, including a traffic simulator and dedicated diagnostics
Quality		
CO_2	++	++
H_2O	++	++
NO_x -O_3	+	∘
NO_x -CH_4	+	–

II

Literature Study

1

Summary

The aviation industry needs to change to become more sustainable. Researchers are exploring different ways to accomplish this by studying alternative fuel types, novel aircraft designs like climate-optimized aircraft designs and aircraft suitable for those alternative fuels, and operational mitigation measures. The proposed research combines these three and aims to explore the research gap created through this combination.

The climate impacts from aviation can be divided into CO_2 and non-CO_2 emissions. The latter depends not only on the amount of fuel burned, but also on the altitude, latitude, time of emission, and atmospheric conditions. Different fuel types have different climate impacts, such as a lowered ice particle count, and thus different radiative forcings for contrails from sustainable aviation fuel (SAF) and liquid hydrogen combustion. Teoh et al. [94] argue that drop-in SAF is heavily constrained in the near future, and careful allocation of the available fuel can significantly reduce the climate impacts from non-CO_2 emissions.

The goal is to examine changes in the fleet and the overall profit and climate impact by allocating different types of aircraft employing different fuels to a network. Kerosene, SAF, and liquid hydrogen are considered, as well as cost and climate-optimized aircraft. The CLIMaCCF model [21] could be used to calculate the climate impacts of flights, which would be converted to monetary values using a climate impact tax. This, together with the cost calculations, provides the input for the fleet allocation model, which uses dynamic programming to maximize the overall profit.

2

Introduction

The year 2024 has been reported the warmest year on record by the World Meteorological Organization (WMO) with 1.55° C ± 0.13° C above the 1850-1900 average [102]. They highlight that increased efforts are necessary to reach the goal of the Paris Agreement: to keep the global average temperature well below 2° C [75].

In 2005, Lee et al. [55] found that radiative forcing from the aviation sector contributed 4.9% (range 2-14%, with 90% likelihood range) to the net global anthropogenic radiative forcing. Later, in 2018, the net radiative forcing due to aviation was estimated to be around +100.9 $(mW)m^{-2}$ (range 55-145, with 95% likelihood range), with more than half of the radiative forcing contributions due to non-CO_2 effects [54]. With a global growth forecast of 3.8% passenger increase per year from 2023 to 2043 [40], the impact of aviation on the climate is expected to grow and continue in the next decades. This means that there is a strong need for the aviation sector to reduce its climate impact and become more sustainable.

Aircraft emissions influence anthropogenic climate change due to CO_2 and non-CO_2 effects. The CO_2 emissions from kerosene aircraft on the climate are proportional to the amount of fuel burned. Increased atmospheric CO_2 concentrations contribute to global warming, and have other negative effects on Earth's climate, such as rising sea levels, ocean acidification, decreased water supplies, severe droughts and increased health risks for humanity and nature (e.g. [56, 90]). The complete carbon cycle is complex; however, the radiative forcing from CO_2 has been estimated with high confidence levels: 34.3 mWm^{-2} (range 29-40 mWm^{-2}, with a 95% likelihood range). CO_2 can remain in the atmosphere for thousands of years, and the main long-term natural carbon sinks are the absorption by the ocean, the reaction with $CaCO_3$, and the reaction with igneous Rocks [8].

Climate effects from non-CO_2 emissions are more complicated, as they significantly depend on the altitude, latitude, time of emission, and atmospheric conditions (e.g. [26, 83]). These non-CO_2 effects include, but are not limited to, contrail formation, nitrogen oxides (NO_x) emissions, and water vapor (H_2O) emissions. Contrail formation occurs if the mixture of exhaust and ambient air becomes saturated with respect to water to form droplets, which sequentially freeze due to cold atmospheric conditions. If the ambient air is saturated with respect to ice, the contrails can become persistent. Persistent contrails remain in the atmosphere for more than 10 minutes and can last up to several hours [40]. Such contrails can form contrail-cirrus clouds when spread by winds, covering up to a few kilometers in width. They can also interact and merge with other induced cirrus clouds or natural clouds. Contrails usually have a net positive (warming) effect on the surface temperature of the Earth [54]; however, in particular cases, the effect can be negative (cooling) [103]. Calculations of the climate impact of contrails involve large uncertainties [54]. Moreover, NO_x emissions influence various other atmospheric concentrations in the atmosphere, which induce cooling and warming effects. Cooling effects include a decrease in methane (CH_4), a long-term decrease in stratospheric ozone, and a decrease in stratospheric water vapor, whereas the warming effect of NO_x emissions is caused by the short-term increase in tropospheric ozone (O_3). The net effect of these NO_x emissions is positive, thus contributing to global warming [54]. The atmospheric chemistry in the troposphere resulting from NO_x emissions is shown in Figure 2.1. Lastly, H_2O emissions also result in a net warming effect through a combination of different warming and cooling effects: a higher concentration of water vapor, a greenhouse gas (GHG), in the atmosphere increases the radiative forcing of the atmosphere (warming); a higher concentration in-

creases the formation of HO_x which depletes the stratospheric ozone concentration (cooling); and a higher concentration increases the probability of contrail formation (net warming) [55].

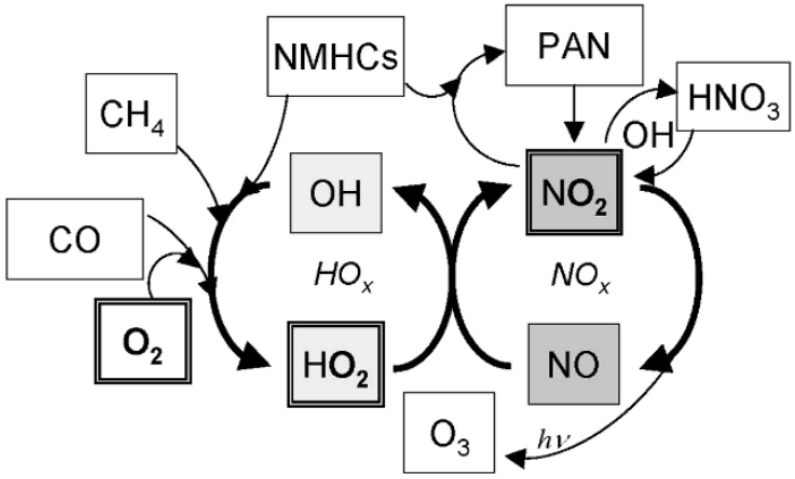

Figure 2.1: Main tropospheric chemical reactions from Reference [30]

Given the complexities of non-CO_2 climate impact mitigation, there are various research areas, which can be categorized into three main fields: 1) the research towards the use of more sustainable fuels (e.g. [41, 71]), 2) the design of climate-optimized aircraft or aircraft employing novel fuels (e.g. [20, 76]), and 3) operational climate impact mitigation measures. The latter includes improved route planning (e.g. [31, 62, 94]), and emission regulations, such as the carbon offsetting and reduction scheme for international aviation (CORSIA) [41].

In line with these developments, this thesis aims to bridge the knowledge gap between these three research areas. Specifically, this research aims to explore how the climate impact of aviation can be reduced using eco-efficient fleet allocation, using climate-optimized aircraft and/or aircraft employing alternative fuels. This study considers two types of fuel next to kerosene: sustainable aviation fuel (SAF) and liquid hydrogen (LH_2), and two types of aircraft designs: climate and cost-optimized aircraft. Through the fleet allocation model, the changes in the fleet, overall climate impact, and costs are examined.

This research proposal continues with a review of the literature in chapter 3 to provide the relevant background information, followed by chapter 4, which describes the identification of the research gaps and the proposed research questions. The methodology is explained in chapter 5 and in chapter 6 and chapter 7, the analysis framework with the expected results and the timeline of the project are discussed, respectively.

3

Literature Review

Sustainable air transport has been studied for several decades, and this chapter aims to provide the relevant state-of-the-art background information. Sustainable aircraft developments are presented in section 3.1, and the use of different fuel types and their emissions and effect on contrail formation are discussed in section 3.2. Other sustainable measures, in addition to sustainable aircraft and fuel types, are described in section 3.3, and the different climate metrics are discussed in section 3.4.

3.1. State-of-the-art for Sustainable Aircraft

There are various developments towards more sustainable aircraft, such as using different fuel types, like hydrogen, SAF, electricity, or a hybrid thereof.

Cabrera and Sousa [16] reviewed the state of alternative aviation fuels in 2022 for solutions toward carbon-neutral aviation. They find that hydrogen and electric aircraft would be the preferred options, because the contribution to global carbon emissions is zero with these aircraft, given that hydrogen and electricity production and transportation are green. However, these technologies require substantial changes to aircraft design and airport infrastructure, and therefore, short-term fleet-wide implementation of these aircraft types is unrealistic. Furthermore, they argue that electric aircraft have to carry a larger weight penalty due to battery storage. Current development plans for future large electric or hybrid electric commercial aircraft are presented in Table 3.1.

Drop-in SAF is an alternative solution for the aviation industry. SAF is a certified jet fuel up to a 50% blending ratio with kerosene, but this also depends on the type of SAF. It is different from conventional jet fuel, as it is derived from renewable sources, such as cooking oils, fats, plant oils, waste, etc [74]. SAF is blended with kerosene (called drop-in SAF) to reduce the climate impact and net-CO_2 emissions from aircraft. It is argued to be the best solution for aviation's climate impact reduction for short-term implementation, as it requires minimal changes to the aircraft and infrastructure [16]. On the other hand, SAF is scarce because the production levels are low and expensive. The production capacity is currently being improved to meet the RefuelEU aviation regulations [79], which forces EU airports to use fuel containing at least 2% SAF in 2025, 6% SAF in 2030, and 70% SAF in 2050.

The even distribution of SAF among aircraft may not be the most effective way of allocating the available SAF and reducing the climate impact. As CO_2 scales with fuel burn, the SAF blending ratios do not influence the climate impact from CO_2 emissions as long as the same amount of SAF is allocated. On the other hand, for non-CO_2 effects, this cannot be said. For maximum reduction of non-CO_2 climate effects, a careful allocation is necessary because the magnitude of the effects depends on the time, location, altitude, and atmospheric conditions (e.g. [26, 48, 94]). Thus, equally dividing the SAF among all flights might not be the most effective way to reduce the climate impact. Further information on this is presented in subsection 3.2.2.

Table 3.1: Development plans for future electric or hybrid large commercial aircraft, adjusted from Reference [22]

Organization/Project	Seats	Type	Range	Target date	Source
Electric Aviation Group	100	Hybrid H_2-electric	Regional	2028	[97]
Wright	100	Full electric	1 hour flights	2027	[98]
Boeing sugar VOLT	135	Hybrid electric	Regional	2040	[22]
Elysian	90	Electric	800 km	2033	[23]
JetZero	250	Hybrid-electric	5000 nm	2030	[46]
Heart Aerospace ES-3	30	Electric (hybrid)	200 km (800km)	2029	[38]
MAEVE Jet	76-100	Hybrid-electric	950-1450 nm	2033	[58]

3.2. Different Fuel Types

With the increased pressure to develop climate-neutral aircraft to mitigate aviation's climate impact, the introduction of these new aircraft types in the near future is realistic. In section 3.1, the current state of sustainable aircraft development is explained, which shows that future fleets may consist of electric, hydrogen, drop-in SAF, and kerosene aircraft, or a combination (hybrid). These aircraft use different fuel types: kerosene, drop-in SAF, or hydrogen. The emissions of the different fuel types are described in this section, and the differences in contrail properties are discussed. Full electric aircraft have zero in-flight emissions and are therefore not included in this section. Moreover, in the next chapters, the assumption is made that the powertrain makes use of turbofan engines, since it is the most widely used propulsion technology for commercial aircraft [77].

3.2.1. Emissions

Kerosene

The ideal combustion of kerosene leads to the production of CO_2 and H_2O. However, during actual combustion (incomplete combustion), there are various other byproducts: unburned hydrocarbons, NO_x, CO, soot, aerosols, and SO_x [28]. CO_2 and H_2O are proportional to the amount of fuel burned, but the other molecules depend on factors such as fuel quality, flight altitude, and thrust settings. The optimal altitude for kerosene aircraft is complicated, as the impact and magnitude differ per emission. For example, the effect of CO_2 is independent of the emission altitude; however, the amount of emissions generally increases with decreasing altitude. Moreover, at lower cruise altitudes, the effect of NO_x increases slightly, leading to a higher global warming potential [92]. On the other hand, the effect of water vapor decreases with decreasing altitude. These contributions are contrasting, and the trade-off between them leads to the optimal cruise altitude.

Hydrogen

Aircraft using hydrogen fuel produce no CO_2, SO_x or black carbon [40]. Although the use of such aircraft eliminates the climate effects of these emissions, the formation of contrails, H_2O emissions, and NO_x emissions are different from the kerosene aircraft and the effects cannot be neglected (e.g. [54, 71]). For example, hydrogen combustion leads to increased levels of H_2O. Moreover, the contrail characteristics change compared to kerosene aircraft, because hydrogen engines generally do not emit soot particles. However, during hydrogen (H_2) combustion, NO_x and H_2O particles are produced, which lead to the formation of OH. OH is highly reactive and can form compounds such as nitric acid and ammonia [11], which in turn can form ultrafine volatile particles (UFPs) such as volatile ammonium nitrate. These contribute to contrail ice crystal formation by increasing the ice particle number, because water vapor can condense on these particles and freeze. The formation process from H_2 combustion to UFPs is not sufficiently understood [11], as well as the significance of UFPs concerning contrail formation. Current studies on the climate impact of contrails from H_2 combustion rely on multiple assumptions that are found not to be completely accurate in reality, such as assuming a fixed aerosol number concentration in the ambient atmosphere [11] or assuming uniform mixing of particles across the exhaust plume cross-section [60].

Moreover, increased OH leads to the depletion of methane (CH_4) and the production of tropospheric ozone (O_3). At lower altitudes, the climate impact is generally smaller because precipitation decreases the lifetime of H_2O [92]. At altitudes below 8-10 kilometers, the effects of H_2O are insignificant, as clouds and precipitation are very common. The optimal cruise altitude for hydrogen aircraft is more dependent on the amount of water vapor emissions [92], compared to kerosene aircraft, where the optimal altitude also considers the impact of the other emissions.

The storage of hydrogen has various practical complexities. It must be stored as a compressed gas or

as cryogenic liquid (LH_2). Hydrogen has a low energy density with respect to volume compared to kerosene and thus requires a lot of volumetric storage space. The hydrogen is pressurized to either a gas or a liquid. Highly compressed hydrogen requires specialized tanks, and liquid hydrogen requires an additional heat management system to prevent the liquid from boiling, as this would increase the pressure even further. The most efficient way to design a tank, equipped to withstand high pressures and insulate against ambient temperature, is a tank with a low surface area compared to volume capacity [1]. An example is a spherical tank; however, the design of the aerodynamics of an aircraft is more complicated with this shape.

The two most common ways to use hydrogen for aircraft propulsion are through turbo-machinery or hydrogen fuel cells. Turbofans and turboprops would need to be redesigned to suit hydrogen; however, it is possible to convert existing machinery for kerosene to hydrogen ([13] as cited in [1]). Hydrogen fuel cells convert hydrogen to electricity to power the aircraft with electric propulsion. The downside of the use of hydrogen fuel cells is that it is difficult to produce electricity with sufficient power, and compared to hydrogen combustion, the energy efficiency is lower, requiring a larger amount of hydrogen on board. On the other hand, the greatest upside to hydrogen fuel cells is that they generally do not produce any NO_x emissions [1]. This means that hydrogen combustion is preferred for medium to long-range aircraft, whereas fuel cells are more often used for concepts for regional or short-range aircraft (e.g. [1, 22, 95]).

Sustainable Aviation Fuel

The International Civil Aviation Organization (ICAO) adopted the Carbon Offsetting and Reduction Scheme for International Aviation (CORSIA) [1]. As the name implies, this is a carbon offsetting scheme, which plans to regulate the CO_2 emissions from the aviation sector for all member states. One way to do this is to make use of sustainable aviation fuel (SAF). The ICAO defines renewable fuel as SAF (or CORSIA SAF) when it meets specific criteria. Such criteria include that the life cycle should achieve at least 10% of greenhouse gas (GHG) emissions reduction, the production should not be made from biomass sourced from areas with high biogenic carbon stock, the production should maintain water quality, soil health, biodiversity, and minimize negative effects on air quality [41].

SAF is currently blended with conventional kerosene, because of the differences in chemical composition. A SAF-kerosene blend is referred to as 'drop-in SAF', but this is usually implied when referred to as SAF. The blending ratios are approved by the European Union Aviation Safety Agency (EASA) and the Federal Aviation Administration (FAA) in the US for up to 50%, but developments towards the use of 100% SAF are being made [2, 14]. SAF is an appealing option for the aviation industry as it reduces the net CO_2 emission and requires little to no adjustments to the aircraft and infrastructure (e.g. [5, 16]). On the other hand, the effects from emissions from SAF combustion, such as NO_x, black carbons, H_2O, contrails, and aerosols remain, and SAF is only to a certain extent more sustainable than conventional aviation fuel. Important to note is that the climate impact from contrails may be lower than for kerosene aircraft due to changes in the exhaust particles, such as changes in mean particle size, contrail lifetime, and sedimentation rate [94]. A more elaborate discussion on the differences in contrail properties is presented in the next section.

3.2.2. Contrail Cirrus

The words *contrails*, *persistent contrails*, and *contrail cirrus* are often used in the literature. In general, *contrails* is used as an abbreviation of the other two, or to describe the characteristics or the formation process; *persistent contrails* applies to contrails remaining for at least 10 minutes in the atmosphere; and *contrails cirrus* usually implies persistent contrails as well as remaining cirrus clouds from aircraft.

Contrail formation depends on the exhaust temperature and ambient temperature and relative humidity [85]. Contrail properties can differ for different emissions, such as the number of formed droplets, the number of ice particles, the ice mass, the size of the particles, and the optical visibility of the contrail [94].

Kerosene

The exhaust from conventional kerosene aircraft can form contrails, depending on the atmospheric conditions and aircraft exhaust characteristics. Schmidt [84] and Appleman [7] were the first to formulate the criteria for contrail formation, called the Schmidt-Appleman Criterion (SAC) [29, 85]. This states that contrails are formed when the exhaust of the engine is hot and humid; the atmospheric conditions are dry and cool; the exhaust mixes with the ambient air; the mixing air is saturated with respect to water to form water droplets; and the temperature is low enough for formed water droplets to freeze [29]. In Figure 3.1 the Schmidt-Appleman criterion is depicted. The right straight dotted line shows the maximum temperature for

[1] https://www.icao.int/environmental-protection/CORSIA

which contrail formation can occur, and the left straight dotted line shows the mixing line. The slope (G) of these lines can be calculated using the (approximated) formula in Equation 3.1 [29]. M(X) represents the molar mass of X in kg/kmol, EI(X) is the emission index in kg(X)/kg(fuel), p_a is the atmospheric pressure (Pa), c_p is the specific heat capacity (J/kg/K), Q is the specific heat content (J/kg), and μ is the aircraft propulsion efficiency (-).

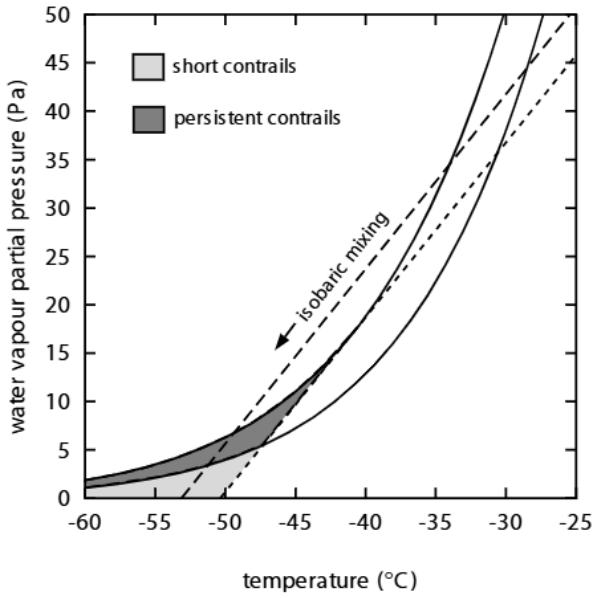

Figure 3.1: Sketch of the Schmidt-Appleman Criterion. The upper curved line represents the saturation curve with respect to liquid water, and the lower line represents the saturation curve with respect to ice. Figure is from Reference [27].

$$G \approx p_a c_p \frac{M(\text{air})}{M(H_2O)} \frac{EI(H_2O)}{(1-\mu)Q} \tag{3.1}$$

When the warm exhaust cools down, water forms droplets on non-volatile particles such as soot and ambient aerosols. When the atmospheric temperature is low enough, usually below -38° C, these droplets freeze and form a contrail. When the end of the mixing line ends in the dark gray region in Figure 3.1, the contrail becomes persistent. This is because the ice particles do not dissolve in the atmospheric air when the air is saturated with respect to ice. Persistent contrails remain in the atmosphere for a minimum of 10 minutes [40], and they generally have a warming effect on the Earth (e.g. [54, 103]). Lee et al. [54] showed that the confidence levels for radiative forcing and effective radiative forcing are low. They argue 111.4 $(mW)m^{-2}$ for radiative forcing and 57.4 $(mW)m^{-2}$ for effective radiative forcing, with 95% confidence intervals of [33,189] $(mW)m^{-2}$ and [17,98] $(mW)m^{-2}$ respectively. Effective radiative forcing considers the direct and indirect effects of emissions, such as changes in cirrus clouds or atmospheric compositions of other molecules, whereas radiative forcing only examines direct effects. Both show a net warming effect on the climate.

Hydrogen

The impact of hydrogen aircraft on climate is not fully understood, because the radiative impact depends significantly on the formation of the contrails, and the climate impact of the contrails is difficult to define, as it depends on multiple factors such as the optical depth of the contrails, the lifetime, and the surrounding clouds ([12] as cited in [48]). Kaufmann, Dischl, and Voigt [48] argue that the climate impact from hydrogen-powered aircraft, similar to kerosene aircraft, depends on the propulsion type, season, region, and flight altitude. These conclusions are expected because the dominant radiative forcing factors from conventional aircraft are CO_2, contrail cirrus, NO_x and H_2O, and the latter three are also relevant for hydrogen aircraft. Kaufmann, Dischl, and Voigt [48] perform a statistical evaluation of the probability of contrail formation based on the ambient atmospheric conditions for kerosene and hydrogen-powered aircraft. They argue that the probability of contrail formation for hydrogen and kerosene propulsion is similar, as ambient temperatures are usually low enough for water droplets to freeze, and that the formation is typically dependent only on the ice-supersaturated regions (ISSRs). They argue that only when the atmospheric conditions are close

to the threshold conditions for contrail formation, a difference of up to 15% in contrail cirrus frequency can be found, due to the difference in water vapor in the emissions. They assume hot gaseous emission, similar to kerosene exhaust, whereas Adler and Martins [1] provide further insights into the impact of cooler exhaust on the climate. They argue that hydrogen can be burned leaner than kerosene to reduce NO_x production with lowered exhaust temperature ([49] as cited in [1]), however, this simultaneously increases the contrail formation probability [36].

Ström and Gierens [91] presented the first numerical simulation of contrails from LH_2 combustion. They compared the contrails from LH_2 combustion to kerosene for two different temperatures representing different flight levels, at a constant relative humidity of 110% with respect to ice. They found that for both cases, the contrails from hydrogen combustion are optically thinner (2D evaluation) and showed lower ice crystal number density; however, they measured similar amounts of ice mass. They also argue that the sedimentation of LH_2 contrails is not significantly faster than kerosene contrails, even though the average ice crystal size is 4 to 6 times larger. This study does not consider the effect of background ambient particles, which have been found to influence the contrail formation and characteristics [11]. Bier et al. [11] model ambient aerosol particles back into the plume, instead of keeping the concentration of aerosol particles fixed. They find that the ice crystal number is reduced by 80-90% and that the optical visibility is significantly reduced. By comparing the two combustion types, they find that for kerosene, the number of ice particles depends on the amount of emitted soot particles at low enough temperatures, whereas the number of ice particles for LH_2 combustion continues to increase when temperature decreases, because of the high amount of emitted of water vapor and the entrainment of aerosol particles back into the plume. Moreover, they argue that contrail formation starts at temperatures around 10 Kelvin higher than for kerosene contrail formation, which means contrail formation can occur at lower altitudes for LH_2 aircraft, and that the probability of persistent contrail formation is higher for LH_2 aircraft. This research is in line with other findings (e.g. [48, 85]). Megill and Grewe [66] argue that LH_2 aircraft would significantly increase persistent contrail formation, but they stress the importance of recognizing the difference between persistent contrail formation and the resulting contrail cirrus coverage and climate impact. They show that LH_2 aircraft could increase persistent contrail formation by 71.4%, and Rap et al. [78] argue an increase of 70%, but there is a consensus that this does not mean that the resulting radiative forcing and temperature change increase similarly [66, 78, 85].

Sustainable Aviation Fuel

The use of drop-in SAF has been found to increase persistent contrail occurrence compared to kerosene fuel; however, it increases the mean ice particle size, which in turn shortens the contrail lifetime as it increases the sedimentation rate. The slight increase in the probability of contrail occurrence due to a higher amount of water vapor emission is counteracted by the larger decrease in contrail lifetime due to lower amounts of non-volatile particle matter and larger ice particle size [94]. Teoh et al. [93] argue that around 12% of all flights over the North Atlantic are responsible for around 80% of the net radiative forcing due to contrail formation, and Teoh et al. [94] elaborate on this by pointing out that the availability of SAF is heavily constrained in the near future and that careful allocation of the available SAF to flights could therefore mitigate significant climate impact. They conclude that if the available SAF is provided with higher blending ratios to the flights responsible for the most strongly warming contrails, climate impacts can be decreased by a factor of 9-15 compared to uniformly distributing the available SAF among aircraft.

3.3. Sustainable Operational Measures

There are other methods besides the use of different fuel types and aircraft designs to reduce the climate impact of aircraft. One way is to reroute aircraft to avoid climate-sensitive regions. These regions refer to ice-supersaturated regions (ISSRs) where the probability of contrail formation is high. Studies have shown that rerouting aircraft to avoid these regions can reduce the climate impact (e.g. [31, 62, 69, 88]). However, the results come with high uncertainties, because it is very difficult to predict these ISSRs [39]. The climate-sensitive regions can be approximated by a time resolution of a month, leading to less accurate results [70].

Another method is flying at lower altitudes (e.g. [26, 63, 92]). Hydrogen aircraft could fly at or below 8-10 kilometers to significantly reduce the climate impact, as precipitation and cloudiness are very common at this height. For conventional turbofan aircraft, the altitude impacts fuel usage: decreasing the altitude decreases fuel efficiency. Therefore, the optimal altitude is a careful trade-off between the climate impacts of different emissions [63].

Formation flying is another example of an operational measure to reduce the climate impact. Dahlmann et al. [18] propose a complete assessment of the total climate impact of formation flights, including CO_2 and

non-CO_2 effects (including contrail formation). They argue that the climate impact (ATR_{100}) can be reduced by about 23% using formation flying. The idea originated from birds known to fly together in V-shaped formations to save energy. While the flight distance increases 1-3% as aircraft detour past rendezvous points to form a formation with another aircraft, the overall emissions and climate impact are reduced. The downside of this proposed mitigation method is that it could only be applied to a small fraction of flights, based on current flight plans ([61] as cited in [18]).

The use of intermediate stop operations (ISO) is another technique that has been researched in the past decade. ISO have long-range aircraft land at an in-between stop for refueling. Various studies have shown that ISO reduces the total fuel burn, as well as the operating costs for the flights (e.g. [33, 53]). However, Grewe et al. [33] demonstrate a 2.3% increase in the average temperature response over 100 years (ATR_{100}) for ISO compared to conventional long-range flights, even though a 4.8% decrease in fuel consumption is observed. They argue that the increase is due to the climate impact of NO_X and H_2O emissions at higher altitudes. As the aircraft are lighter due to a lower fuel mass, the fuel-optimal cruise altitude is higher.

3.4. Climate Metrics

To quantify the climate impact of aircraft emissions (CO_2 and non-CO_2 effects) and their contribution to anthropogenic climate change, the climate impact must be expressed in terms of appropriate metrics. Megill, Deck, and Grewe [65] study climate metrics and explore their suitability for existing aircraft as well as future aircraft using alternative fuels. They compare the standard climate metric Global Warming Potential (GWP) with 6 other metrics: Radiative Forcing (RF), Efficacy-weighted Global Warming Potential (EGWP), Global Temperature Change Potential (GTP), Average Temperature Response (ATR), Integrated GTP (iGTP), and GWP* and EGWP* (which are different from GWP and EGWP as short-lived emissions are related to CO_2 pulses ([4, 17, 89] as cited in [65])).

Table 3.2: Overview of the performance of the analyzed climate metrics with respect to 4 requirements, from Reference [65]. The four requirements refer to how well the climate metric is suitable for policy makers. Neutrality refers to the bias or lack thereof towards specific aircraft design changes. Stability means that the climate metric is reliable when assessing the effectiveness of climate impact reduction policies through annual or quarterly reports. Compatibility refers to whether the new climate metric is able to perform equal to or better than the existing climate metric. The last requirement, simplicity, means how easily policymakers and non-specialists are able to grasp the meaning of the metric and interpret results.

Requirement	**Neutrality**	**Stability**	**Compatibility**	**Simplicity**
RF	Very low	Generally stable	Compatible	Simple to understand and implement
GWP	Low & consistent	Stable	Compatible	Complex to understand, simple to implement
EGWP	High	Stable	Compatible	Complex to understand and implement
GTP	Low & inconsistent	Generally stable	Compatible	Simple to understand, complex to implement
ATR & iGTP	High	Stable	Compatible	Simple/complex to understand, complex to implement
GWP*	Low & consistent	Highly unstable	Not compatible	Highly complex to understand and implement
EGWP*	High & consistent	Highly unstable	Not compatible	Highly complex to understand and implement

As shown in Table 3.2, the first 5 metrics in the table are considered possible options for the climate metric. The metrics based on the calculations used by Megill, Deck, and Grewe [65] are presented below. The start time of the emissions is presented with t_0, H is the horizon, r is the efficacy of species i ΔT is the change in temperature, and A stands for the absolute climate metric.

Radiative Forcing (RF): $$RF_H = RF(t_0 + H) \tag{3.2}$$

Global Warming potential (GWP): $$AGWP_H = \int_{t_0}^{t_0+H} RF(t)\,dt \tag{3.3}$$

Efcacy-weighted GWP (EGWP): $$AEGWP_{i,H} = r_i \int_{t_0}^{t_0+H} RF_i(t)\,dt \tag{3.4}$$

Global Temperature Change Potential (GTP): $$AGTP_H = \Delta T(t_0 + H) \tag{3.5}$$

Integrated GTP (iGTP): $$iAGTP_H = \int_{t_0}^{t_0+H} \Delta T(t)\,dt \tag{3.6}$$

Average Temperature Response (ATR): $$ATR_H = \frac{1}{\mathrm{H}} \int_{t_0}^{t_0+H} \Delta T(t)\,dt \quad (= \frac{1}{\mathrm{H}}\, iAGTP_H) \tag{3.7}$$

4

Identification of the Research Gaps

This chapter will explain the existing research gap and present the research questions for this thesis. The research gap is framed by two key areas of existing knowledge and remaining unknowns:

1. Sustainable aircraft designs employing alternative fuels are being researched and developed, but their impact on both the overall climate and profit when used in a fleet remains largely unknown.

2. There is limited knowledge on how different aircraft types and fuel types can be used by a fleet to minimize the overall climate impact.

These two aspects are in more detail discussed in this chapter in section 4.1 and in section 4.2.

4.1. Sustainable Aircraft Designs and Alternative Fuels

Proesmans [76] compares the changes in aircraft design variables when minimizing aircraft for operating cost (COC), fuel usage, and climate impact (ATR_{100}) for kerosene, SAF and LH_2. He compares these aircraft for regional (REG), medium- (SMR) and long-range (LR) categories, and he studies the trade-off between climate impact reduction and operating cost. For the kerosene aircraft, he presents Figure 4.1, demonstrating the trade-off between operating costs and climate impact (as the average temperature response in 100 years).

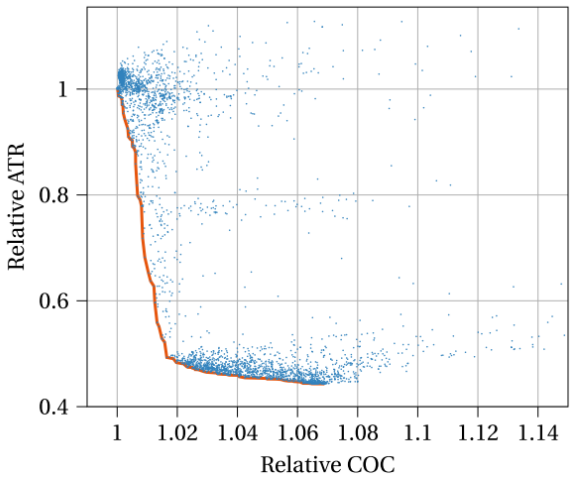

Figure 4.1: Eco-efficient distribution presenting the trade-off between operating costs and climate impact, from Reference [76].

Moreover, Proesmans [76] compared the trade-off for LH_2 and SAF aircraft, and performed a fleet allocation on a simplified hub-and-spoke network to demonstrate the changes in the number of aircraft in the fleet, when optimizing the aircraft for three objectives: minimal operating costs (COC), minimal average temperature response over 100 years(ATR_{100}), and minimizing the multi-objective (MO) corresponding to the

eco-efficient solution (the kinks in the Pareto distribution, as shown in Figure 4.1). In all optimizations, he assumed all aircraft in the fleet use the same fuel type, either kerosene, SAF, or LH_2. The differences in the number of aircraft is presented in Table 4.1, for REG, SMR and LR aircraft.

Table 4.1: Comparison of number of aircraft allocated to the fleet, from Reference [76].

		Kerosene	**SAF**	**LH_2**
COC	REG	9	9	9
	SMR	21	22	23
	LR	8	8	5
	Total	38	39	37
MO	REG	9	10	8
	SMR	21	21	24
	LR	8	8	6
	Total	38	39	38
ATR_{100}	REG	8	8	8
	SMR	28	28	25
	LR	10	10	7
	Total	46	46	40

Table 4.1 shows that more ATR-optimized (climate-optimized) aircraft are needed compared to a fleet that uses COC-optimized (cost-optimized aircraft), due to a higher block time and thus a lower productivity for climate-optimized aircraft. To keep the same level of productivity for the fleet, more aircraft are needed, which increases production and the overall climate impact. His research focused on the allocation of those aircraft types to obtain the maximum profit, but it has not considered a mixed-fleet (climate- and cost-optimized aircraft in one fleet, and/or different fuels in one fleet), nor has it looked at climate-optimal fleet allocation.

4.2. Eco-Efficient Fleet Allocation

Research by Niklass et al. [69] examines the changes in climate impact and operating costs when rerouting aircraft to avoid climate-sensitive regions. Their research introduces penalties for certain geographical locations, and their results demonstrate a similar Pareto-distribution as shown in Figure 4.1. They highlight the need to mitigate the climate impact of flights, and they focus on this by avoiding climate-sensitive regions. However, mitigation could potentially also be achieved by allocating aircraft and fuel types with lower climate impacts to these regions.

For example, Teoh et al. [94] focus on the allocation of drop-in SAF to flights to mitigate the climate impact of those flights. They argue that SAF allocation should be examined at fleet-level, because they find that allocating SAF at higher blending ratios to the few flights responsible for the highest climate impact leads to an overall climate benefit increase of a factor of 9-15 compared to uniformly distributing the available SAF over all flights. They highlight the need for intelligent allocation of the scarce amounts of SAF in the future to reduce the climate impact of aviation. These conclusions are in line with research from Burkhardt, Bock, and Bier [15], who found that only a small percentage of flights produce large-scale contrail cirrus outbreaks responsible for a high percentage of the radiative forcing. They also argue that the mitigation of the climate impact of those flights could reduce aviation's overall climate impact significantly.

Noorafza et al. [72] developed a multi-objective framework for network planning and design, incorporating the objective of minimizing the climate impact. This objective is relatively new, as airlines primarily focus on maximizing profit, which only extends to incorporating the fuel costs in the objective function (e.g., [45, 57]). Noorafza et al. [72] evaluated intermediate-stop operations and lower flight altitudes in their research, examining the climate impact reduction potential of these operational improvements. Even though their framework includes the climate impact objective, it only considers conventional kerosene aircraft and does not account for a mixed fleet with different aircraft and fuel types.

As explained before, three main research directions for the climate mitigation of aviation are sustainable fuels (e.g. SAF, hydrogen), novel aircraft designs and performance improvements (e.g. climate- or cost-optimal aircraft), and operational improvements (e.g. ISO, lower flight altitude, rerouting flight trajectories, fleet allocation). These three directions have been researched in the past; however, the use of sustainable fuels (SAF & L2), different aircraft designs (climate & cost-optimized aircraft), and climate-optimal fleet allocation altogether have not. This forms the topic of this research proposal.

4.3. Research Questions

The proposed research aims to bridge the presented knowledge gap, by researching the impact of sustainable aircraft and fuels on the climate and the overall profit at fleet level. This research will use the aircraft designed by Proesmans [76], and because the SAF-powered aircraft and kerosene-powered aircraft are nearly identical, this research will only use the LH_2 and kerosene aircraft, with the possibility to add drop-in SAF with a 50% blending ratio to the kerosene aircraft. More elaboration on the fleet selection is given in subsection 5.3.3.

The goal is: **to examine the fleet, the allocation of SAF, and the changes in the overall profit and climate impact by allocating different types of aircraft employing different fuels to a network**. An optimized fleet allocation model for the climate impact, the profit, and the trade-off thereof will be developed. Such a trade-off is often referred to as an *eco-efficient* solution. With this, changes in the fleet, network, satisfied demand, overall climate impact, and profit can be researched. Knowledge on the impact of sustainable aircraft and alternative fuels at fleet level is gained, as well as insights into the use of these aircraft to reduce the overall climate impact and/or operating costs.

The research questions addressed in this paper are presented below.

Research questions

RQ: To what extent can a future airline reduce its climate impact while considering changes in operating costs by allocating climate-optimized aircraft and alternative fuels in its fleet?

SQ1 To what extent do the fuel and aircraft type affect the fleet composition, the satisfied demand, the flight frequencies, and the flight routes when reducing the overall climate impact?

SQ2 What is the trade-off between climate impact and profit for the allocation of different aircraft types, sizes, fuels, and combinations thereof in a network?

The trade-off between climate impact and profit is often discussed for different climate-mitigation strategies (e.g. [31, 69, 72, 94]); however, there is limited research on fleet allocation that incorporates the climate impact in the objective function (e.g. [72]). The proposed research will focus on this by incorporating a climate impact tax, and will be the first to also include different aircraft types and fuel types in the fleet. A climate/profit trade-off is expected, similar to the eco-efficient distribution shown in Figure 4.1. It is expected that patterns in the allocation of specific aircraft and fuel types on the network arise for different trade-offs in climate impact and profit. Also, it is anticipated that changes in the number of aircraft used in the fleet and volumetric changes for the different fuel types can be found.

The current knowledge will be extended by examining the changes at fleet level for varying levels of climate impact and profit, and by researching the allocation of aircraft types and aviation fuels to particular flight legs on the network, for varying levels of climate impact tax. A multi-fuel mixed-fleet (kerosene, SAF, LH_2; climate- and cost-optimized aircraft) will be considered.

By answering the above research questions, various other insights for the aviation industry could be expected. For example, this research could demonstrate how efficient allocation of SAF and LH_2 across flights and airports can reduce the climate impact, and if shown that SAF and LH_2 are allocated to a couple of particular airports, allocation decisions could be made to lower the pressure on the supply chains.

Moreover, it could provide insights into the effect of a climate impact tax incentive. It could investigate whether such taxes would drive profits down, or whether sufficient climate impact mitigation is possible using the sustainable alternatives. As airlines perform their fleet allocation to maximize profits and keep their market position [100], the integration of cost incentives may be an effective measure to stimulate them

to reduce their climate impact and adopt new sustainable developments.
Airlines and aircraft manufacturers could benefit from this research, as it could lead to insights into the future use and profitability of sustainable aircraft types and alternative fuel types. Results could potentially indicate that particular aircraft types are preferred over others. This could influence development plans, infrastructure investments, and aircraft orders.

5

Methodology

The method proposed to be used to answer the research questions is explained in this chapter. The research consists of three parts: 1) the calculation of the climate impact per flight leg for different aircraft types and fuel types (section 5.1), and 2) the cost calculations including the aircraft acquisition costs and flight costs, and 3) the fleet allocation to a network for different objectives (cost, climate impact, or a combination thereof) (section 5.2). Step 2, the cost calculations, will be further elaborated upon in later stages of the research. Therefore, the first and third steps are discussed in this chapter. Besides these steps, there are some important decisions and assumptions that need to be made, such as the fleet composition and network selection, which are discussed thereafter in section 5.3. At the end in section 5.4, the scope of the project is summarized.

5.1. Climate Impact per Flight Leg

For a climate-optimal fleet allocation, the climate impact of individual flights needs to be calculated. This depends on the flight altitude, geographical location, atmospheric conditions, time of emissions, fuel type, and aircraft design characteristics (e.g. [26, 76, 83]). To quantify the climate impacts of flights, there are various approaches available in the literature

Grewe et al. [34] calculate the climate impact of transatlantic flights within the air traffic simulator (SAAM), for the EU FP7 Project REACT4C [1]. The authors use the European Centre HAMburg general circulation model (ECHAM)/Modular Earth Submodel System (MESSy) Atmospheric Chemistry (EMAC) model, which is a numerical chemistry-climate model system consisting of submodels describing various processes in the atmosphere and the interactions with oceans and land ([47] as cited in [105]). Grewe et al. [34] simulate the atmospheric reactions from different emissions, and the climate impact in terms of various climate indicators is calculated using five-dimensional climate change functions (CCFs).

These CCFs are computationally expensive, and therefore the EU-project ATM4E developed approximate versions called algorithmic CCFs (aCCFs) [59]. Yin et al. [105] present the first version of the aCCF submodel called ACCF 1.0 for the EMAC model framework. They implement the aCCFs and elaborate on contrail aCCF development. The model can be used with a flight trajectory optimization model such as AirTraf 2.0 to assess changes between trajectories optimized for climate or cost objectives [104, 105].

Dietmüller et al. [21] present an open-source Python library called CLIMaCCF to calculate the climate impact of flights. The tool calculates the CO_2 aCCF, the individual non-CO_2 aCCFs, and the merged non-CO_2 aCCFs, given a geographical location and meteorological input data. The authors argue the tool to be user-friendly and efficient, and it is possible to estimate the climate impact as different physical climate metrics, such as pulse or future ATR for different time horizons.

The CLIMaCCF model is designed for conventional jet-powered aircraft, similar to the other available methods (e.g. [72, 87]). Therefore, the CLIMaCCF model can be used to calculate the climate impact of kerosene flights. However, for the LH_2 and SAF flights, weight factors should be used to compensate for the difference in contrail characteristics, and different emission indices based on the fuel type would have to be used. The model uses meteorological input data, such as ECWMF weather forecast or ERA5 reanalysis data.

[1] http://www.react4c.eu/

Another option to calculate the climate impact is to use the OpenAirClim model, developed by Völk et al. [99]. This model has recently been released and can be used to calculate the general atmospheric composition and climate change from different emissions. It incorporates CO_2 response models, and non-CO_2 climate impacts from NO_X, contrails, H_2O, O_3, primary mode ozone (PMO), and CH_4. It also includes the option to distinguish between kerosene, SAF, and LH_2-powered aircraft.

The CLIMaCCF model and the OpenAirClim model are both options for this research. The user-friendliness and the accessibility of the code are very important due to the time constraints for this thesis. There is more documentation available for the CLIMaCCF model, which is why this model has been chosen for this research.

The climate impact, expressed in the relevant climate metric F-ATR_{100} as discussed in section 3.4, will be calculated for every flight for each aircraft type and fuel type, for different departure times, and for different days and seasons based on the input data. This output will be used in the second part of this research: the fleet allocation.

5.2. Fleet Allocation

Early work from Hane et al. [37] describes a basic fleet assignment model, calculated using a mixed-integer linear programming method (MILP). The model determines which aircraft type should fly what leg; however, it uses a given flight schedule and fleet; the model does not include the aircraft routing problem, as the flight schedule is already provided.

Currently, much more complex models are being examined and implemented in the aviation industry. Airlines face many other logistical problems next to their fleet assignment: aircraft routing, crew pairing, crew rostering, and more [9, 51, 86]. Many of these problems influence each other, and trying to solve them all simultaneously is unrealistic, as the model becomes too complex and inefficient. Instead, a combination of a couple of problems can be solved to increase the optimality, but keep the model within a reasonable scope. For example, Salazar-González [81] proposes an integrated problem that solves the aircraft routing, crew pairing, and fleet assignment model.

For this research, a model is necessary that combines the aircraft routing and the fleet assignment, usually referred to as the fleet allocation. Based on the chosen network and demand, the goal is to research what routes should be performed with what aircraft and fuel type (referring to Table 5.1), to reach the most optimal objective (highest overall profit).

The fleet allocation can be done in different ways, and a decision should be made on what method to use. The fleet allocation is generally performed using either a mixed-integer linear programming (MILP) method, or a dynamic programming method (e.g. [72, 81, 82]).

For mixed-integer linear programming, the expectation is that the computational time of this method will be an issue. The input (the climate impact per aircraft type per flight leg for different times) will constitute a large data set, but also the possible flight legs including departure and arrival times, and the origin-destination matrix for passenger demand are expected to weigh on the computational time of the model. Solution techniques can be applied, such as a column generation technique or a heuristic procedure [81]; however, due to the time constraints of this research, the model should be refrained from becoming too complex.

Therefore, the choice is made to use the dynamic programming method. This allows for non-linear calculations, and it uses a divide and conquer concept: the idea is to break down a large problem into incremental steps, recursively solved using a greedy policy, to obtain sub-solutions that solve the large problem. The computational time is expected to be lower compared to the MILP method.

The dynamic programming model is largely based on the method described in [76], which uses the Bellman-Ford algorithm and the solving method from Noorafza et al. [72], and (Álvarez [6] as cited in [76]). The approach is depicted in Figure 5.1. As shown in the figure, the path generation and the aircraft selection will be performed based on an objective function, which includes the costs as well as the climate impact of flights.

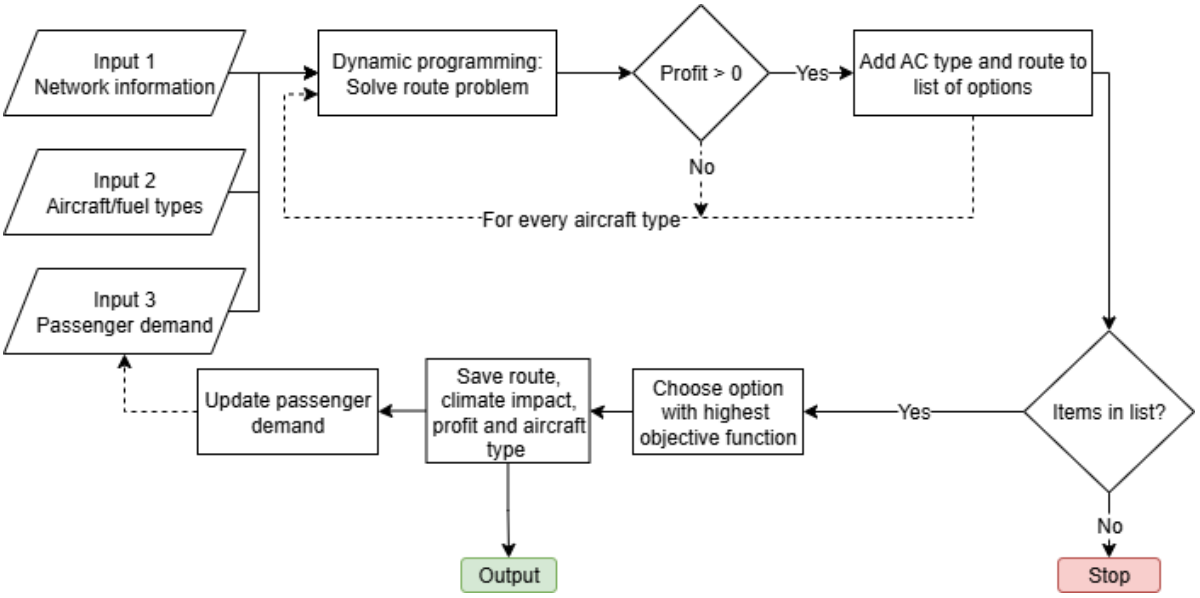

*The best option and the route calculation will be done according to the highest objective (profit).

Figure 5.1: Block diagram of dynamic programming model used to solve the fleet allocation problem. Diagram adapted from [82], and ([6] as cited in [76])

5.3. Decisions and Assumptions

There are various decisions and assumptions made for this research. The most important ones are discussed in chronological order in this section:

- the F-ATR$_{100}$ climate metric
- the Delta-network used by Proesmans [76]
- twelve different aircraft, also from Proesmans [76], including the use of SAF
- conversion factors for the CLIMaCCF model for the climate impact of contrails from hydrogen and SAF.

5.3.1. Metric Selection

In section 3.4 the different climate metrics are discussed and the calculations used by Megill, Deck, and Grewe [65] are provided. The authors state that the metric ATR$_H$, shown with Equation 3.7, is suitable for calculating the climate impact of aircraft, but also for future aircraft employing different fuels. They argue that a time horizon of at least 70 years would be most appropriate, as long-term climate effects need to be considered, such as long term effects from CO_2 emissions. A 100-year time horizon is commonly used in the literature (e.g. [72, 76]), and also compatible with the chosen method described in section 5.1. The CLIMaCCF model differentiates between pulse (P-ATR) and future ATR (F-ATR). F-ATR is appropriate when examining future emission scenarios, and therefore, the climate metric F-ATR$_{100}$ is chosen for this research.

5.3.2. Network Selection

To assess the climate impact of different aircraft types employing different fuels at fleet level, the fleet allocation needs to be performed on a chosen network and demand. Preferably, the chosen network represents the reality as closely as possible to achieve the most accurate results. The aCCFs used in the CLIMaCCF library are developed for winter and summer meteorological conditions for the area east and around the North Atlantic [59], and thus the use of CLIMaCCF for spring, autumn, and tropical regions is discouraged [21]. This narrows down the scope for the use of weather data for winter or summer, but also for the choice of network. This leads to the first requirement of the chosen network: the network operates within Europe, North America, or both.

The second requirement for the network refers to its complexity. A complex network leads to increased complexity for the fleet allocation, and increases the timeline of the project, which must stay within the maximum duration of 9 months. There are different types of networks: a point-to-point network, a hub-and-spoke

network, or a combination thereof. For example, Delta and Lufthansa operate on hub-and-spoke systems having multiple hubs, (e.g. in Salt Lake City, Atlanta, Minneapolis, and Seoul[2], and in Brussels, Frankfurt, Munich, and Vienna[3] respectively), KLM operates a single-hub network with its hub in Amsterdam, but collaborates with partner airlines (e.g. AirFrance and Delta) forming a multi-hub global network system[4], and Ryanair operates a point-to-point airline, not facilitating transfer passengers or baggage[5].

The aim is to research the effect of different types of aircraft and fuels at fleet level on the overall climate impact and profit, and therefore the fleet allocation should be flexible. In a point-to-point network, the allocation is less flexible as legs are usually operated by only one aircraft type [10]. A hub-and-spoke network would be the most appropriate option since it allows for a more dynamic fleet allocation. The second requirement then follows: the network should be a hub-and-spoke network.

The third requirement is that the network should cover short, medium, and long-range flights. Firstly, the transition from kerosene to H_2-powered aircraft is expected to take place for short and medium-haul aircraft first [48]. Secondly, the probability of contrail formation is higher for long-haul flights, due to a higher percentage of time spent in cruise than time spent in climb or descent [93]. Since contrail cirrus has the largest contribution to anthropogenic global warming from aviation [54], long-range flights should be included to investigate how the climate, as well as the costs, are affected. Thus, short- and medium-range aircraft are included because they are expected to be the most relevant in near-future sustainable practices, and long-range aircraft are included because they are expected to have a high impact on the changes in climate impact and costs.

The network and demand are chosen based on the available data and the above requirements. The decision was made to use the simplified Delta Airlines network as introduced by Jansen and Perez [45] and modified and expanded by Proesmans [76]. The network is a hub-and-spoke network with the hub in Atlanta Airport, consisting of 19 domestic and 11 international airports. The demand for this network is per week and assumed to be symmetric.

5.3.3. Fleet Selection

The fleet selection for this research is based on a couple of assumptions. As shown in Table 3.1 in section 3.1, the current development plans for electric aircraft and H_2-fuel cell aircraft are mostly only for regional flights, due to large weight penalties for the battery storage or the powertrain. With the focus of this research on a network covering short- to long-haul flights, the contribution of electric aircraft and H_2-fuel cell aircraft will be neglected.

Proesmans [76] designed kerosene, SAF, and LH_2-powered aircraft for cost-optimal (COC) and climate-optimal (ATR) objectives, and a multi-objective (MO) including cost, climate, and fuel consumption. These aircraft form the basis of this research. He designed REG, SMR, and LR aircraft. The multi-objective aircraft will be ignored in this research because of the focus on the climate and cost impact of climate-optimal aircraft and alternative fuels. The multi-objective blurs the distinction between cost-optimal and climate-optimal aircraft. SAF aircraft will also not be included in this research. It will instead be assumed that SAF can be allocated to kerosene aircraft (climate-optimal and/or cost-optimal), because of the following three arguments: the SAF aircraft are very similar to kerosene aircraft, current (kerosene) aircraft need hardly any adjustments to use drop-in SAF [5], and it best represents the current situation: SAF is blended with kerosene and allocated to conventional aircraft. Therefore, in this research, the possibility of allocating SAF is included, but aircraft specifically optimized for the use of drop-in SAF are not. Table 5.1 shows the final selection of possible aircraft types to be used in this research. This leaves 12 aircraft types, all designed by Proesmans [76].

Long-range LH_2 aircraft are included in the fleet as shown in the table, even though the use of H_2-powered aircraft is expected to occur for short- to medium-range aircraft first [48]. This decision was made because this forecast is expected to be reflected in the results of this research as well. As can be seen in results from Proesmans [76] in Figure 5.2, the relative network profit for all three long-range LH_2 aircraft is very low compared to regional- and medium-range aircraft and kerosene aircraft. It is therefore expected that long-range LH_2 aircraft are used only for the fleet allocation and when the climate objective dominates the cost objective in the fleet allocation. For realistic future scenarios - a careful trade-off between climate and cost - no or hardly any use of long-range LH_2 aircraft is expected.

[2] https://news.delta.com/
[3] https://business.lufthansagroup.com/
[4] https://www.klm.nl/en/information/corporate/network-alliances
[5] https://www.ryanair.com/tr/en/useful-info/help-centre/terms-and-conditions/termsandconditions

Table 5.1: The aircraft types designed by Proesmans [76] selected for this research.

Aircraft type (Fuel type)	**Kerosene Aircraft** (Kerosene, SAF)			**SAF Aircraft** (SAF)			**LH_2 Aircraft** (LH_2)		
Design objective	**ATR**	**COC**	**MO**	**ATR**	**COC**	**MO**	**ATR**	**COC**	**MO**
Regional	✓	✓	-	-	-	-	✓	✓	-
Medium	✓	✓	-	-	-	-	✓	✓	-
Long	✓	✓	-	-	-	-	✓	✓	-

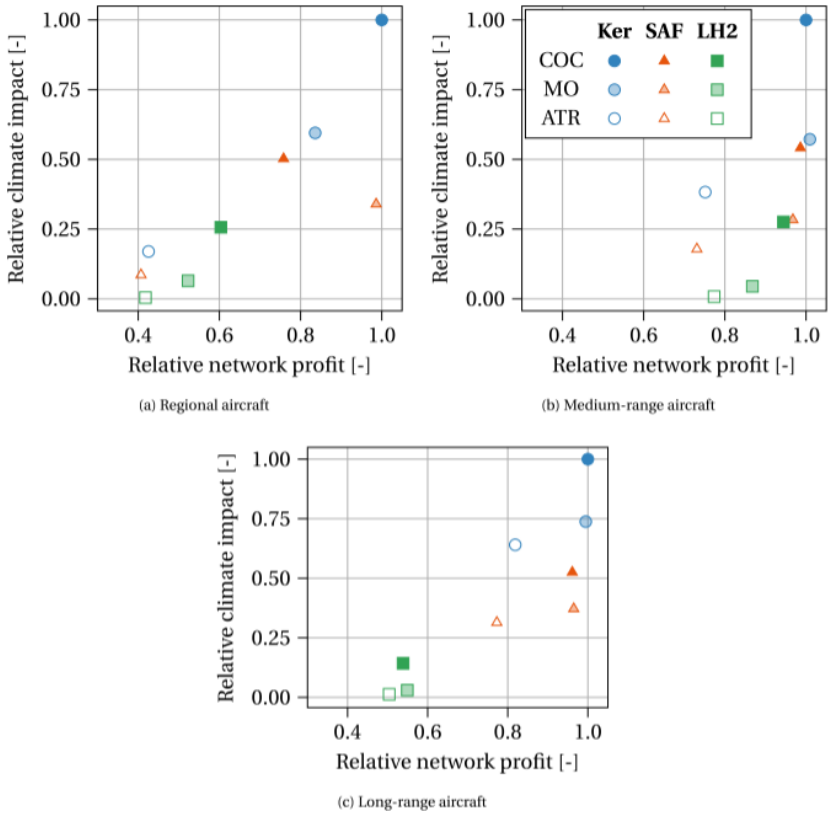

Figure 5.2: Relative climate impact vs. relative network profit for REG, SMR, and LR aircraft, from Reference [76].

5.3.4. Conversion Factors for Contrails

In subsection 3.2.2 the contrails from kerosene, LH_2 and SAF aircraft are presented. The CLIMaCCF model is developed for kerosene flights, and while the emission indices for different fuel types can be modified to include SAF and LH_2 fuel, a conversion factor for the contrails from different fuel types is necessary.

Burkhardt, Bock, and Bier [15] discuss the influence of the number of ice crystals on the contrail cirrus net radiative forcing. They argue that the net radiative forcing of contrail cirrus decreases with 50% when the ice particle number decreases with 80%. This is shown in Figure 5.3. Bier et al. [11] show that ice crystal numbers in contrails from hydrogen combustion decrease by around 80-90% compared to kerosene combustion. These two findings support the assumption that contrail cirrus from hydrogen aircraft leads to 80% reduced ice crystal number, and consecutively to 50% less net radiative forcing, compared to kerosene aircraft. This means that a conversion factor of 0.5 will be introduced for contrails from hydrogen aircraft.

Moreover, Burkhardt, Bock, and Bier [15] argue that by reducing the number of ice crystals by 50% through the use of a 50% SAF blending ratio, a reduction of 21% in the net radiative forcing from contrail cirrus can be achieved. Therefore a conversion factor of 0.79 will be used for contrails from aircraft employing 50% drop-in SAF. Since different blending ratios would affect the conversion factor, it was chosen to simplify the SAF allocation by allowing only a 50% blending ratio for SAF.

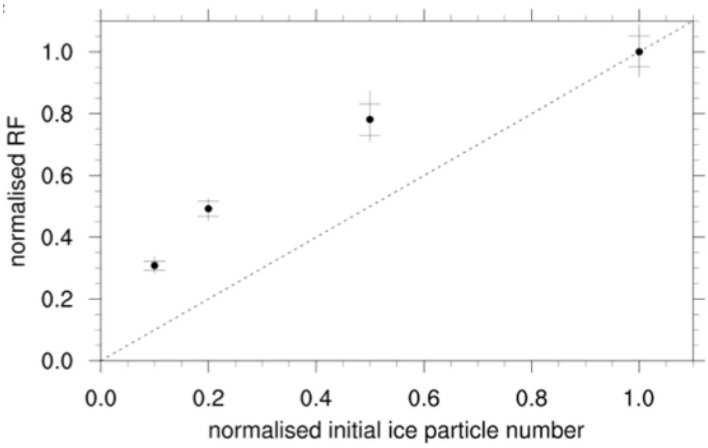

Figure 5.3: The global net radiative forcing from contrail cirrus, normalized to present day soot numbers, versus the initial ice particle number concentration of contrails, from Reference [15]

5.4. Research Scope

This research should remain within a reasonable scope. Additional research areas that could be added to the scope later on are discussed in section 6.1. For the clarity of this research proposal, the scope and decisions made in this paper are summarized below.

The research starts by calculating the climate impacts of all possible flight legs flown at different times by different aircraft and fuels (using CLIMaCCF [21]). Also, the costs of all possible flights are calculated. Then, for the chosen network and demand, and for the selected aircraft types in the fleet, the fleet allocation will be performed using dynamic programming.

The focus of this research will be on the summer season. Grewe et al. [31] study a climate-optimized routing strategy for trans-Atlantic flights, during summer and winter days, and they find that for summer days, the variability and the climate-reduction potential are the highest. The variability of the climate impact of different aircraft types is expected to be highest in summer as well, since the largest contributor to the climate impact is the formation of contrails [54]. It is therefore that the summer season has been chosen. The summer season lasts from June to September, and therefore, one or more summer weeks will be picked, based on the available data. The same weeks will be used for multiple years, to get a representative dataset for the summer weather conditions. For all weeks and years, the network demand (with a 1-week duration) will remain the same.

The costs/operating costs, as referred to in this proposal, will include the direct operating costs only. A more detailed cost breakdown will be created in later stages of the research.

6

Analysis Framework and Expected Results

The research can be split into three main components: the climate impact calculations using the CLIMaCCF tool, the cost calculations, and the fleet allocation optimization for different objectives using dynamic programming.

The first part of the research relies on the input data for the CLIMaCCF tool [21]: aircraft design characteristics from Proesmans [76], and ECMWF meteorological weather data. This part will provide the datasets containing the aCCFs for all the grids at the selected flight level. After processing the data and performing the calculations for the flight trajectories, the climate impacts will be found for all possible flight legs, at different departure times, and for each aircraft type and fuel.

The second part of this research calculates the costs, which include the flight costs as well as the landing fees, overnight parking costs, and aircraft acquisition costs per week. The output of this part consists of the costs per flight, as well as the acquisition costs and overnight parking costs. The climate impacts calculated per flight, in part 1, are included in the costs by introducing a climate impact tax. A more detailed cost breakdown will be provided in later stages of this research.

The third part of this research uses the output of the climate impact analysis and cost calculations as input, together with network and demand data, containing REG, SMR, and LR flights.

The resulting optimal allocations for different objective values for the climate-profit trade-off will be researched. The climate impact per flight and the total impact per flight leg will be calculated and compared to investigate whether specific flight legs or flights are responsible for a higher climate impact than others. The results are expected to be in line with the research from Teoh et al. [94], who argue that for the North Atlantic region, ~12% of all flights is responsible for ~80% of the climate impact.

The change in fleet composition and fleet allocation is evaluated for the trade-off between profit and climate impact. It is expected that the trade-off will show a Pareto-front similar to Figure 4.1, and a pattern in the introduction of certain aircraft will be reflected in the results. For example, it is hypothesized that long-range hydrogen aircraft will only be used when high levels of profit are sacrificed.

The changes in the network will also be researched. Changes in the total number of flights, the number of flights per leg, the number of flights per aircraft type, the served demand, and the arrival and departure times of flights will be considered. It is expected that, for example, longer flight times due to the use of slower aircraft (climate-optimal aircraft) could influence the total number of flights per aircraft, the total amount of aircraft in the fleet, and the served demand.

The results will include a sensitivity analysis to investigate the influence of various assumptions on the final results.

6.1. Additional Research Ideas

The timeline of the thesis is 9 months, and estimating the duration is difficult. Various ideas have come up during the literature research and progress meetings that have been saved for later purposes. If and when there is room, one or more of these ideas can be implemented in this research. The current list consists of the

following items:

- The energy consumption in terms of fuel volume can be included to provide additional insights into the required infrastructure for different fuel types. These insights could lead to additional constraints on fuel availability, and including these could provide a more realistic future scenario. For example, it may not be realistic for an airport to support hydrogen flights when results show that hardly any hydrogen flights are expected to arrive and depart from this airport. Moreover, these results could provide insights into a more efficient and effective development of the hydrogen (and SAF) supply chain.
- The use of more than one network would increase the scope of the research. Starting with the network and demand data from Proesmans [76] in North America, the research could include a European network, such as Lufthansa's network, if available.
- The use of electric regional aircraft could be included in the fleet to investigate their impact on the overall results.
- The research scope could be increased by, for example, expanding the analysis to more days and/or years, or to the winter season.
- With the sensitivity analysis, the effect of different prices (such as fuel costs) on the outcomes can be examined.

6.2. Gained Insights

This research aims to answer the research questions posed in chapter 4, to provide key insights for the aviation industry. Such insights include:

- The impact of climate-optimal aircraft and alternative fuels in a future fleet.
- The trade-off between climate impact and profit for optimal fleet allocation.
- Efficient allocation of SAF and hydrogen across flights and airports to reduce the climate impact and lower the pressure on the supply chain.
- The need for cost incentives or policy implications in the aviation industry to promote more sustainable aircraft and fleet allocation.
- Forecasts on the development and profitability of climate-optimal aircraft and different aviation fuels.

7

Timeline

The thesis consists of four phases: the literature review, the research phase 1, the research phase 2, and the research dissemination. Research phases 1 and 2 are separated with a mid-term review, and due to the tight timeline of the project, the following goals have been set to achieve at the end of the first research phase:

- Finalize the implementation of the CLIMaCCF model.
- Complete the analysis of the ISSRs from the CLIMaCCF model (visual plots).
- Finish the calculation of the climate impact for all kerosene flight legs.
- Finalize the calculation of the climate impact for SAF and H_2 flight legs.
- Developed prototype of the dynamic programming model.
- Finalize the network and demand data to be used in phase 2.

The timeline of this thesis is presented in Figure 7.1. This preliminary planning depicts the 5 important deliverables/moments in the thesis trajectory: the kick-off, the research proposal, the mid-term review, the green light draft, and the final hand-in. The four phases are shown with different colors. Important to note is that a full-time thesis should take 32-39 weeks. In this timeline 2 weeks of vacation are added, resulting in 34 weeks. However, students are allowed to spend a maximum of 39 weeks on their thesis to accommodate for some delays in their research, or illnesses, or vacations. These extra 5 weeks are not included in the timeline but provide a contingency if needed.

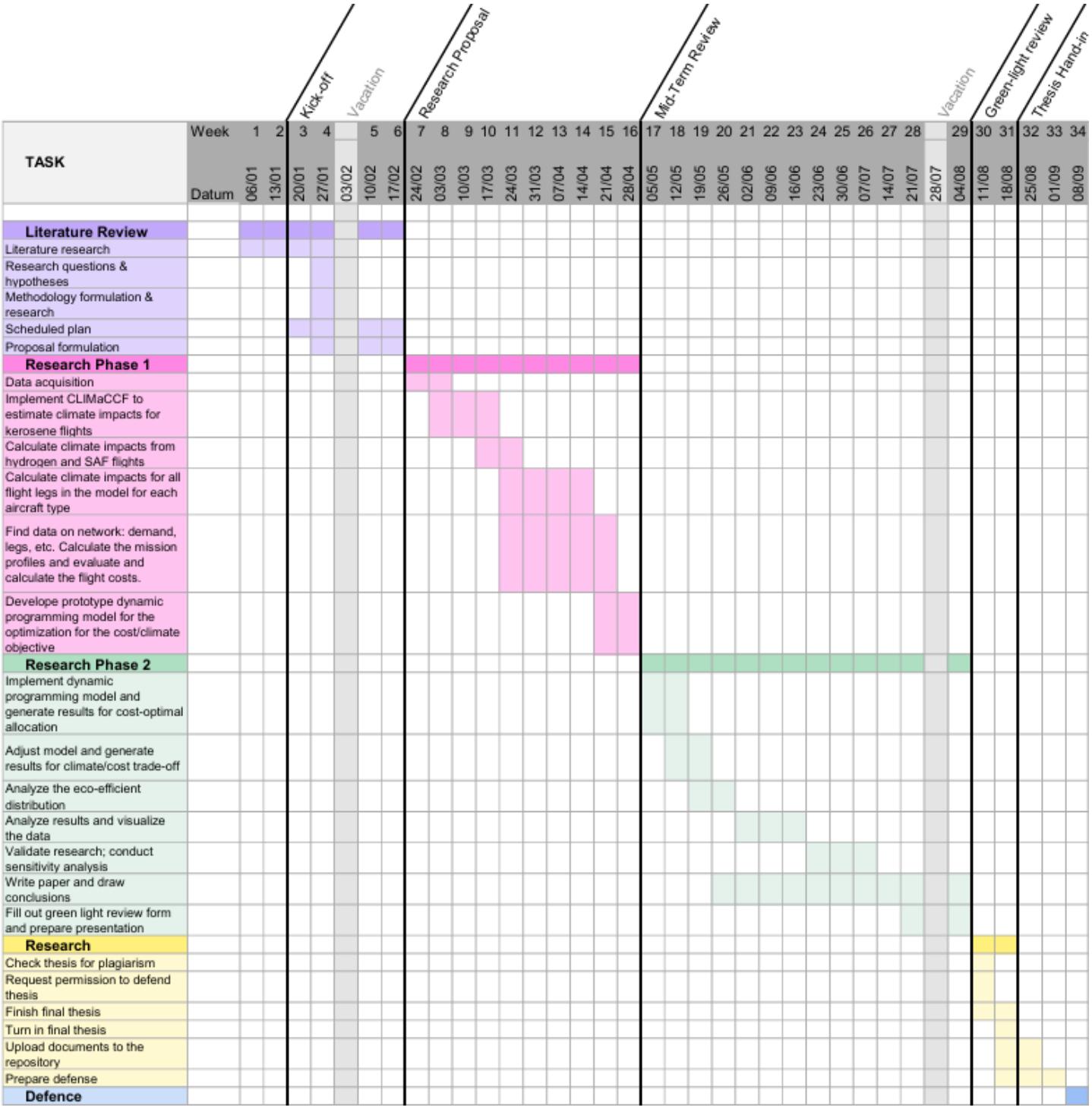

Figure 7.1: Gantt chart for the initial timeline for this research

III

Supporting work

1

CLIMaCCF Calculation

CLIMaCCF is an open-source Python library, presented by Dietmüller et al. [21]. It calculates the aCCFs for CO_2 and non-CO_2 emissions, as well as the total *merged* aCCF, which combines the effects from CO_2, O_3, CH_4, PMO, day-contrails, night-contrails, and H_2O. The formula is shown in Equation 1.1.

All formulas presented in this chapter are for the Pulse ATR_{20} calculation and are obtained from Reference [21]. For F-ATR_{100}, the $aCCF_x$ value has to be converted using a climate metric conversion factor CM_x. The conversion factors CM_x as well as the efficacies r_x are presented in Table 1.1.

$$\mathrm{aCCF}_{\mathrm{merged}} = \begin{cases} \mathrm{aCCF}_{\mathrm{CO_2}} \times \mathrm{CM}_{\mathrm{CO_2}} \\ +\mathrm{aCCF}_{\mathrm{O_3}} \times \mathrm{EI(NO}_x\mathrm{)} \times r_{\mathrm{O_3}} \times \mathrm{CM}_{\mathrm{O_3}} \\ +\mathrm{aCCF}_{\mathrm{CH_4}} \times \mathrm{EI(NO}_x\mathrm{)} \times r_{\mathrm{CH_4}} \times \mathrm{CM}_{\mathrm{CH_4}} \\ +\mathrm{aCCF}_{\mathrm{PMO}} \times \mathrm{EI(NO}_x\mathrm{)} \times r_{\mathrm{PMO}} \times \mathrm{CM}_{\mathrm{PMO}} \\ +\mathrm{aCCF}_{\mathrm{contrail}} \times F_{\mathrm{km}} \times r_{\mathrm{contrail}} \times \mathrm{CM}_{\mathrm{contrail}} \\ +\mathrm{aCCF}_{\mathrm{H_2O}} \times r_{\mathrm{H_2O}} \times \mathrm{CM}_{\mathrm{H_2O}}, \end{cases} \tag{1.1}$$

$$F_{km} = km/kg(fuel) \tag{1.2}$$

$$EI_{NO_x} = g(NO_2)/kg(fuel) \tag{1.3}$$

$$PV = 10^{-6} Km^2 s^{-1} \tag{1.4}$$

$$OLR = Wm^{-2} \tag{1.5}$$

$$T = K \tag{1.6}$$

$$\Phi = m^2 s^{-2} \tag{1.7}$$

Table 1.1: Climate metric conversion factors CM_x from P-ATR_{20} to F-ATR_{100}, values from References [21, 54]

aCCF	F-ATR_{100} (CM_x)	efficacies (r_x)
CO_2	125.0	1
H_2O	58.3	1
O_3	58.3	1.37
CH_4	98.2	1.18
PMO	98.2	1.18
$contrail$	48.9	0.42

The corresponding formula for the algorithmic climate change function for CO_2 is given in Equation 1.8. The climate impact of CO_2 scales directly with fuel burn, and the constant factor of 7.48e-16 K/kg(fuel) is taken from Yin et al. [105].

$$\mathrm{aCCF}_{\mathrm{CO_2}} = 7.48 \times 10^{-16} \quad \text{[K/kg(fuel)]} \tag{1.8}$$

The climate impact from NO_x results in 3 types of climate effects: NO_x-induced O_3, NO_x-induced CH_4, and NO_x-induced PMO. NO_x-induced O_3 depends on the temperature T[K] and the geopotential Φ $[m^2 s^{-2}]$. The formula is presented in Equation 1.9.

$$\text{aCCF}_{\text{O}_3}(T,\Phi) = \begin{cases} -2.64\times10^{-11} + 1.17\times10^{-13}\times T \\ +2.46\times10^{-16}\times\Phi - 1.04\times10^{-18}\times T\times\Phi \quad [\text{K/kg}(NO_x)], & \text{if aCCF}_{\text{O}_3} \geq 0 \\ 0, & \text{if aCCF}_{\text{O}_3} < 0 \end{cases} \tag{1.9}$$

For NO_x-induced CH_4, the climate change function depends on the geopotential, and the incoming solar radiation at the top of the atmosphere F_{in} $[Wm^{-2}]$. Note that methane has a cooling effect (thus negative), and is set to 0 otherwise. The formula is shown in Equation 1.10. The aCCF for methane is also used to determine climate impact from primary mode ozone (PMO) (Equation 1.11), using a constant factor of 0.29 ([19] as cited in [21]).

$$\text{aCCF}_{\text{CH}_4}(\Phi,F_{\text{in}}) = \begin{cases} -4.84\times10^{-13} + 9.79\times10^{-19}\times\Phi \\ -3.11\times10^{-16}\times F_{\text{in}} + 3.01\times10^{-21}\times\Phi\times F_{\text{in}} \quad [\text{K/kg}(NO_x)], & \text{if aCCF}_{\text{CH}_4} < 0 \\ 0, & \text{if aCCF}_{\text{CH}_4} \geq 0 \end{cases} \tag{1.10}$$

$$\text{aCCF}_{\text{PMO}} = 0.29\times\text{aCCF}_{\text{CH}_4} \quad [\text{K/kg(fuel)}] \tag{1.11}$$

The climate impact from water vapor depends on the potential vorticity (PV), units: $[10^{-6}\ \text{K}m^2 s^{-1}]$. The calculation is shown in Equation 1.12. For the calculation for the southern hemisphere, the absolute value should be taken for PV. The aCCF is adjusted to account for different fuels (LH_2 or SAF) by scaling the aCCF with the emission index.

$$\text{aCCF}_{\text{H}_2\text{O}}(\text{PV}) = \left(2.11\times10^{-16} + 7.70\times10^{-17}\times\text{PV}\right)\times\frac{\text{EI}_{\text{fuel}}(\text{H}_2\text{O})}{\text{EI}_{\text{kerosene}}(\text{H}_2\text{O})} \quad [\text{Kkg}^{-1}\text{(fuel)}] \tag{1.12}$$

The climate impact from contrails depends on the incoming solar radiation. Thus, a distinction between day- and nighttime contrails is made, and the climate impact is calculated by obtaining the radiative forcing for both scenarios [105]. The climate impact from daytime contrails depends on the outgoing long-wave radiation at the top of the atmosphere (OLR). The climate impact of nighttime contrails depends on the temperature. If below 201 Kelvin, the value is set to zero. For both calculations (Equation 1.13 and 1.14), the values are only included for locations where the Schmidth-Appleman criterion [7] holds. This depends on the emission indices of H_2O, the fuel-specific caloric values, and the overall engine efficiencies, as described in subsection 3.2.2.

$$\text{aCCF}_{\text{contrails,day}} = 0.0151\times\text{RF}_{\text{aCCF-day}}(\text{OLR}) = 0.0151\times10^{-10}\times(-1.7 - 0.0088\times\text{OLR}) \quad [K/km] \tag{1.13}$$

$$\text{aCCF}_{\text{contrails,night}} = 0.0151\times\text{RF}_{\text{aCCF-night}}(\text{T}) = 0.0151\times10^{-10}\times(0.0073\times10^{0.0107\times T} - 1.03) \quad [K/km] \tag{1.14}$$

2

NO_x Modeling in this Thesis

During this thesis, different decisions, solutions, and analyses are made regarding the climate impact from NO_x. Part I explains the final methodology used in this thesis; however, this chapter aims to provide the reader with additional information regarding these decisions, as well as the steps taken to come to those decisions. The following summarizes this chapter.

To begin, the aCCFs are designed for cruise altitudes. During this thesis, it is investigated whether the flight conditions other than cruise could also be included in the analysis, thus that the climate impact from all flight phases could be calculated (based on the mission profiles). The biggest issue with this is the dataset, which is part of the CLIMaCCF model. It contains averaged NO_x emission indices (EI) for different aircraft at different altitudes, but does not include values below 20000 feet. Therefore, the steps taken to extend this data are described in section 2.1.

It is examined whether EI(NO_x) values below 20000 feet could be used, and whether the climate impact calculations at these altitudes would be justified. How the verification steps are performed is explained in section 2.2. First, the aCCF for NO_x, O_3, and CH_4 are verified and compared with literature. Then, the climate impact (K/kg(NO_x) is calculated for all pressure levels, and it is concluded that these are not in line with existing literature, as the impact of NO_x should decrease with decreasing altitude. Additionally, it is investigated whether this difference would significantly influence the overall climate impact of flights. These last two steps support the conclusion: aCCF for NO_x is not suitable for lower altitudes.

Nevertheless, to continue with the thesis, an assumption on the NO_x values has to be made. It is decided to only include NO_x for cruise altitudes; however, since ATR-optimized aircraft fly below 20000 ft, the data needs to be extended to 18000 ft, in order to enable the analysis performed in this thesis. The data is extended linearly as explained in section 2.1. Furthermore, evaluating Figure 2.5, it is decided to include scaling factors for aCCF O_3 for altitudes below 250 hPa, since O_3 heavily influenced the climate impact of NO_x. The scaling factors and the calculation thereof are described in section 2.3.

2.1. NO_x Emission Indices and Fuel Efficiencies

The CLIMaCCF model includes the emission indices of NO_x and the fuel efficiency (km/kg(fuel)). The data consists of altitudes between 20000 ft and 45000 ft, for REG, SMR, and LR kerosene aircraft. The data is extended down to 0 ft to examine whether the climate impact calculations using the CLIMaCCF model could be possible.

To do this, the ICAO Aircraft Engine Emissions Databank is used to estimate the NO_x emissions at lower altitudes [42]. In Figure 2.1, the NO_x emission indices for climb-out are plotted against the emission indices for take-off, and as can be seen, there is a regression line drawn with a slope of 0.63. This value is assumed to be the linear conversion factor between the NO_x emissions at 0 ft and 20000 ft.

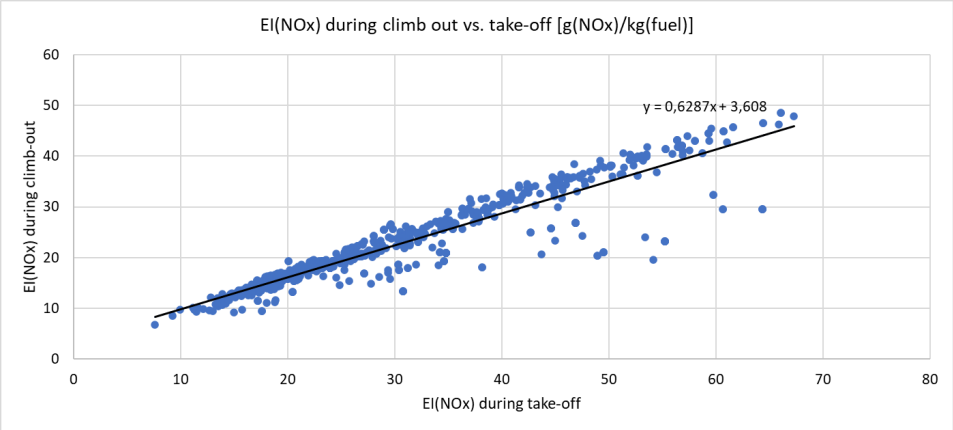

Figure 2.1: NO_x emission indices during climb out vs. during take-off. Values obtained from Reference [42].

Since the data does not include values for the ATR-optimized aircraft, these are estimated by multiplying the COC-optimized data columns with a scaling factor. The scaling factor is the ratio between the average values ($EI(NO_x)$ and fuel efficiency) for ATR-optimized and COC-optimized aircraft, obtained from the mission profiles. The scaling factors and the average values are presented in Table 2.2.

Table 2.1: Average $EI(NO_x)$ and average fuel efficiency for cruise for different aircraft types, including the conversion factors used for the initial emission indices, to account for climate-optimized aircraft

	$EI(NO_x)$					**Fuel Efficiency**				
	COC	**Alt. [ft]**	**ATR**	**Alt. [ft]**	**ATR/COC**	**COC**	**Alt. [ft]**	**ATR**	**Alt. [ft]**	**ATR/COC**
REG	26.75	33536	20.33	21763	0.543	0.831	33536	0.924	21763	1.332
SMR	26.43	33873	18.88	21915	0.502	0.495	33873	0.510	21915	1.273
LR	22.97	33370	14.88	26557	0.524	0.195	33370	0.191	26557	0.975

For SAF, the same emission indices are assumed, as well as the fuel efficiencies. However, for hydrogen aircraft, the data is multiplied by scaling factors that are presented in Part I.

Table 2.2: Average fuel efficiency for cruise for different hydrogen aircraft, including the conversion factors used for the initial emission indices, to account for climate-optimized aircraft

	Fuel Efficiency					
	COC	**Alt. [ft]**	**ATR**	**Alt. [ft]**	**LH_2/Kerosene**	**ATR/COC**
REG	2.487	35935	2.126	20544	5.06	1.07
SMR	1.376	36438	1.233	20665	4.04	1.19
LR	0.480	33576	0.455	21967	2.46	0.94

When comparing the NO_x emission indices and the fuel efficiencies from the dataset from Dietmüller et al. [21] with the emission indices from the mission profiles for the lower altitudes, it can be seen that the emission indices for NO_x are higher for the mission profiles. This could be explained by NO_x emission index equation (see Equation 2.1), which is designed for engines with an overall pressure ratio of below 50. This difference is, however, not a problem, since underestimating the NO_x emissions at lower altitudes does not change the outcome of the NO_x emission verification in subsection 2.2.1.

2.2. NO_x Emissions and Climate Impact using CLIMaCCF

This section focuses on the verification step of the CLIMaCCF model, calculating the climate impact of emissions and specifically those of NO_x emissions. The aCCFs are designed for cruise conditions, and it is investigated whether extending the CLIMaCCF model to altitudes below 20000 ft until 0 ft can be justified (using the $EI(NO_x)$ calculated in the previous section).

The structure is as follows: subsection 2.2.1 verifies the climate impact calculations and subsection 2.2.2 examines the climate impact of NO_x for different altitudes according to the CLIMaCCF model and the mission profiles.

2.2.1. Calculation verification

To begin, the climate impact calculations using CLIMaCCF for the climate metric F-ATR_{20} are performed at pressure level 250 hPa, to compare the results from the model with the results from the paper by Dietmüller et al. [21]. The figure is presented in Figure 2.2. It shows that the results for O_3, CH_4 (CH_4 + PMO), and NO_x are in line with the results from Dietmüller et al. [21]. All three figures present similar magnitudes, and it can therefore be concluded that the NO_x calculation is verified.

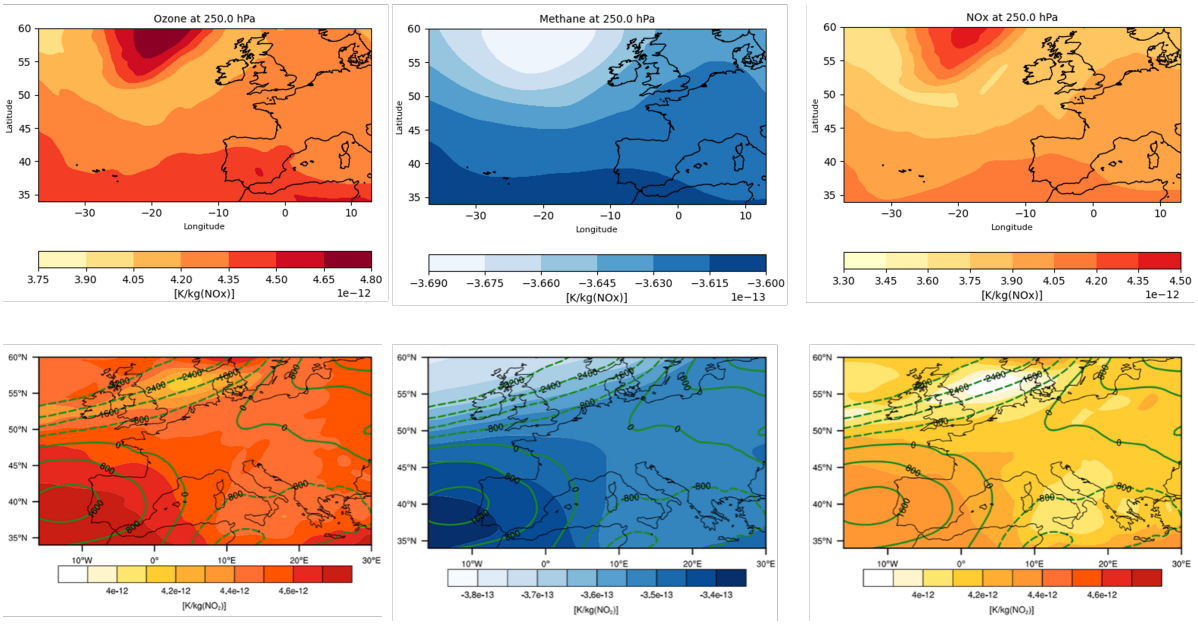

Figure 2.2: Top three figures present the results from the calculations, at noon UTC on August 5th 2024. The bottom three figures are taken from Reference [21], and represent the results for June 15th 2018, at noon UTC. All units are in [K/kg(NO_x)]. In all figures the results are for the pressure level of 250 hPa. All results are calculated for F-ATR_{20}.

Because the geographical area differs from the reference, the top three figures in Figure 2.2 are zoomed in on the eastern part, to facilitate the visual comparison between the plots. The results for the full geographical scope are presented in Figure 2.3.

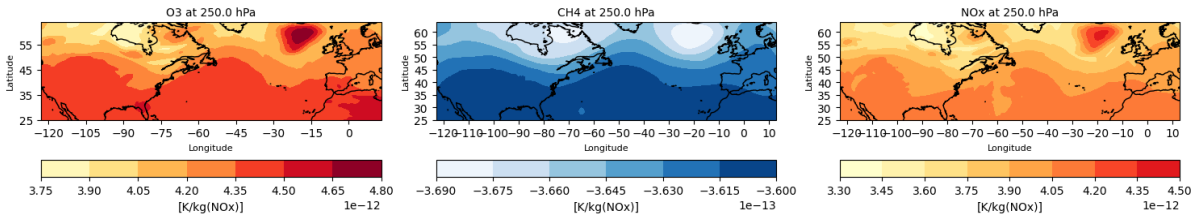

Figure 2.3: Results from NO_x calculations, at noon UTC on August 5th 2024. Results are in [K/kg(NO_x)], for the pressure level of 250 hPa. All results are calculated for F-ATR_{20}.

2.2.2. NO_x at different altitudes

The aCCF calculations for NO_x using CLIMaCCF are verified, and this section examines whether CLIMaCCF could also be used for lower altitudes, when looking at the NO_x emissions.

Therefore, it starts by calculating the impact of NO_x at different altitudes (subsection 2.2.2). Then, it calculates the amount of NO_x emissions per altitude according to the mission profiles (Figure 2.2.2), and thereafter, it combines both results and examines the climate impact contribution of NO_x per flight for different altitudes.

Impact at different altitudes

The climate impact for NO_x, as can be seen in the third figure in Figure 2.3, is plotted for all pressure levels in the data set, from 1000 hPa to 100 hPa. The results are shown in Figure 2.4.

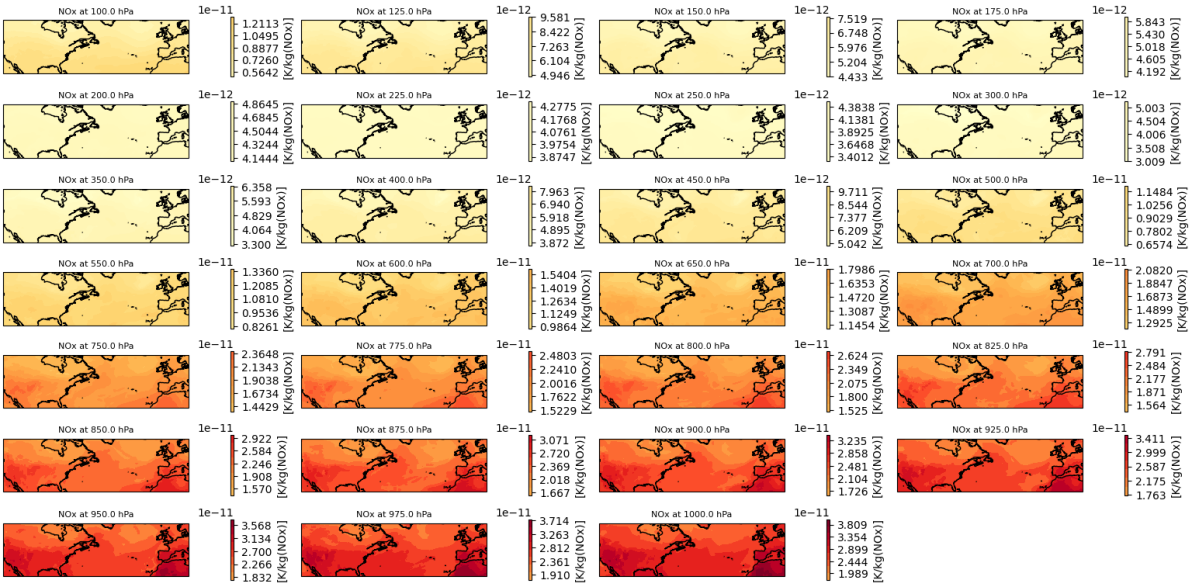

Figure 2.4: All results are calculated for F-ATR_{20}.

The average from each graph in Figure 2.4 is plotted in Figure 2.5 to provide a quick overview of the relative changes in climate impact (F-ATR_{20}) in [K/kg(NO_x)].

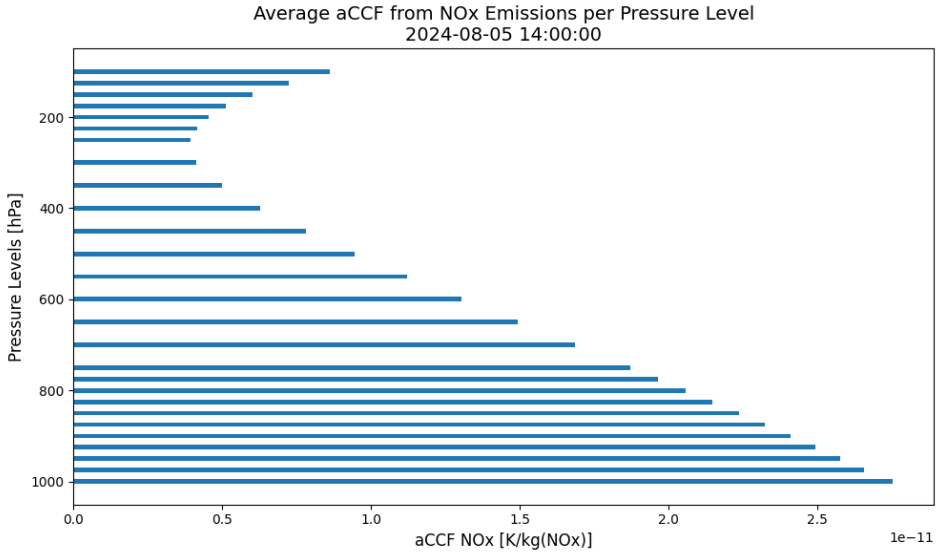

Figure 2.5: Average climate impact in [K/kg(NO_x] per pressure level

These results contradict existing literature. Because the climate impact contribution from O_3 dominates CH_4, results are compared with literature describing the climate impact of O_3: Lacis, Wuebbles, and Logan [52] describe the radiative forcing of O_3 as a function of altitude, and demonstrate that the radiative forcing decreases for decreasing altitudes below ~12 km. Their results are shown in Figure 2.6.

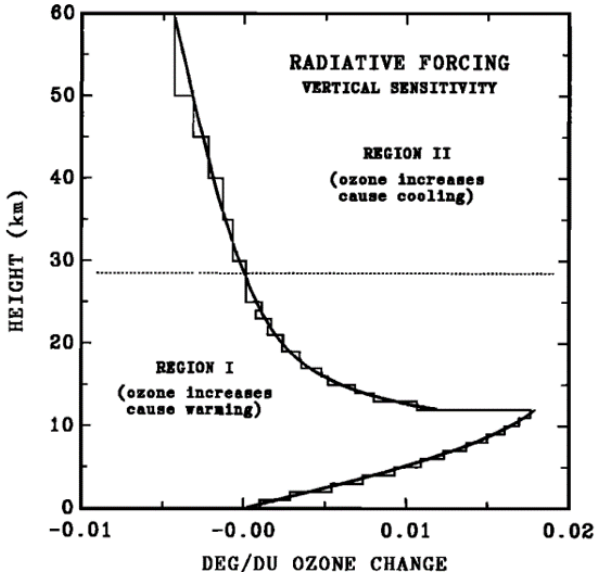

Figure 2.6: Radiative forcing sensitivity of global surface temperature changes in vertical ozone distribution. Figure from Reference [52].

Additionally, Fichter [25] argues that the radiative forcing from O_3, PMO, and CH_4 is reduced for lower flight altitudes, and the total radiative forcing increases for higher altitudes. She argues that at lower altitudes, less O_3 is formed due to a quicker removal of O_3 precursor species (e.g. O, O_2, Volatile Organic Compounds (VOCs), CO). This is in line with research from Grewe et al. [32], which argues that the O_3 perturbations are lower at lower altitudes, although the amount of NO_x emissions is higher.

Amount of NO_x at different altitudes

To examine the amount of NO_x emissions per flight altitude, two flights are chosen: Atlanta (ATL) - Miami (MIA), and Atlanta (ATL) - Seattle (SEA). Respectively, the first flight can be flown with either a REG or SMR aircraft, and the second flight can be flown with a SMR and a LR aircraft. For those flights, Figure 2.7 and Figure 2.8 demonstrate the amount of NO_x emissions according to the mission profiles.

The NO_x emissions increase when the engine overall pressure ratio increases, as well as the combustor temperature. On the other hand, this would also increase the engine's thermal efficiency and thus fuel consumption and CO_2 and H_2O emissions. Proesmans [76] used Equation 2.1 to calculate the NO_x emission index, which is taken from Reference [20]. Respectively, p_{T3}, T_{T3}, and H_0 are the pressure and temperature ahead of the engine combustor, and the specific humidity.

$$\mathrm{EI}_{\mathrm{NO_x}} = 0.0986 \cdot \left(\frac{p_{T3}}{101325}\right)^{0.4} \cdot e^{T_{T3}/194.4 - H_0/53.2} \tag{2.1}$$

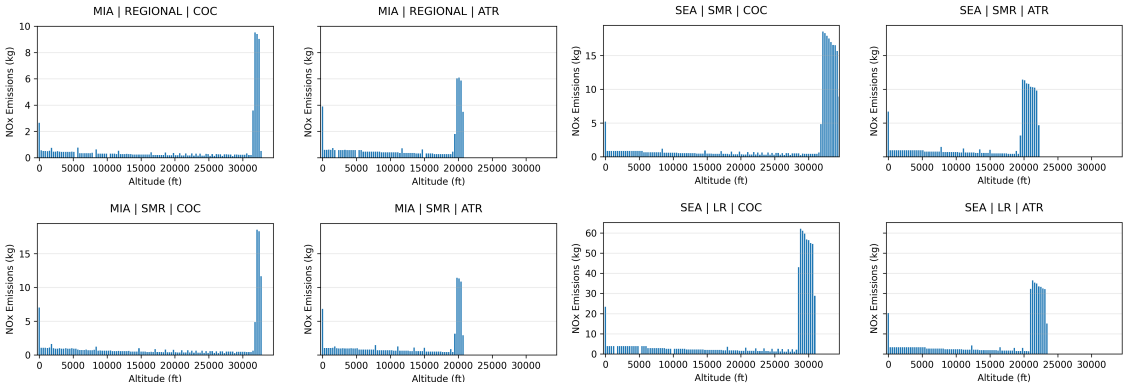

Figure 2.7: NO_x emissions per altitude for flight between ATL-MIA, for regional and small-medium range aircraft.

Figure 2.8: NO_x emissions per altitude for flight between ATL-SEA, for small-medium range and long-range aircraft.

These amounts of NO_x are compared with existing literature. Mulder and Ruijgrok [68] argue that a 500 nm flight (926 km) corresponds to 7.0 kg NO_x during takeoff and landing, and 65.3 kg NO_x during climb, cruise, and descent. Comparing this to the ATL-MIA flight (957 km), the values appear to be in line with these numbers, as can be seen in Table 2.3. For the regional aircraft, the NO_x emissions are quite close to the estimated values presented by Mulder and Ruijgrok [68], and for SMR aircraft, the NO_x values are much higher, which could be explained by the increased payload and fuel flow.

Table 2.3: Comparison of NO_x and fuel emissions. *Cruise includes climb and descent.

	Source [68]	**REG**				**SMR**			
	NO_x [kg]	**NO_x [kg]**		**Fuel [kg]**		**NO_x [kg]**		**Fuel [kg]**	
		COC	**ATR**	**COC**	**ATR**	**COC**	**ATR**	**COC**	**ATR**
LTO (<1500 ft)	7.0	4.8	6.3	91.6	65.4	11.3	10.9	233.2	125.1
Cruise* (>1500 ft)	65.3	60.7	47.8	1701.3	1350.1	114.2	84.4	3210	2525.1

Next to this flight, a long-range flight from ATL-SEA is used to compare values from Mulder and Ruijgrok [68] with. They present NO_x emissions for a flight from London to Tokyo, which corresponds to around 9600 km. The flight distance from ATL-SEA is about 2.7 times shorter than from London to Tokyo. While comparing these two flights (ALT-SEA with cruise x 2.7, and London-Tokyo) is not an accurate comparison, especially because assuming a linear scaling factor does not include the impact of the additional fuel mass, it does provide a starting point for comparison. In Table 2.4, the emissions per flight phase for Reference [68] and for the NO_x emissions calculated using the mission profiles are presented. The flight phase altitude boundaries are used as defined by Mulder and Ruijgrok [68]. Only for the LTO phase, a 300ft altitude boundary is assumed because it is undefined in the paper, and therefore the 300 ft is based on the visual interpretation of the plots in Figure 2.8. While the values from Table 2.4 demonstrate a rough comparison based on general assumptions, it can be concluded that the NO_x emission calculations are in the right order or magnitude.

Table 2.4: Comparison of NO_x and fuel emissions by flight phase and aircraft model. Values are based on data from [68].

	NO_x [kg] [68]	**NO_x [kg] for LR**	
		COC	**ATR**
LTO (<300 ft)	15	23.4	20.3
Climb-out (<1500 ft)	27	15.5	13.5
Cont. climb (>1500 ft)	158	205.4	146.1
Cruise (>1500 ft)	1113	480.7	295.4
Cruise x 2.7 (>1500 ft)		**1297.9**	**797.6**
Total NO_x emissions	1321	708.6	461.02
Total NO_x emissions with Cruise x 2.7		**1541.9**	**963.2**

Climate impact contribution from different altitudes

The last verification step combines the results from the aCCF calculations for NO_x emissions per altitude, with the amount of NO_x emissions per altitude. This demonstrates the contribution to the overall climate impact of NO_x per altitude, for one flight. Instead of altitude, the height is presented in terms of pressure level, because this is the method that is used to calculate the total climate impact of a flight. The result for the ATL-MIA flight for the SMR aircraft and the result for the ATL-SEA flight for the LR aircraft are depicted in Figure 2.10 and Figure 2.9, respectively.

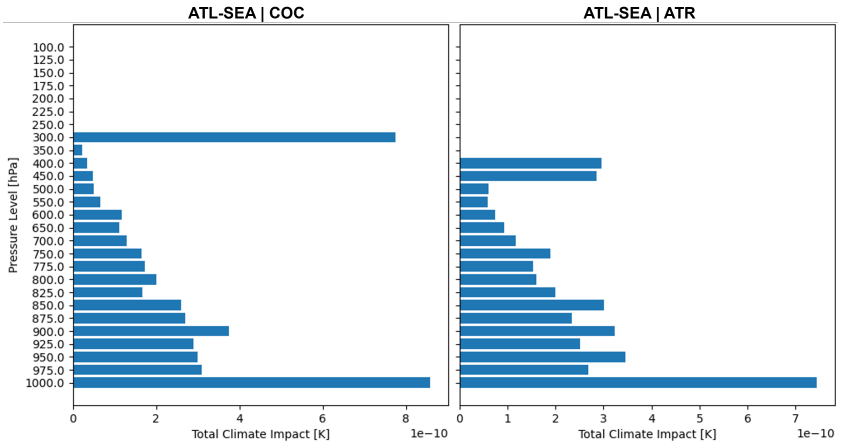

Figure 2.9: Climate impact calculated with aCCF for NO_x emissions per altitude for flight between ATL-SEA (F-ATR$_{20}$, for LR COC and ATR-optimized aircraft.

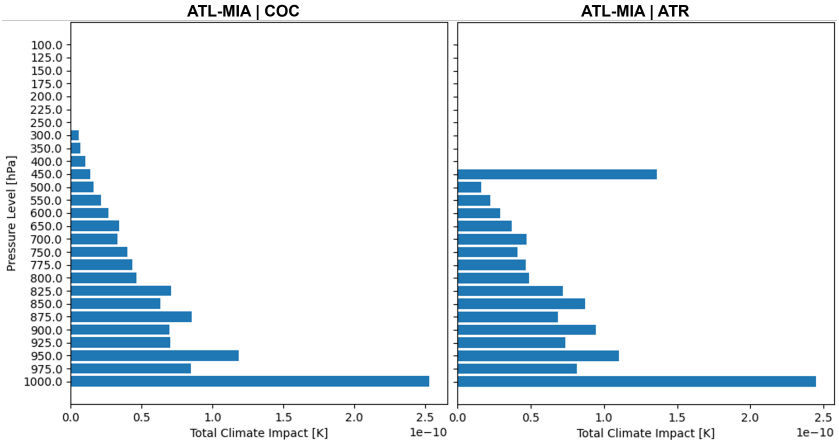

Figure 2.10: Climate impact calculated with aCCF for NO_x emissions per altitude for flight between ATL-MIA (F-ATR$_{20}$, for SMR COC- and ATR-optimized aircraft.

These figures further demonstrate that the climate impact calculations for NO_x emissions at lower altitudes are not in line with the available literature. The climate impact of NO_x at lower altitudes should be much less compared to the climate impact at cruise altitudes. It is therefore that the climate impact of NO_x emissions at lower altitudes are not considered in this research. This decision is also supported by Meuser, Lau, and Gollnick [67], who excluded NO_x emissions for altitudes below 20000 ft.

2.3. NO_x Scaling Factors

It is established that there is a problem with the NO_x climate impact values, since the climate impacts in K/kg(NO_x) from O_3 are found to be in contrast to the available literature for lower cruise altitudes (pressures between 250 hPa and 550 hPa). O_3 dominates the climate impact contribution for NO_x, thus it is chosen to only introduce scaling factors for O_3.

Köhler et al. [50] present the radiative forcings of NO_x and O_3 as a function of altitude, and demonstrate that they both decrease with lower altitudes, which is in line with References [25, 32, 52]. It is therefore that the scaling factors, presented in Table 2.5, are introduced. Based on Figure 2.11, the linear decrease in radiative forcing and the relative size of the forcing factors are used to derive the scaling factors. The resulting average climate impact from O_3 and NO_x as a function of altitude is presented in Figure 2.12.

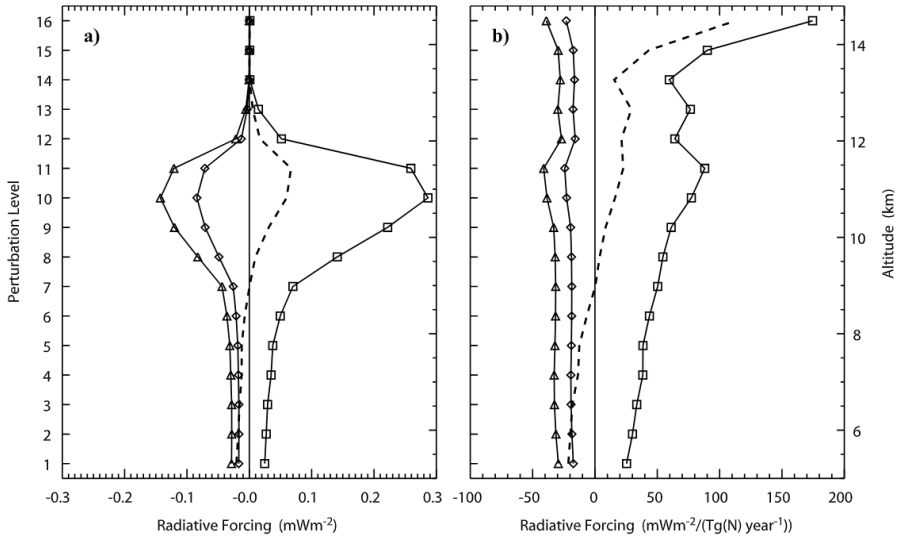

Figure 2.11: Radiative forcings due to changes in NO_x emissions. O_3 is represented with squares; CH_4 with triangles; PMO with diamonds; net forcing from NO_x with dashed line. Figure from Reference [50].

Table 2.5: Scaling factors for O_3 at different pressure levels

Pressure (hPa)	250	300	350	400	450	500	550
Scaling factor	0.94	0.81	0.59	0.41	0.28	0.20	0.15

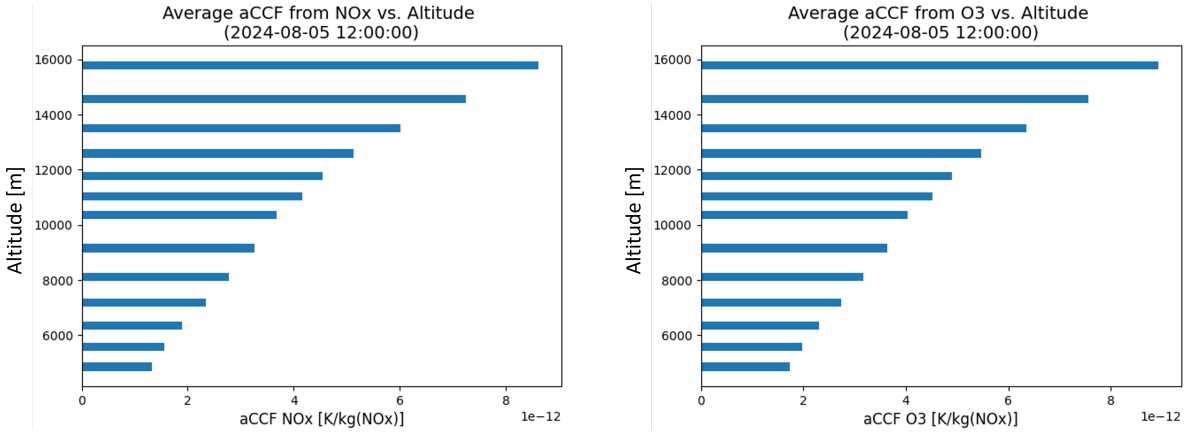

Figure 2.12: Average climate impact from NO_x and O_3 for different altitudes (F-ATR_{100}) in [K/kg(NO_x)]. Results for August 5th, 2024, at 12:00:00 UTC.

To conclude, this chapter shows that the current understanding of NO_x emissions is limited. The climate impact due to NO_x is difficult to determine, because it contains lots of assumptions, already starting at the amount of NO_x production during flights. Current methods to determine NO_x production from aircraft engines depend on various factors such as the bypass ratio, the combustor temperature, the fuel flow, and the overall pressure ratio (e.g. [76]).

3

Resource Availability

This research provides insights into how airlines could use ATR-optimized aircraft and alternative fuels to lower the overall climate impact. It does this by assuming the availability of these resources. While the sensitivity analysis provides additional insights into the influence of different fuel prices, this chapter aims to provide a more detailed understanding of the resource availability. The availability will be related to the results of this research. The SAF availability is discussed in section 3.1, the LH_2 is discussed in section 3.2, and the aircraft availability is discussed in section 3.3. The implications of the resource availability are discussed in section 3.4.

3.1. SAF Availability

The SAF production is increasing significantly in Europe, the United States, and Asia. In 2024, the European SAF production capacity reached around 1.2 million tonnes. This is equivalent to around 2.4% of the fuel consumption of the European aviation sector [80]. Neste is the global leading SAF supplier, supplying European airports as well as some North American airports such as San Francisco International Airport. Neste expanded its SAF production by opening a renewables refinery in Rotterdam, where they produce 500.000 tonnes of SAF per year, leading to a total of 900.000 tonnes of SAF per year. SkyNRG is an example of a company that is currently in development, aiming to open a factory that will produce 100.000 tonnes of SAF per year. When compared to a major airline like KLM, such an amount would replace around 1-2% of the yearly kerosene uptake. The SAF availability at European airports is depicted in Figure 3.1[1]. As for North America, Montana Renewables[2] and World Energy[3] are the leaders, with each the capacity to produce approximately 1 million tonnes of SAF per year.

Most of the SAF developments have taken place in Europe and the US. However, since 2023, increased SAF activity has been observed in the Asia Pacific. For example, Japan announced it will replace 10% of the aviation fuel with SAF in 2030, India is working on developing a SAF road-map, and Thai Airways announced they will use 2% SAF by 2024 and 60% by 2050 [44].

On a global scale, the SAF production reached 1 billion tonnes in 2024, double the amount produced in 2023[4]. Although one billion tonnes sounds like a lot, this translates to only 0.2-0.3% of the global jet fuel use.

While significant global progress has been made in recent years, there is concern regarding the availability of feedstock in the long term, such as the availability of vegetable oils, waste, residue oils, etc. (e.g. [44, 101]), as well as the sustainability of the feedstock. For example, CORSIA SAF has clear requirements on the supply chain; however, with high levels of SAF production, the regulation can become complicated, and exporting countries may have an incentive to commit fraud by mixing used cooking oils with (cheaper) virgin oil [24].

[1] https://www.eurocontrol.int/article/sustainable-aviation-fuels-saf-europe-eurocontrol-and-ecac-cooperate-saf-map, accessed June 4th, 2025.
[2] https://montanarenewables.com/, accessed June 4th, 2025.
[3] https://worldenergy.net/, accessed June 4th, 2025.
[4] https://www.iata.org/en/iata-repository/pressroom/fact-sheets/fact-sheet---alternative-fuels/, accessed June 4th, 2025.

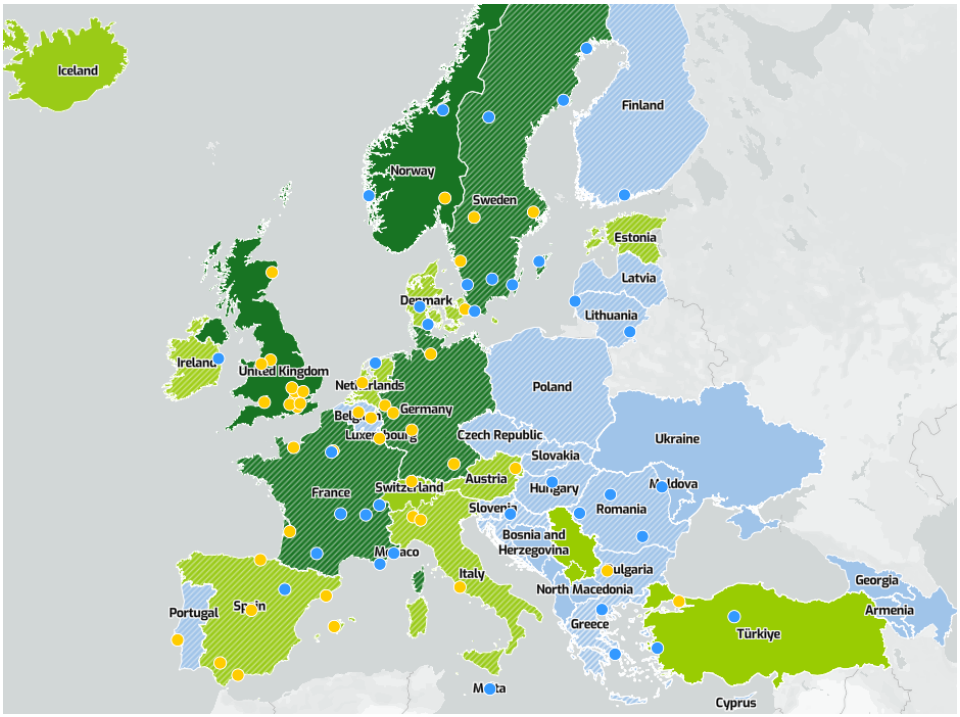

Figure 3.1: SAF supply at airports. Yellow: Airport offering SAF; blue: Base of aircraft operator using SAF; striped: EU SAF obligations apply; light green: national SAF road-maps under development; green: national SAF measures promulgated; gray: other European Council Aviation Conference (ECAC) state.

3.2. Hydrogen Availability

For the aviation sector, Oesingmann, Grimme, and Scheelhaase [73] forecast a global demand in 2050 for LH_2 around 15.4 million tonnes per year, and Grimme and Braun [35] forecast a similar demand of around 17.4 million tonnes per year. LH_2 produced with zero or few emissions (low-emission LH_2) is scarce, with less than 1 million tonnes produced in 2023, and forecasts for 2030 estimate 4 million tonnes per year [43]. The current state of low-emission LH_2 production, either using carbon capture, utilization, and storage (CCUS) or electrolysis, is presented in Figure 3.2.

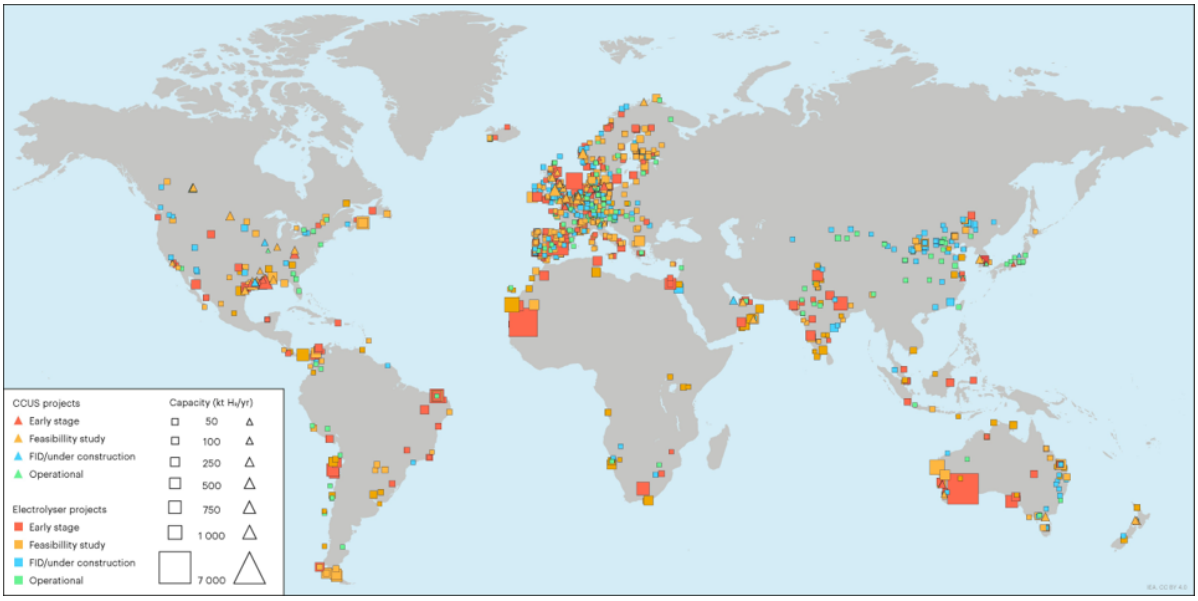

Figure 3.2: Global hydrogen production. Figure from Reference [43]. CCUS = carbon capture, utilization and storage; FID = final investment decision.

While there are quite some low-emission LH_2 production locations, researchers have argued that the realization of a steady LH_2 supply chain also depends on the demand from other sectors [3], such as the automotive industry. The LH_2 demand for road transport is decreasing, while the demand for the aviation sector is increasing, and as a result, some production initiatives have stopped.

3.3. Aircraft Availability

Deciding upon certain aircraft types within an airline's fleet, such as ATR-optimized aircraft or LH_2 aircraft, may come with high waiting times. Currently, it takes up to 10 years for aircraft to be designed, developed, and certified [64]. Additionally, it takes around 7 years between aircraft orders and deliveries [96]. Moreover, the introduction of hydrogen-powered commercial aircraft is not expected within the next couple of years. Airbus, for example, has reported that the development of their commercial hydrogen aircraft has been delayed to the late 2040s, due to insufficient green hydrogen supply and infrastructure[5]. Meanwhile, researchers are also studying fuel-flexible engines, which can accommodate multiple fuels[6]. Fuel flexibility may support the transition between kerosene and other sustainable fuels, as the availability is unreliable. Nevertheless, the design, licensing, and manufacturing takes time.

3.4. Implications

This chapter has demonstrated the scarcities of sustainable fuels and aircraft. As SAF is expected to be heavily constrained in the future, this implies that relying solely on SAF to mitigate significant climate impact is insufficient. However, the LH_2 production is also not expected to be able to cover the energy needs of the industry; moreover, the introduction of commercial LH_2 aircraft on the aviation market is not expected within the next couple of years. These resource constraints could be mitigated by leveraging the combination of the available resources and operational measures. Airlines, airports, aircraft manufacturers, and policymakers should develop and anticipate mixed fleets with mixed fuel types and aircraft types in the future, to reduce the climate impact of the aviation industry.

[5] https://energydigital.com/articles/airbus-delays-plans-for-commercial-hydrogen-aircraft, accessed July 8th, 2025.

[6] https://www.tudelft.nl/en/stories/articles/flying-on-liquid-hydrogen-outstanding-challenges-and-solutions, accessed July 8th, 2025.

References

[1] E. J. Adler and J. R. R. A. Martins. "Hydrogen-powered aircraft: Fundamental concepts, key technologies, and environmental impacts". In: *Elsevier: Progress in Aerospace Sciences* 141 (2023). DOI: 10.1016/j.paerosci.2023.100922.

[2] European Union Aviation Safety Agency. *Sustainable Aviation Fuels*. 2025. URL: https://www.easa.europa.eu/en/domains/environment/eaer/sustainable-aviation-fuels.

[3] International Energy Agency. *Global Hydrogen Review 2024*. Tech. rep. 2024. URL: www.iea.org.

[4] M. R. Allen et al. "A solution to the misrepresentations of CO2-equivalent emissions of short-lived climate pollutants under ambitious mitigation". In: *npj Climate and Atmospheric Science* 1 (1 Dec. 2018). ISSN: 23973722. DOI: 10.1038/s41612-018-0026-8.

[5] *Alternative Fuels Data Center: Sustainable Aviation Fuel*. URL: https://afdc.energy.gov/fuels/sustainable-aviation-fuel.

[6] M. Seaone Álvarez. "Assessment of Climate Impact Mitigation Potential of Intermediate Stop Operations". MA thesis. Delft University of Technology, 2021.

[7] H. Appleman. "The Formation of Exhaust Condensation Trails by Jet Aircraft". In: *Bull. Am. Meteorol* 34 (1953), pp. 14–20.

[8] D. Archer and V. Brovkin. "The millennial atmospheric lifetime of anthropogenic CO2". In: *Climatic Change* 90 (3 Oct. 2008), pp. 283–297. ISSN: 01650009. DOI: 10.1007/s10584-008-9413-1.

[9] C. Barnhart, T. S. Kniker, and M. Lohatepanont. "Itinerary-based airline fleet assignment". In: *Transportation Science* 36 (2 2002), pp. 199–217. ISSN: 00411655. DOI: 10.1287/trsc.36.2.199.566.

[10] T. Bieger and A. Wittmer. "Airline Strategy: From Network Management to Business Models". In: Springer Berlin Heidelberg, 2011, pp. 77–102. DOI: 10.1007/978-3-642-20080-9_5.

[11] A. Bier et al. "Contrail formation on ambient aerosol particles for aircraft with hydrogen combustion: a box model trajectory study". In: *Atmospheric Chemistry and Physics* 24 (2024), pp. 2319–2344. DOI: 10.5194/acp-24-2319-2024.

[12] L. Bock and U. Burkhardt. "Contrail cirrus radiative forcing for future air traffic". In: *Atmospheric Chemistry and Physics* 19 (12 June 2019), pp. 8163–8174. ISSN: 16807324. DOI: 10.5194/acp-19-8163-2019.

[13] J. Brand et al. "Potential use of hydrogen in air propulsion". In: *AIAAInternational Air and Space Symposium and Exposition: The Next 100 Years*. American Institute of Aeronautics and Astronautics Inc., 2003. DOI: 10.2514/6.2003-2879.

[14] N. Brown and A. Oldani. *Sustainable Aviation Fuel*. 2022. URL: https://www.faa.gov/media/74261.

[15] U. Burkhardt, L. Bock, and A. Bier. "Mitigating the contrail cirrus climate impact by reducing aircraft soot number emissions". In: *npj Climate and Atmospheric Science* 1 (1 Dec. 2018). ISSN: 23973722. DOI: 10.1038/s41612-018-0046-4.

[16] E. Cabrera and J. M. Melo de Sousa. "Use of Sustainable Fuels in AviationA Review". In: *Energies* 15 (7 Apr. 2022). ISSN: 19961073. DOI: 10.3390/en15072440.

[17] M. Cain et al. "Improved calculation of warming-equivalent emissions for short-lived climate pollutants". In: *npj Climate and Atmospheric Science* 2 (1 Dec. 2019). ISSN: 23973722. DOI: 10.1038/s41612-019-0086-4.

[18] K. Dahlmann et al. "Assessing the climate impact of formation flights". In: *Aerospace* 7 (12 Dec. 2020), pp. 1–12. ISSN: 22264310. DOI: 10.3390/aerospace7120172.

[19] K. Dahlmann et al. "Can we reliably assess climate mitigation options for air traffic scenarios despite large uncertainties in atmospheric processes?" In: *Transportation Research Part D: Transport and Environment* 46 (July 2016), pp. 40–55. ISSN: 13619209. DOI: 10.1016/j.trd.2016.03.006.

[20] E. S. Dallara and I. M. Kroo. “Aircraft Design for Reduced Climate Impact”. In: This paper investigates the design of future aircraft for reduced climate impacts, which is distinct fromlow fuel burn design because of the importance of non-CO2 emissions. In particular, the eects of reducedcruise speed and altitude, low emissions and fuel burn technologies, and an operational contrail mitigationstrategy are explored. American Institute of Aeronautics and Astronautics (AIAA), Jan. 2011. DOI: 10.2514/6.2011-265.

[21] S. Dietmüller et al. “A Python library for computing individual and merged non-CO2 algorithmic climate change functions: CLIMaCCF V1.0”. In: *Geoscientific Model Development* 16 (15 Aug. 2023), pp. 4405–4425. ISSN: 19919603. DOI: 10.5194/gmd-16-4405-2023.

[22] *Electric and Hybrid Aircraft Platform for Innovation*. URL: https://www.icao.int/environmental-protection/Pages/electric-aircraft.aspx.

[23] Elysian Aircraft. *Elysian Aircraft*. Accessed: 2025-04-23. 2025. URL: https://www.elysianaircraft.com/.

[24] *Europes imports of dubious used cooking oil set to rise, fuelling deforestation*. 2021. URL: https://www.transportenvironment.org/articles/europes-imports-dubious-used-cooking-oil-set-rise-fuelling-deforestation#:~:text=Press%20Release-,Europe's%20imports%20of%20dubious%20'used'%20cooking%20oil,set%20to%20rise%2C%20fuelling%20deforestation&text=Europe's%20demand%20for%20used%20cooking,imports%2C%20a%20new%20study%20shows..

[25] C. Fichter. “Climate Impact of Air Traffic Emissions in Dependency of the Emission Location and Altitude”. PhD thesis. DLR, 2009.

[26] C. Frömming et al. “Aviation-induced radiative forcing and surface temperature change in dependency of the emission altitude”. In: *Journal of Geophysical Research Atmospheres* 117 (19 2012). ISSN: 01480227. DOI: 10.1029/2012JD018204.

[27] K. Gierens, L. Lim, and K. Eleftheratos. “A Review of Various Strategies for Contrail Avoidance”. In: *The Open Atmospheric Science Journal* 2 (1 Feb. 2008), pp. 1–7. ISSN: 18742823. DOI: 10.2174/1874282300802010001.

[28] V. Grewe. *Climate Impact of Air Traffic Part 1*. Lecture. 2023.

[29] V. Grewe. *Climate Impact of Air Traffic Part 3*. Lecture. 2023.

[30] V. Grewe. “Lightning: Principles, Instruments and Applications”. In: *Springer* (2008). Ed. by Hans Dieter Betz, Ulrich Schumann, and Pierre Laroche. DOI: 10.1007/978-1-4020-9079-0.

[31] V. Grewe et al. “Feasibility of climate-optimized air traffic routing for trans-Atlantic flights”. In: *Environmental Research Letters* 12.3 (2017). DOI: 10.1088/1748-9326/aa5ba0.

[32] V. Grewe et al. “Impact of aircraft NOx emissions. Part 2: Effects of lowering the flight altitude”. In: *Meteorologische Zeitschrift* 11 (3 2002), pp. 197–205. ISSN: 09412948. DOI: 10.1127/0941-2948/2002/0011-0197.

[33] V. Grewe et al. “Mitigating the climate impact from aviation: Achievements and results of the DLR WeCare project”. In: *Aerospace* 4 (3 Sept. 2017). ISSN: 22264310. DOI: 10.3390/aerospace4030034.

[34] V. Grewe et al. “Reduction of the air traffic’s contribution to climate change: A REACT4C case study”. In: *Atmospheric Environment* 94 (2014), pp. 616–625. ISSN: 18732844. DOI: 10.1016/j.atmosenv.2014.05.059.

[35] W. Grimme and M. Braun. “Estimation of potential hydrogen demand and CO2mitigation in global passenger air transport by the year 2050”. In: *Transportation Research Procedia*. Vol. 65. Elsevier B.V., 2022, pp. 24–33. DOI: 10.1016/j.trpro.2022.11.004.

[36] F. Haglind. “Potential of lowering the contrail formation of aircraft exhausts by engine re-design”. In: *Aerospace Science and Technology* 12 (6 Sept. 2008), pp. 490–497. ISSN: 12709638. DOI: 10.1016/j.ast.2007.12.001.

[37] C. A. Hane et al. *The fleet assignment problem: 1 solving a large-scale integer program*. 1995.

[38] Heart Aerospace. *Heart Aerospace*. Accessed: 2025-04-23. 2025. URL: https://heartaerospace.com/es-30/.

[39] S. Hofer, K. Gierens, and S. Rohs. “How well can persistent contrails be predicted? An update”. In: *Atmospheric Chemistry and Physics* 24 (13 July 2024), pp. 7911–7925. ISSN: 16807324. DOI: 10.5194/acp-24-7911-2024.

[40] IATA. “Global Outlook for Air Transport: Deep Change”. In: *IATA Sustainability and Economics* (June 2024). URL: https://www.iata.org/en/iata-repository/publications/economic-reports/global-outlook-for-air-transport-june-2024-report/.

[41] ICAO. *ICAO document - CORSIA Sustainability Criteria for CORSIA Eligible Fuels*. Nov. 2022. URL: https://www.icao.int/environmental-protection/CORSIA/Documents/CORSIA_Eligible_Fuels/ICAO%20document%2005%20-%20Sustainability%20Criteria%20-%20November%202022.pdf.

[42] *ICAO Aircraft Engine Emissions Databank*. July 2024. URL: https://www.easa.europa.eu/en/domains/environment/icao-aircraft-engine-emissions-databank%20https://www.easa.europa.eu/en/downloads/131424/en.

[43] International Energy Agency (IEA). *Hydrogen Production Projects Database*. Accessed May 2025. 2024. URL: https://www.iea.org/reports/global-hydrogen-review-2024/executive-summary.

[44] *Is Asia Pacific a global game changer for the global SAF industry?* Tech. rep. KPMG, 2023. URL: https://kpmg.com/content/dam/kpmgsites/uk/pdf/2023/09/is-asia-pacific-a-game-changer-for-the-global-saf-Industry.pdf.coredownload.inline.pdf.

[45] P. W. Jansen and R. E. Perez. “Coupled optimization of aircraft design and fleet allocation with uncertain passenger demand”. In: *2013 Aviation Technology, Integration, and Operations Conference*. American Institute of Aeronautics and Astronautics Inc., 2013. ISBN: 9781624102257. DOI: 10.2514/6.2013-4392.

[46] JetZero. *JetZero*. Accessed: 2025-04-23. 2025. URL: https://www.jetzero.aero/.

[47] P. Jöckel et al. “Development cycle 2 of the Modular Earth Submodel System (MESSy2)”. In: *Geoscientific Model Development* 3 (2 2010), pp. 717–752. ISSN: 1991959X. DOI: 10.5194/gmd-3-717-2010.

[48] S. Kaufmann, R. Dischl, and C. Voigt. “Regional and seasonal impact of hydrogen propulsion systems on potential contrail cirrus cover”. In: *Atmospheric Environment: X* 24 (Dec. 2024). ISSN: 25901621. DOI: 10.1016/j.aeaoa.2024.100298.

[49] B. Khandelwal et al. *Hydrogen powered aircraft: The future of air transport*. 2013. DOI: 10.1016/j.paerosci.2012.12.002.

[50] M. O. Köhler et al. “Impact of perturbations to nitrogen oxide emissions from global aviation”. In: *Journal of Geophysical Research Atmospheres* 113 (11 June 2008). ISSN: 01480227. DOI: 10.1029/2007JD009140.

[51] M. Kühlen et al. “An explanatory approach to modeling the fleet assignment in the global air transportation system”. In: *CEAS Aeronautical Journal* 14 (2022), pp. 255–269. ISSN: 18695590. DOI: 10.1007/s13272-022-00622-1.

[52] A. A. Lacis, D. J. Wuebbles, and J. A. Logan. *Radiative Forcing of Climate by Changes in the Vertical Distribution of Ozone*. Tech. rep. 1990. DOI: 10.1029/JD095iD07p09971.

[53] S. Langhans et al. “System analysis for an intermediate stop operations concept on long range routes”. In: *Journal of Aircraft* 50 (1 2013), pp. 29–37. ISSN: 15333868. DOI: 10.2514/1.C031446.

[54] D. S. Lee et al. “The contribution of global aviation to anthropogenic climate forcing for 2000 to 2018”. In: *Atmospheric Environment* 244 (Jan. 2021). ISSN: 18732844. DOI: 10.1016/j.atmosenv.2020.117834.

[55] D. S. Lee et al. “Transport impacts on atmosphere and climate: Aviation”. In: *Atmospheric Environment* 44 (1352-2310 2010), pp. 4678–4734. DOI: 10.1016/j.atmosenv.2009.06.005.

[56] R. Lindsey. *Climate Change: Atmospheric Carbon Dioxide*. 2024.

[57] M. Liu et al. “Green Airline-Fleet Assignment with Uncertain Passenger Demand and Fuel Price”. In: *Sustainability (Switzerland)* 15 (2 Jan. 2023). ISSN: 20711050. DOI: 10.3390/su15020899.

[58] Maeve. *Maeve*. Accessed: 2025-08-03. 2025. URL: https://maeve.aero/maeve-jet.

[59] J. van Manen and V. Grewe. “Algorithmic climate change functions for the use in eco-efficient flight planning”. In: *Transportation Research Part D: Transport and Environment* 67 (Feb. 2019), pp. 388–405. ISSN: 13619209. DOI: 10.1016/j.trd.2018.12.016.

[60] R. S. Märkl et al. “Powering aircraft with 100% sustainable aviation fuel reduces ice crystals in contrails”. In: *Atmospheric Chemistry and Physics* 24 (2024), pp. 3813–3837. DOI: 10.5194/acp-24-3813-2024.

[61] T. Marks et al. “Climate impact mitigation potential of formation flight”. In: *Aerospace* 8 (1 Jan. 2021), pp. 1–18. ISSN: 22264310. DOI: 10.3390/aerospace8010014.

[62] S. Matthes et al. “Climate-optimized trajectories and robust mitigation potential: Flying atm4e”. In: *Aerospace* 7 (11 Nov. 2020), pp. 1–15. ISSN: 22264310. DOI: 10.3390/aerospace7110156.

[63] S. Matthes et al. “Mitigation of non-CO2 aviations climate impact by changing cruise altitudes”. In: *Aerospace* 8 (2 Feb. 2021), pp. 1–20. ISSN: 22264310. DOI: 10.3390/aerospace8020036.

[64] S. Matthews, D. Naughton, and D. Griffin. *Fuelling the future of flight*. Tech. rep. SMBC Aviation Capital, 2024.

[65] L. Megill, K. Deck, and V. Grewe. “Alternative climate metrics to the Global Warming Potential are more suitable for assessing aviation non-CO2 effects”. In: *Communications Earth and Environment* 5 (1 2024). ISSN: 26624435. DOI: 10.1038/s43247-024-01423-6.

[66] L. Megill and V. Grewe. “Investigating the limiting aircraft design-dependent and environmental factors of persistent contrail formation”. Preprint. Nov. 2024. DOI: 10.5194/egusphere-2024-3398.

[67] M. Mendiguchia Meuser, A. Lau, and V. Gollnick. “Investigation on the effects of weather patterns on strategic climate impact mitigation measures: a data-based approach”. In: *ECATS conference*. Oct. 2023. URL: https://elib.dlr.de/200550/.

[68] T. J. Mulder and G.J.J. Ruijgrok. “On the reduction of NOx-emission levels by performing low NOx flights”. In: *26th International Congress of the Aeronautical Sciences*. ICAS 2008, 2008. URL: http://icas.org/icas_archive/ICAS2008/PAPERS/532.PDF.

[69] M. Niklass et al. “Implementation of eco-efficient procedures to mitigate the climate impact of non-CO2 effects.” In: *Proceedings of the 31st Congress of the International Council of the Aeronautical Sciences* (2018).

[70] M. Niklass et al. “Potential to reduce the climate impact of aviation by climate restricted airspaces”. In: *Elsevier* (2019). DOI: 10.1016/j.tranpol.2016.12.010.

[71] H. Nojoumi, I. Dincer, and G. F. Naterer. “Greenhouse gas emissions assessment of hydrogen and kerosene-fueled aircraft propulsion”. In: *International Journal of Hydrogen Energy* 34 (3 Feb. 2009), pp. 1363–1369. ISSN: 03603199. DOI: 10.1016/j.ijhydene.2008.11.017.

[72] M. Noorafza et al. “Airline Network Planning Considering Climate Impact: Assessing New Operational Improvements”. In: *Applied Sciences (Switzerland)* 13 (11 June 2023). ISSN: 20763417. DOI: 10.3390/app13116722.

[73] K. Oesingmann, W. Grimme, and J. Scheelhaase. “Hydrogen in aviation: A simulation of demand, price dynamics, and CO2 emission reduction potentials”. In: *International Journal of Hydrogen Energy* 64 (Apr. 2024), pp. 633–642. ISSN: 03603199. DOI: 10.1016/j.ijhydene.2024.03.241.

[74] *Operating Life*. 2025. URL: https://www.airbus.com/en/products-services/commercial-aircraft/the-life-cycle-of-an-aircraft/operating-life.

[75] *Paris Agreement*. 2015.

[76] P. Proesmans. “Climate-Optimal Aircraft Design and Fleet Allocation: Evaluating the Impact of Sustainable Aviation Fuels”. Dissertation at TU Delft, Delft University of Technology. PhD thesis. Delft University of Technology, 2024. DOI: 10.4233/uuid:295a037d-02ef-4bb9-bd4e-c6e346f0fefa.

[77] K. Ranasinghe et al. “Review of advanced low-emission technologies for sustainable aviation”. In: *Energy* 188 (Dec. 2019). ISSN: 03605442. DOI: 10.1016/j.energy.2019.115945.

[78] A. Rap et al. “The climate impact of contrails from hydrogen combustion and fuel cell aircraft”. In: *EGU General Assembly 2023*. Apr. 2023. DOI: 10.5194/egusphere-egu23-5520.

[79] *Refuel EU aviation initiative: Council adopts new law to decarbonise the aviation sector*. Council of the EU. 2023. URL: https://www.consilium.europa.eu/en/press/press-releases/2023/10/09/refueleu-aviation-initiative-council-adopts-new-law-to-decarbonise-the-aviation-sector/.

[80] *Report from the commission to the European parliament and the council: The ReFuelEU Aviation SAF flexibility mechanism*. Tech. rep. European Commission, 2025. URL: https://eur-lex.europa.eu/legal-content/EN/TXT/?uri=COM:2025:59:FIN.

[81] J. J. Salazar-González. "Approaches to solve the fleet-assignment, aircraft-routing, crew-pairing and crew-rostering problems of a regional carrier". In: *Omega (United Kingdom)* 43 (2014), pp. 71–82. ISSN: 03050483. DOI: 10.1016/j.omega.2013.06.006.

[82] B. F. Santos. *AE4423 Lect 6.2 Aircraft Routing Dynamic Programming*. 2022. URL: https://www.youtube.com/watch?v=bUiaxFiHtmU.

[83] R. Sausen et al. "A Diagnostic Study of the Global Distribution of Contrails Part I: Present Day Climate Ā". In: *Springer: Theoretical and Applied Climatology* (61 1998), pp. 127–141.

[84] E. Schmidt. "Die Entstehung von Eisnebel aus den Auspuffgasen von Flugmotoren". In: *Schriften der Deutschen Akademie der Luftfahrtforschung* 44 (1941), pp. 1–15.

[85] U. Schumann. "On conditions for contrail formation from aircraft exhaust". In: *Meteorol Zeitschrift* 5 (1996), pp. 4–23.

[86] H. D. Sherali, E. K. Bish, and X. Zhu. "Airline fleet assignment concepts, models, and algorithms". In: *European Journal of Operational Research* 172 (1 July 2006), pp. 1–30. ISSN: 03772217. DOI: 10.1016/j.ejor.2005.01.056.

[87] A. Simorgh et al. *A Comprehensive Survey on Climate Optimal Aircraft Trajectory Planning*. Mar. 2022. DOI: 10.3390/aerospace9030146.

[88] A. Simorgh et al. "Concept of robust climate-friendly flight planning under multiple climate impact estimates". In: *Transportation Research Part D: Transport and Environment* 131 (June 2024). ISSN: 13619209. DOI: 10.1016/j.trd.2024.104215.

[89] M. A. Smith, M. Cain, and M. R. Allen. "Further improvement of warming-equivalent emissions calculation". In: *npj Climate and Atmospheric Science* (1 Dec. 2019). ISSN: 23973722. DOI: 10.1038/s41612-019-0086-4.

[90] S. Solomon et al. *Irreversible climate change due to carbon dioxide emissions*. 2009. URL: www.pnas.org/cgi/content/full/.

[91] L. Ström and K. Gierens. "First simulations of cryoplane contrails". In: *Journal of Geophysical Research Atmospheres* 107 (18 2002), AAC 2-1-AAC 2–13. ISSN: 01480227. DOI: 10.1029/2001JD000838.

[92] F. Svensson, A. Hasselrot, and J. Moldanova. "Reduced environmental impact by lowered cruise altitude for liquid hydrogen-fuelled aircraft". In: *Elsevier: Aerospace Science and Technology* 8 (2004), pp. 307–320. DOI: 10.1016/j.ast.2004.02.004.

[93] R. Teoh et al. "Aviation contrail climate effects in the North Atlantic from 2016-2021". In: *Atmospheric Chemistry and Physics* 22 (2022), pp. 10919–10935. DOI: 10.5194/acp-22-10919-2022.

[94] R. Teoh et al. "Targeted Use of Sustainable Aviation Fuel to Maximize Climate Benefits". In: *Environmental Science and Technology* 56 (23 Dec. 2022), pp. 17246–17255. ISSN: 15205851. DOI: 10.1021/acs.est.2c05781.

[95] *The Clean Future of Flight*. URL: https://zeroavia.com/.

[96] *The Growing Challenge of Capacity Planning*. Tech. rep. IATA, 2025.

[97] *The jetzero consortium to deliver the true zero flight*. URL: https://www.electricaviationgroup.com/jet-zero-consortium/.

[98] *The Wright Spirit*. URL: https://www.weflywright.com/aircraft.

[99] S. Völk et al. *OpenAirClim*. 2024. DOI: 10.5281/zenodo.14283277. URL: https://github.com/dlr-pa/oac/tree/v0.9.0.

[100] Y. Wang et al. “Optimization model and algorithm design for airline fleet planning in a multiairline competitive environment”. In: *Mathematical Problems in Engineering* 2015 (2015). ISSN: 15635147. DOI: 10.1155/2015/783917.

[101] *Wat houdt ons tegen? - Veelvliegers*. Geraadpleegd op 9 mei 2025. May 2025. URL: https://npo.nl/start/serie/wat-houdt-ons-tegen/seizoen-5/wat-houdt-ons-tegen_22/afspelen.

[102] *WMO confirms 2024 as warmest year on record at about 1.55řC above pre-industrial level*. Jan. 2025. URL: https://wmo.int/news/media-centre/wmo-confirms-2024-warmest-year-record-about-155degc-above-pre-industrial-level.

[103] K. Wolf, N. Bellouin, and O. Boucher. “Sensitivity of cirrus and contrail radiative effect on cloud microphysical and environmental parameters”. In: Copernicus Publications (on behalf of the European Geosciences Union), Nov. 2023. Chap. 23, pp. 14003–14037. DOI: 10.5194/acp-23-14003-2023.

[104] H. Yamashita et al. “Newly developed aircraft routing options for air traffic simulation in the chemistryclimate model EMAC 2.53: AirTraf 2.0”. In: *Geoscientific Model Development* 13 (10 Oct. 2020), pp. 4869–4890. ISSN: 19919603. DOI: 10.5194/gmd-13-4869-2020.

[105] F. Yin et al. “Predicting the climate impact of aviation for en-route emissions: the algorithmic climate change function submodel ACCF 1.0 of EMAC 2.53”. In: *Geoscientific Model Development* 16 (11 June 2023), pp. 3313–3334. ISSN: 19919603. DOI: 10.5194/gmd-16-3313-2023.